ANALYSIS OF THE MECHANISMS OF HEPACAM-MEDIATED TUMOUR SUPPRESSION

WU MEIHUI

(B.Sc. (Hons.), National University of Singapore)

A THESIS SUBMITTED

FOR THE DEGREE OF DOCTOR OF PHILOSOPHY

DEPARTMENT OF PHYSIOLOGY

NATIONAL UNIVERSITY OF SINGAPORE

2015

DECLARATION

I hereby declare that this thesis is my original work and it has been written by me in its entirety. I have duly acknowledged all the sources of information which have been used in the thesis.

This thesis has also not been submitted for any degree in any university previously.

_____

Wu Meihui

15 January 2015

ACKNOWLEDGEMENTS

TABLE OF CONTENTS

ix

ABSTRACT

HEPACAM is a gene encoding a novel immunoglobulin-like cell adhesion molecule that is frequently downregulated in human hepatocellular carcinoma and several other solid cancers including carcinomas of the breast and colon. Re-expression of hepaCAM in several cancer cell lines inhibits proliferation, suggesting a putative role as a tumour suppressor. However, the underlying mechanisms of hepaCAM-mediated tumour suppression are not understood. Expression of hepaCAM, also known as GlialCAM, has been observed in the central nervous system and mutations in *HEPACAM* can give rise to the leukodystrophy, megalencephalic leukoencephalopathy with subcortical cysts (MLC). In this study, I show a hitherto unknown interaction of hepaCAM with the gap junction protein connexin 43 in the human glioblastoma cell line U373 MG. Connexin 43, which has an aberrant intracellular localisation in U373 MG cells, is re-targeted to the plasma membrane at cellular junctions upon hepaCAM expression. Furthermore, hepaCAM expression increases connexin 43 protein levels by enhancing its protein stability. Mutations in hepaCAM which cause MLC, or neutralisation of hepaCAM with an antagonistic antibody disrupt its interaction with connexin 43 at cellular junctions. It is proposed that hepaCAM-mediated targeting of connexin 43 to cellular junctions increases cell-cell contact and gap junction transfer between glioblastoma cells, making it more difficult for them to detach from the primary tumour and disseminate during metastasis. I also show in this study that proteolytic cleavage of the hepaCAM cytoplasmic domain occurs in different human cancer cell lines, and is inhibited by the MLC-causing mutations in hepaCAM and the antagonistic hepaCAM antibody. Upon

integrin-mediated adhesion of U373 MG cells to the extracellular matrix protein fibronectin, hepaCAM undergoes endocytosis and is concomitantly cleaved. The presence of the cleaved hepaCAM fragment in the nucleus suggests that it may have functions in regulating gene expression and mediating the tumour suppressive activities of hepaCAM.

LIST OF TABLES

LIST OF FIGURES

LIST OF ABBREVIATIONS

7-AAD	7-Aminoactinomycin D
A595	Absorbance at 595 nm
ADAM	A Disintegrin And Metalloproteinase
ALCAM	Activated leukocyte cell adhesion molecule
AMPK	5' adenosine monophosphate-activated protein kinase
ANOVA	Analysis of variance
ATP	Adenosine triphosphate
BSA	Bovine serum albumin
CAM	Cell adhesion molecule
cAMP	Cyclic adenosine monophosphate
CAR	Coxsackie and adenovirus receptor
CDK	Cyclin dependent kinase
cDNA	Complementary DNA
CHO	Chinese hamster ovary
CHX	Cycloheximide
CNS	Central nervous system
Co-IP	Co-immunoprecipitation
DAPI	4',6-Diamidino-2-phenylindole
DMEM	Dulbecco's Modified Eagle Medium
DMSO	Dimethyl sulfoxide
DNA	Deoxyribonucleic acid
DNase	Deoxyribonuclease
dNTP	Deoxyribonucleoside triphosphate
DSP	Dithiobis[succinimidyl propionate]
EBAG9	Estrogen receptor-binding fragment-associated gene 9

ECM	Extracellular matrix
EDTA	Ethylenediaminetetraacetic acid
EEA1	Early endosome antigen 1
EGFR	Epidermal growth factor receptor
EMT	Epithelial-mesenchymal transition
EpCAM	Epithelial cell adhesion molecule
ER	Endoplasmic reticulum
ESAM	Endothelial cell-selective adhesion molecule
FACS	Fluorescence activated cell sorting
FAK	Focal adhesion kinase
FBS	Fetal bovine serum
GAPDH	Glyceraldehyde 3-phosphate dehydrogenase
GFAP	Glial fibrillary acid protein
GJIC	Gap junctional intercellular communication
HCC	Hepatocellular carcinoma
HDAC2	Histone deacetylase 2
HEK	Human embryonic kidney
HRP	Horseradish peroxidase
HUVECs	Human umbilical vein endothelial cells
ICAM-1	Intercellular cell adhesion molecule 1
Ig	Immunoglobulin
Ig-CAM	Immunoglobulin-like CAM
ILK	Integrin-linked kinase
IP	Immunoprecipitation
IP_3	Inositol trisphosphate
JAM	Junctional adhesion molecule
LB	Luria-Bertani

MAGUK	Membrane-associated guanylate kinase
MAPK	Mitogen-activated protein kinase
MLC	Megalencephalic leukoencephalopathy with subcortical cysts
MMP	Matrix metalloproteinase
mRNA	Messenger RNA
mTOR	Mammalian target of rapamycin
NCAM	Neural cell adhesion molecule
NEB	Nuclear extraction buffer
ORF	Open reading frame
PBS	Phosphate-buffered saline
PCR	Polymerase chain reaction
PDGF	Platelet derived growth factor
PDI	Protein disulfide isomerase
PECAM-1	Platelet endothelial cell adhesion molecule 1
PKC	Protein kinase C
PMA	Phorbol-12-myristate-13-acetate
PNGase F	Peptide-N-glycosidase F
Poly-HEMA	Polyhydroxyethylmethacrylate
PVDF	Polyvinylidene difluoride
RACE	Rapid amplification of cDNA ends
RIPA	Radioimmunoprecipitation assay
RNA	Ribonucleic acid
RNase	Ribonuclease
RT-PCR	Reverse transcription-PCR
SD	Standard deviation
SDS	Sodium dodecyl sulfate

SDS-PAGE	SDS-polyacrylamide gel electrophoresis
SE	Standard error
siRNA	Small interfering RNA
TAE	Tris-acetate-EDTA
TBS	Tris-buffered saline
TBST	TBS containing 0.1% Tween-20
TIMP	Tissue inhibitors of metalloproteinase
UTR	Untranslated region
VCAM-1	Vascular cell adhesion molecule 1
VEGF	Vascular endothelial growth factor
VEGFR2	Vascular endothelial growth factor receptor 2
WT	Wild-type
ZO	Zona occludens

CHAPTER 1   INTRODUCTION

1.1.   Cell adhesion

Cell adhesion is essential for the assembly of individual cells into three-dimensional tissues in multicellular organisms. It is both a stable and dynamic process. Stable cell adhesion mechanisms maintain tissue structural integrity, while dynamic cell adhesion events mediate tissue morphogenesis by regulating cellular processes such as growth, migration, differentiation and apoptosis (Gumbiner, 1996).

Cell adhesion is mediated by multi-protein complexes comprising three general classes of proteins: cell adhesion molecules (CAMs), the extracellular matrix (ECM) proteins, and peripheral membrane proteins (or cytoplasmic plaque proteins). CAMs are typically transmembrane glycoproteins that mediate diverse cell-cell and cell-ECM interactions at the plasma membrane, allowing cells to communicate with one another and with the external environment. CAMs on the cell surface are able to bind strongly to ECM proteins, most of which are large glycoproteins that assemble into fibrils or other structural networks in the extracellular milieu. CAMs also associate with peripheral membrane proteins on the intracellular surface of the plasma membrane and these interactions serve to connect CAMs to the cytoskeletal network, as well as to mediate the functions and signal transduction of CAMs (Gumbiner, 1996).

1.2. Cell adhesion molecules

The pioneering work on cell adhesion and CAMs began at the turn of the twentieth century, and significant progress was made in the identification of major CAM families in the late 1970s to 80s (reviewed in Horwitz, 2012). To date, hundreds of CAMs have been identified and characterised. Most CAMs can be classified into four broad categories: the immunoglobulin-like CAMs (Ig-CAMs), cadherins, integrins and selectins.

1.2.1. Immunoglobulin-like cell adhesion molecules

Ig-CAMs belong to the immunoglobulin (Ig) superfamily, a large group of structurally related proteins which possess one or more Ig-like domains. The Ig-like domain is a characteristic sandwich structure made up of two opposing anti-parallel beta sheets (Barclay, 2003). Ig-CAMs are calcium (Ca^{2+})-independent glycoproteins containing one or more Ig-like loops in their extracellular domain, as well as a single transmembrane domain and a cytoplasmic tail. Most Ig-CAMs are type I transmembrane proteins, while some are linked to the cell surface by a glycosylphosphatidylinositol anchor. The cytoplasmic tail of Ig-CAMs is able to interact with cytoskeletal proteins such as actin and spectrin, as well as adaptor proteins such as ankyrin (Cavallaro and Christofori, 2004; Cavallaro and Dejana, 2011).

Ig-CAMs establish homophilic *trans* interactions in which an Ig-CAM on one cell binds to the same Ig-CAM type on an adjacent cell. The combination of homophilic *trans* interactions and lateral *cis* interactions between Ig-CAMs on the same cell generate zipper-like structures which stabilise cell-cell adhesion. In addition, Ig-CAMs are able to exhibit heterophilic *cis* and *trans* interactions

with other molecules, including the different members of the Ig-CAM superfamily, integrins, cadherins, growth factor receptors and components of the ECM. These Ig-CAM mediated intercellular contacts are able to activate various proteins involved in signalling pathways, such as receptor tyrosine kinases and focal adhesion kinase (FAK) (Cavallaro and Christofori, 2004; Cavallaro and Dejana, 2011).

Ig-CAMs are expressed in diverse cell types throughout the human system including epithelial cells, endothelial cells, cells of the nervous system and leukocytes. They are implicated in many important cellular processes such as tissue morphogenesis, angiogenesis, brain development and immune responses (Cavallaro and Christofori, 2004). Some of the well-studied Ig-CAMs include NCAM (neural cell adhesion molecule), ICAM-1 (intercellular cell adhesion molecule 1), ALCAM (activated leukocyte cell adhesion molecule), VCAM-1 (vascular cell adhesion molecule 1), PECAM-1 (platelet endothelial cell adhesion molecule 1) and the L1 family.

1.2.2. Integrins

Integrins are a major family of cell adhesion receptors which mediate cellular attachment to the ECM, as well as cell-cell adhesions in vertebrates. Integrins are transmembrane heterodimeric glycoproteins consisting of non-covalently bound α and β subunits, each of which is a single-pass type I transmembrane protein. To date, 18 α and 8 β subunits have been identified in mammals, and are known to assemble into 24 distinct heterodimers. The integrin heterodimers have different tissue distribution and have been shown to have specific and non-redundant functions (Hynes, 2002).

The major ligands of integrins are the ECM proteins, including fibronectin, laminin, collagen, fibrinogen and vitronectin. In addition to interacting with ECM proteins, the extracellular domains of integrins also interact with cell surface counter receptors on adjacent cells such as Ig-CAMs, selectins and cadherins. The cytoplasmic domains of integrins interact with cytoskeletal proteins, providing a transmembrane mechanical link from the extracellular contacts to the intracellular cytoskeleton (Calderwood, 2004; Harburger and Calderwood, 2009; Hynes, 2002). This large complex of proteins interacting with integrins is known as a focal adhesion (Zamir and Geiger, 2001).

Integrins play important roles in bi-directional signal transduction between the extracellular environment and the cell. Integrins mediate "outside-in signalling" by binding to their external ligands and transmitting signals into the cell, providing information on its location, local environment and adhesive state. By activating downstream signalling proteins such as FAK and integrin-linked kinase (ILK), integrins modulate many aspects of cellular behaviour including proliferation, differentiation, survival and migration. Integrins also mediate "inside-out signalling" via the cytoplasmic tails to the extracellular domains, which then undergo conformational changes and modify their affinity to extracellular ligands in a rapid and reversible process known as integrin activation. Integrins and their ligands are essential in diverse cellular processes including growth, development, immune responses, leukocyte traffic and haemostasis (Calderwood, 2004; Harburger and Calderwood, 2009; Hynes, 2002; Miranti and Brugge, 2002).

1.2.3. Cadherins

Cadherins are a large superfamily of Ca^{2+}-dependent single-span transmembrane proteins involved in diverse processes such as cell-cell adhesion, cell polarity, cell sorting during development and tissue morphogenesis. Cadherins often engage in homophilic *trans* interactions in which a cadherin molecule binds to the same type of cadherin molecule on another cell (Takeichi, 1991). The cadherin superfamily consists of classical cadherins and non-classical cadherins. Classical cadherins are primarily associated within adherens junctions and are expressed in almost all solid tissues. The extracellular domain of classical cadherins contains five cadherin-type tandem repeats bound together by Ca^{2+} in a rod-like structure, while the cytoplasmic domain binds to the cytoplasmic proteins β-catenin and p120-catenin, which in turn are linked to α-catenin and the actin cytoskeleton. Of the classical cadherins, E-cadherin (epithelial cadherin) is the most commonly studied cadherin. Other classical cadherins include N-cadherin (neural cadherin) and VE-cadherin (vascular endothelial cadherin) (Gumbiner, 2005; Shapiro and Weis, 2009; Takeichi, 1995). Non-classical cadherins include desmosomal cadherins which are exclusively expressed in the desmosomes of epithelial cells and cardiac muscle cells and are linked to the intermediate filament cytoskeleton, as well as protocadherins which are mainly involved in neuronal plasticity (Cavallaro and Christofori, 2004; Gumbiner, 2005).

1.2.4. Selectins

Selectins are single-chain transmembrane glycoproteins which mediate the transient attachment and rolling of leukocytes along the vascular endothelial wall during inflammation. Selectins share similar properties to C-type lectins

due to the presence of an N-terminal Ca^{2+}-dependent lectin domain in the extracellular region which binds sugar moieties. The extracellular region also contains an epidermal growth factor-like domain and two to nine short consensus repeat units. There are three main types of selectins: P-selectin, which is stored within endothelial cells and platelets and is translocated to the cell surface within minutes of an inflammatory response to initiate leukocyte recruitment to the site of injury; E-selectin, which is expressed on endothelial cells in response to inflammatory cytokines and serves to augment leukocyte recruitment to the site of injury together with P-selectin; and L-selectin, which is expressed on the surface of leukocytes and acts as a homing receptor for lymphocytes to enter the peripheral lymph nodes via high endothelial venules (Barthel et al., 2007; Tedder et al., 1995).

1.2.5. Signal transduction of cell adhesion molecules

While initial studies on CAMs focused on their structural functions in mediating adhesion, later research showed that CAMs themselves can act as receptors which directly modulate signal transduction by interacting with the downstream components of major cellular signalling pathways (Gumbiner, 1996). The signalling through CAMs can be adhesion-dependent or adhesion-independent. Adhesion-independent signalling is mediated by the direct or indirect interaction of CAMs with growth factor receptors or other signalling proteins (Cavallaro and Dejana, 2011). For example, VE-cadherin has been shown to interact with vascular endothelial growth factor receptor 2 (VEGFR2) and prevent activation of the mitogen-activated protein kinase (MAPK) pathway, thus inhibiting cell proliferation (Lampugnani et al., 2006).

Furthermore, CAMs can undergo cleavage of their extracellular domains by proteases such as matrix metalloproteinases (MMPs) and members of the ADAM (A Disintegrin And Metalloproteinase) family, thus losing their adhesive properties. However, the soluble extracellular domain that is shed may still be able to interact with its signalling partners and regulate downstream signalling pathways (Cavallaro and Dejana, 2011; van Kilsdonk et al., 2010). For example, the ectodomain of L1 is cleaved by ADAM10, and the soluble L1 ectodomain shed can bind to the integrin $\alpha v\beta 5$, thus facilitating the migration of cells on the ECM substrates fibronectin or laminin. As L1 is expressed in several human carcinomas, such a mechanism is proposed to contribute to metastasis (Mechtersheimer et al., 2001).

There is also an emerging view that the cytoplasmic domains of CAMs can support signal transduction in the absence of their extracellular domains. Cleavage of the extracellular domain of CAMs such as cadherins and Ig-CAMs is frequently accompanied by the release of the cytoplasmic domain into the cytosol. Although the biological functions of the resulting cytoplasmic fragments are not completely understood, there is some evidence that they may mediate signalling responses, as well as translocate to the nucleus and regulate gene transcription (Cavallaro and Dejana, 2011). For example, upon ectodomain shedding, L1 undergoes further intramembrane processing by presenilin/γ-secretase, resulting in the release of a soluble intracellular domain which translocates to the nucleus. The cytoplasmic fragment of L1 may regulate the transcription of genes such as $\beta 3$ integrin (Gast et al., 2008; Riedle et al., 2009).

1.3. Cell-cell adhesion

Cells make contact with other cells via four distinct junctional complexes: gap junctions, tight junctions, adherens junctions and desmosomes.

1.3.1. Gap junctions

Gap junctions are cell-cell junctions that directly connect the cytoplasm of two contacting cells. The 2-4 nm gap between two cells is bridged by a gap junction channel which facilitates the direct transfer of small molecules and ions between cells without having to pass through the intercellular space. This gap junctional intercellular communication (GJIC) enables cells to exchange small metabolites such as ATP and cAMP, second messengers such as Ca^{2+} and IP_3, as well as electrical impulses (Laird, 2006; Naus and Laird, 2010; Segretain and Falk, 2004).

Gap junctions are made up of connexins, a family of 21 structurally related transmembrane proteins in humans. Connexins have a structure consisting of cytoplasmic N- and C-termini, four transmembrane domains, two extracellular loops and a cytoplasmic loop (Figure 1). Connexins are assembled in hexamers to form a connexon (also known as a hemichannel), and two connexons combine to form a gap junction channel. Several gap junction channels aggregate together to form a mature gap junction (also known as a gap junction plaque). Different types of connexins can combine as homo- or hetero-hexamers to form a hemichannel. Furthermore, there is increasing evidence that connexin hemichannels can also function as independent entities outside of gap junctions to mediate the exchange of small molecules with the extracellular milieu (Naus and Laird, 2010; Segretain and Falk, 2004).
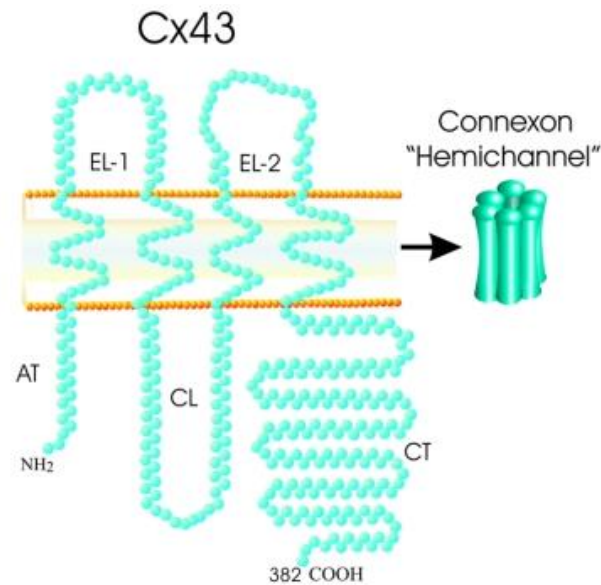
Figure 1. The structure of connexin 43, the most commonly expressed member in the connexin protein family. Connexins are four-pass transmembrane proteins with cytoplasmic N-termini (AT) and C-termini (CT), two extracellular loops (EL-1 and EL-2) and a cytoplasmic loop (CL). Six connexins oligomerise to form a connexon, also known as a hemichannel. From Laird (2006).

Most tissues of the body communicate via gap junctions. In excitable tissues such as cardiac muscles and the neural network, gap junctions are important for the transmission of electrical signals. In non-excitable tissues, gap junctions and connexins play key roles in development, tissue homeostasis, cell growth control and differentiation (Naus and Laird, 2010). The functions of connexins will be discussed in greater detail in section 1.7.

1.3.2. Tight junctions

Tight junctions, also known as occluding junctions, form a paracellular barrier to regulate the movement of solutes between epithelial or endothelial cells (Mitic and Anderson, 1998). They are also important in the establishment and maintenance of cell polarity, by restricting the lateral diffusion of lipid and protein components between a cell's apical and basolateral membrane domains (Shin et al., 2006).

Tight junctions are complex multi-protein structures, of which at least 40 different protein components have been identified. The major components of tight junctions include the transmembrane proteins: claudins, occludins, junctional adhesion molecules (JAMs), and the peripheral membrane proteins: the zona occludens (ZO) proteins ZO-1, ZO-2 and ZO-3, which are members of the membrane-associated guanylate kinase (MAGUK) family (Aijaz et al., 2006; Mitic and Anderson, 1998; Shin et al., 2006). Claudins play an important role in cell-cell adhesion, as well as in regulating tight junction selectivity based on the molecular size and ionic charge of solutes (Anderson and Van Itallie, 2009). Occludins also mediate cell-cell adhesion (Van Itallie and Anderson, 1997), but do not appear to be a critical component of tight junctions, as tight junction morphology is not affected in occludin knockout mice, although histological abnormalities were observed (Saitou et al., 2000). Occludins are linked to the actin cytoskeleton by interaction with the ZO proteins, which are scaffold proteins that mediate signal transduction with many other interacting partners. These interactions of the ZO proteins are important in tight junction assembly (Aijaz et al., 2006; Shin et al., 2006). Furthermore, ZO-1 has been reported to interact with adherens junction proteins such as α-catenin (Itoh et al., 1997), as well as multiple connexins in gap junctions and thus may function in gap junction assembly (Giepmans, 2004; Rhett et al., 2011).

1.3.3. Adherens junctions

Adherens junctions provide strong mechanical attachment between adjacent epithelial or endothelial cells and are important in the maintenance of tissue integrity. They form an interconnected lateral bridge linking the actin

cytoskeleton of neighbouring cells. The key components of adherens junctions are cadherins (discussed in section 1.2.3), which are associated with p120 and β-catenin or plakoglobin (γ-catenin) via their cytoplasmic domains. The association with β-catenin or plakoglobin in turn recruits α-catenin and links the protein complex to the actin cytoskeleton. Besides maintaining cell-cell adhesion in tissues, adherens junctions also play important roles in tissue morphogenesis and remodelling (Meng and Takeichi, 2009; Perez-Moreno et al., 2003).

1.3.4. Desmosomes

Desmosomes maintain strong adhesion between cells and are linked intracellularly to the intermediate filament network. They are important in the maintenance of tissue integrity and are particularly abundant in tissues that experience mechanical stress, such as the epidermis and myocardium. Desmosomes are composed of the desmosomal cadherins, desmocollins and desmogleins, which interact with the cytoplasmic proteins plakoglobin and plakophilins. Plakoglobin and plakophilins in turn interact with desmoplakin and link the desmosomal plaque to intermediate filaments. Desmoplakin interacts with keratin intermediate filaments in epithelial cells and desmin intermediate filaments in cardiomyocytes (Delva et al., 2009; Garrod and Chidgey, 2008).

1.4.   Cell-extracellular matrix adhesion

1.4.1.   The extracellular matrix

The ECM is a complex meshwork of extracellular molecules present in all vertebrate tissues and organs and provides structural support to surrounding cells, as well as biochemical cues for dynamic cellular processes such as growth, differentiation, tissue morphogenesis and wound healing. It is composed of proteoglycans, fibrous proteins, water and minerals. The proteoglycans found in the ECM can be classified into four main groups: hyaluronic acid, chondroitin sulfate, heparan sulfate and keratan sulfate. The major fibrous ECM proteins are collagen, elastin, fibronectin and laminin. The ECM composition varies in the types and amounts of these molecules, depending on the functional requirements of the tissue (Frantz et al., 2010). The basement membrane or basal lamina is a specialised ECM underlying all epithelial tissues and other cell types such as smooth muscle cells (LeBleu et al., 2007).

The ECM is a dynamic entity that undergoes regulated remodelling in response to changes in physiological conditions. Components of the ECM are largely produced and organised by fibroblasts. Tissue homeostasis is maintained by the controlled secretion of fibroblast MMPs which degrade ECM proteins (Mott and Werb, 2004), and is counterbalanced by tissue inhibitors of metalloproteinases (TIMPs) (Cruz-Munoz and Khokha, 2008). However, this process is often deregulated in cancer, as tumour cells secrete MMPs in order to migrate through the basement membrane during metastasis (Frantz et al., 2010).

12

Cellular adhesion to the ECM is regulated by integrins (discussed in section 1.2.2) and can be classified into three major types: focal adhesions, hemidesmosomes and dystroglycan complexes.

1.4.2. Focal adhesions

Focal adhesions are large dynamic complexes that link the ECM to the actin cytoskeleton of the cell. At these sites, integrins are linked to actin via adaptor proteins such as vinculin, paxillin, α-actinin and talin and tyrosine kinases such as Src and FAK, which regulate the assembly of focal adhesions (Zamir and Geiger, 2001).

1.4.3. Hemidesmosomes

Hemidesmosomes play a role in the adhesion of epithelial cells to the basement membrane in stratified epithelia and other complex epithelia such as the skin by connecting the ECM to intermediate filaments such as keratin. A hemidesmosomal plaque comprises the transmembrane proteins α6β4 integrin and BP180, and the cytoplasmic plaque proteins BP230 and plectin (Borradori and Sonnenberg, 1999).

1.4.4. Dystroglycan complexes

In skeletal muscles, dystroglycan complexes link the ECM protein laminin to the actin cytoskeleton, and are composed of α-dystroglycan, β-dystroglycan and the cytoplasmic plaque protein dystrophin. The genetic disease Duchenne muscular dystrophy is caused by a mutation in the dystrophin gene (Campbell, 1995).

1.5. Cell adhesion molecules and cancer

The structural and signalling functions of CAMs are essential in the regulation of diverse cellular processes including proliferation, survival, differentiation, development, migration, tissue repair, immune responses and inflammation. The abundance of CAMs throughout the human body underscores its importance in the maintenance of normal physiological activities and tissue homeostasis. As such, mutations in CAMs or the unregulated expression of CAMs are involved in the pathogenesis of many human diseases. These include cancer (Makrilia et al., 2009), neurological diseases such as Charcot-Marie-Tooth Disease (Kamiguchi et al., 1998), autoimmune diseases such as systemic lupus erythematosus and multiple sclerosis (McMurray, 1996), and cardiovascular diseases such as coronary artery disease and thrombosis (Hillis and Flapan, 1998). In this section, the roles of CAMs in tumourigenesis will be further discussed.

Tumourigenesis is a multi-step process in which the accumulation of genetic alterations and other cancer hallmarks cause the progressive transformation of normal cells into highly malignant cells (Hanahan and Weinberg, 2000, 2011). The aberrant expression of CAMs leads to alterations in cell-cell and cell-ECM adhesion and underlies several hallmarks in cancer, including invasion, metastasis and angiogenesis (Cavallaro and Christofori, 2004; Hanahan and Weinberg, 2011; Makrilia et al., 2009). The following sections will discuss a few examples of CAMs that are involved in these cancer hallmarks.

1.5.1. Roles of cell adhesion molecules in the control of cell proliferation, survival and death

Normal cells move from a quiescent state to a proliferative state in response to growth-promoting signals. The production and release of growth signals is carefully regulated in normal tissues, but deregulated in cancer cells, enabling them to be self-sufficient in their growth signals. Cancer cells also acquire the ability to evade growth suppression mechanisms and resist cell death (Hanahan and Weinberg, 2011). Integrins have been shown to play significant roles in the transformation of cells through their ability to promote proliferation and inhibit apoptosis (Desgrosellier and Cheresh, 2010; Guo and Giancotti, 2004; Makrilia et al., 2009). For example, β4 integrin has been shown to promote tumour progression by amplifying HER2 signalling, which in turn promotes proliferation and invasion by activation of the transcription factors c-Jun and STAT3 (Guo et al., 2006). Integrin signalling via FAK and ILK has also been shown to be upregulated in cancer, thus promoting cell survival and resistance to apoptosis (Guo and Giancotti, 2004; Hannigan et al., 2005). The loss of FAK or ILK activity has been shown to promote anoikis, a form of apoptosis resulting from the loss of attachment to the ECM (Attwell et al., 2000; Duxbury et al., 2004).

1.5.2. Roles of cell adhesion molecules in invasion and metastasis

Alterations in CAMs lead to the progression of low-grade benign tumours to malignancies of higher pathological grades, as characterised by local invasion and distant metastasis. CAMs favouring cytostasis are frequently downregulated, and this allows cells to proliferate in an uncontrolled manner, as well as to detach and escape from the primary tumour. By inhibiting cell

proliferation and migration, these CAMs are conventionally regarded to have tumour suppressor functions. A classical example of such a tumour suppressor CAM is E-cadherin, which is commonly lost in cancers of epithelial origin. E-cadherin is required for the maintenance of adherens junctions with adjacent epithelial cells, and its downregulation leads to the loss of cell polarity and a more invasive phenotype. The loss of E-cadherin-mediated cell-cell adhesion is a rate-limiting step in the progression from adenoma to carcinoma, and an inverse correlation has been observed between E-cadherin levels, tumour grade and mortality rates. Re-expression of E-cadherin in cancer cells causes reversion from an invasive to a benign, epithelial phenotype (Cavallaro and Christofori, 2004; Christofori and Semb, 1999; Hanahan and Weinberg, 2011).

On the other hand, CAMs associated with cell migration are often upregulated in invasive carcinomas (Hanahan and Weinberg, 2011). For example, there is increasing evidence that the loss of E-cadherin in cancers is accompanied by the *de novo* expression of mesenchymal cadherins such as N-cadherin. This cadherin switch during epithelial-mesenchymal transition (EMT) increases the invasiveness of tumour cells and enables interaction with endothelial and stromal cells, promoting intravasation and metastasis (Cavallaro and Christofori, 2004). It has also been reported that Ig-CAMs such as ALCAM, L1 and NCAM are upregulated in metastatic cancers, allowing groups of cancer cells to retain some cell-cell adhesion as they disseminate from the primary tumour and migrate as a unit to distant sites (Wong et al., 2012).

1.5.3. Roles of cell adhesion molecules in angiogenesis

Angiogenesis is an essential step in cancer progression, as tumours are unable to grow beyond a limited size unless there is a growth of new blood vessels within the tumour. Tumour-associated vasculature not only provides nutrients and oxygen to the rapidly proliferating cancer cells, but also enables them to gain access to the blood circulation during metastasis. It also enables leukocytes to infiltrate the tumour stroma and secrete tumour-promoting chemokines and cytokines (Guo and Giancotti, 2004; Hanahan and Weinberg, 2011). The expression of CAMs such as integrins has been shown to be upregulated by vascular endothelial growth factor (VEGF) in tumour angiogenesis (Desgrosellier and Cheresh, 2010; Guo and Giancotti, 2004). For example, the integrin αvβ3 is not normally expressed in quiescent endothelium, but is expressed in angiogenic endothelial cells in tumours. The expression of αvβ3 in endothelial cells may facilitate their adhesion to matrix proteins deposited in the tumour microenvironment, such as fibronectin, fibrinogen and von Willebrand factor. This integrin-mediated adhesion may provide survival cues to and promote the migration of invading endothelial cells (Brooks et al., 1994; Desgrosellier and Cheresh, 2010). VEGF secretion also leads to the upregulation of Ig-CAMs such as ICAM-1, VCAM-1 and PECAM-1 in endothelial cells, facilitating their migration (Wong et al., 2012).

**1.6.	The *HEPACAM* gene**

**1.6.1.	Identification of *HEPACAM* as a gene suppressed in human hepatocellular carcinoma**

HEPACAM was first identified in 2005 as a gene encoding a novel Ig-CAM frequently downregulated in hepatocellular carcinoma (HCC) (Moh et al., 2005a). Its identification was derived from sequence analysis of another gene, *HEPN1*. The novel transcript *HEPN1* was identified by suppression subtractive hybridisation in a study by Moh et al. (2003) to examine genes associated with HCC. *HEPN1* was significantly downregulated in 22 out of 23 HCC patients and in HCC cell lines. Expression of *HEPN1* in HepG2 cells resulted in reduced cell viability and induced apoptosis.

In a subsequent study by Moh et al. (2005a), an updated BLAST search with the *HEPN1* sequence revealed an uncharacterised and incomplete mRNA sequence containing the entire antisense strand of *HEPN1* in its 3' UTR. Using the technique of rapid amplification of cDNA ends (RACE), the full-length sequence was identified from a human normal liver cDNA library and later designated as a new gene, *HEPACAM*. The gene *HEPACAM* maps to human chromosome 11q24 and contains 7 exons (Figure 2).
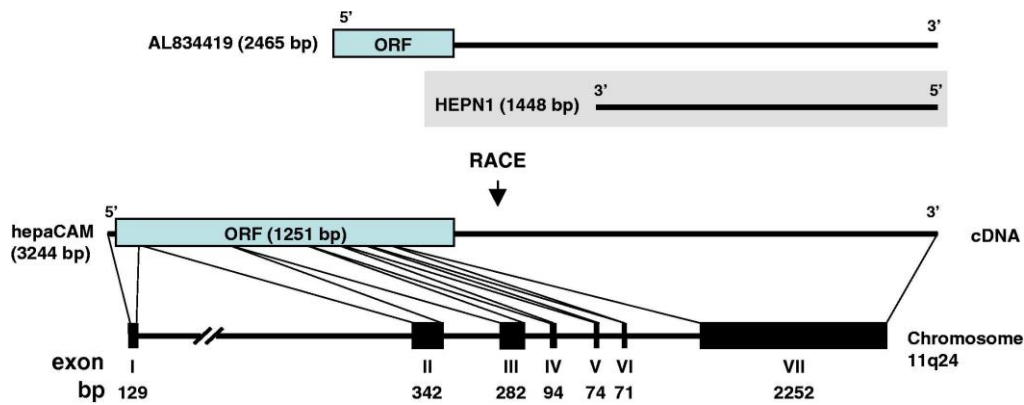
Figure 2. Molecular cloning of *HEPACAM*. An uncharacterised and incomplete mRNA sequence of 2465 bp (GenBank accession number: AL834419) was retrieved from a BLAST search using the *HEPN1* sequence. This sequence contained the entire antisense strand of *HEPN1* in its 3'-UTR and had an incomplete ORF. The full-length cDNA sequence was subsequently isolated from a human normal liver cDNA library by RACE and later designated as *HEPACAM*. The gene *HEPACAM* maps to human chromosome 11q24 and contains 7 exons. Adapted from Moh et al. (2005a).

1.6.2. Sequence analysis and structure of the human hepaCAM protein

Based on sequence analysis, *HEPACAM* was predicted to encode a novel type I transmembrane protein of 416 amino acids. The hepaCAM protein displays the typical structure of an Ig-CAM and consists of a signal peptide (residues 1-33), an extracellular region (residues 34-240), a transmembrane segment (residues 241-261) and a cytoplasmic tail (residues 262-416) (Figure 3). The extracellular region of hepaCAM comprises two Ig-like domains: a V-set domain and a C2-set domain containing a disulfide bond formed between two cysteine residues (Moh et al., 2005a).
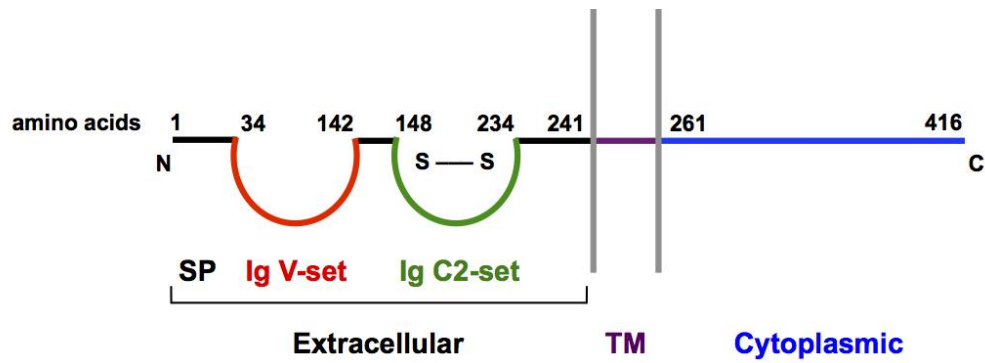
Figure 3. Illustration of the secondary structure of hepaCAM protein. Sequence annotation from UniProtKB/Swiss-Prot (accession number: Q14CZ8). hepaCAM consists of a signal peptide (SP), an extracellular region containing two Ig-like domains (one V-set and one C2-set), a transmembrane (TM) segment and a cytoplasmic tail.

hepaCAM shares structural similarities with JAMs, endothelial cell-selective adhesion molecule (ESAM) and coxsackie and adenovirus receptor (CAR), which also contain two Ig-like folds (one V-set and one C2-set) in their extracellular domains (Moh et al., 2005a).

The presence of N-glycosylation sites in the hepaCAM extracellular domain was predicted by sequence analysis and verified experimentally. A shift in the molecular weight of hepaCAM was observed upon enzymatic digestion with peptide-N-glycosidase F (PNGase F), which cleaves N-linked glycans. This confirmed that hepaCAM is a glycoprotein (Moh et al., 2005a; Moh et al., 2005b). In a later study by Gaudry et al. (2008), the hepaCAM extracellular domain was further shown to be highly glycosylated in two mammalian expression systems, HEK and CHO cells, but with significant differences in their glycosylation patterns. As glycosylation can influence the activity of proteins, hepaCAM expressed in different cell lines may have different glycosylation modifications leading to different properties (Gaudry et al., 2008).

Sequence analysis also predicted the presence of multiple potential serine, threonine and tyrosine phosphorylation sites in the hepaCAM cytoplasmic domain. Moh et al. (2005b) generated a polyclonal antiserum to recognise the hepaCAM cytoplasmic domain by immunising rabbits with recombinant bacterial fusion protein containing residues 260-416 of hepaCAM. However, the rabbit antiserum failed to detect exogenous and endogenous hepaCAM, leading the authors to suspect the presence of post-translational modifications in the cytoplasmic domain. Upon treatment of the cell lysates with calf intestinal alkaline phosphatase, dephosphorylated hepaCAM could be detected with the antiserum, confirming that the hepaCAM cytoplasmic domain is phosphorylated (Moh et al., 2005b).

Furthermore, sequence analysis predicted two potential class III PDZ domain-binding motifs in the cytoplasmic domain of hepaCAM (Moh et al., 2005a), as well as putative binding sites for SH3 domains in its proline-rich region (Moh et al., 2005b). However, the presence of these motifs in the hepaCAM cytoplasmic domain has yet to be verified experimentally.

1.6.3. Homology of the human hepaCAM protein

The hepaCAM protein is highly conserved from humans to other organisms including mice, rats (Favre-Kontula et al., 2008) and zebrafish (Sirisi et al., 2014). The human hepaCAM protein is 94% identical to the mouse protein and 89% identical to the predicted rat protein (Figure 4). Within the extracellular domain of the hepaCAM protein, the conservation between the human amino acid sequence and that of the mouse or the rat is even higher at 99%.
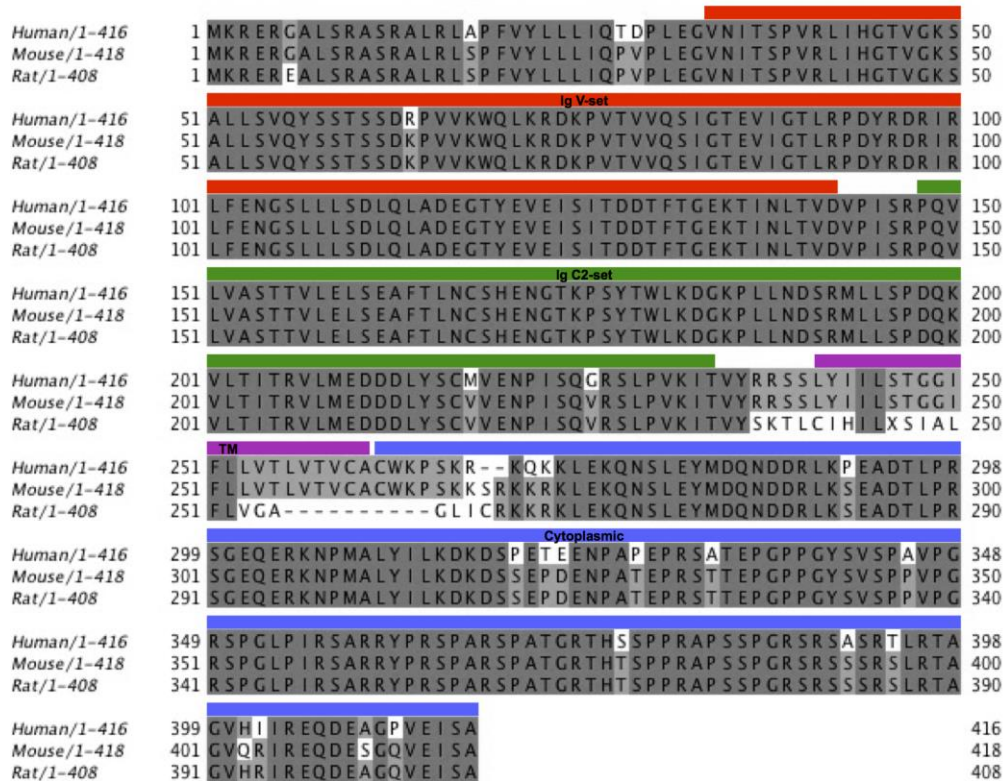
Figure 4. Homology of the human hepaCAM protein to the mouse and rat hepaCAM proteins. Multiple sequence alignment of hepaCAM protein sequences from human (RefSeq: NP_689935.2), mouse (*Mus musculus*; RefSeq: NP_780398.2) and rat (*Rattus norvegicus*, predicted; RefSeq: XP_002729937.2) was computed with Clustal Omega (EMBL-EBI) and visualised with Jalview. Dark grey boxes indicate amino acids conserved in all three species, while light grey boxes indicate those conserved in two of the three species. The Ig-like domains V-set and C2-set are indicated in red and green respectively. The transmembrane (TM) segment is indicated in purple, while the cytoplasmic domain is indicated in blue.

1.6.4. Suppression of hepaCAM in human cancers

The gene *HEPACAM* was initially identified as being frequently downregulated in human HCC. Semi-quantitative RT-PCR showed that *HEPACAM* expression was reduced in 20 out of 23 paired liver tissues of HCC patients, and was not detected in five HCC cell lines. Western blot analysis confirmed the expression of hepaCAM in normal liver tissues, but not in the HCC cell line HepG2 (Moh et al., 2005a).

In a subsequent study using the technique of dot blot analysis with a matched tumour/normal expression array, the *HEPACAM* transcript was detected in various normal human tissues including breast, colon, kidney, liver and lung but was significantly downregulated in tumours of the breast, colon, kidney, rectum, stomach and uterus. In addition, *HEPACAM* mRNA was not detected in 11 human cancer cell lines including the breast cancer cell line MCF7 and the colon cancer cell lines HCT116, HT29 and Colo205. These data indicated that hepaCAM expression is suppressed in diverse human cancers (Moh et al., 2008).

1.6.5. Dimerisation of hepaCAM

Cross-linking experiments in MCF7 cells demonstrated that hepaCAM forms homodimers on the cell surface through *cis* interactions rather than *trans* interactions. Additionally, a deletion mutant of hepaCAM lacking the cytoplasmic domain was able to form dimers, indicating that dimerisation is independent of the cytoplasmic domain (Moh et al., 2005b).

1.6.6. Subcellular localisation of hepaCAM

The subcellular localisation of hepaCAM is dependent on the cell density of HepG2 and MCF7 cells (Moh et al., 2005a; Moh et al., 2005b). In well spread cells, hepaCAM was localised to punctuate structures in the cytoplasm and cell surface protrusions that were about to make contacts with adjacent cells. In confluent cell cultures, hepaCAM was predominantly localised on the plasma membrane at cell-cell contacts (Moh et al., 2005b).

1.6.7. Functional characterisation of hepaCAM in cancer

1.6.7.1. Effects on cell growth and differentiation

hepaCAM exerts an inhibitory effect on cell growth in cancer cell lines. Exogenous expression of hepaCAM in hepaCAM-negative cell lines HepG2, MCF7 and U373 MG (glioblastoma astrocytoma) was demonstrated to inhibit proliferation and colony formation (Lee et al., 2009; Moh et al., 2005a; Moh et al., 2008). Furthermore, hepaCAM expression in MCF7 cells caused cell cycle arrest in the G2/M phase and induced cellular senescence as defined by their flat enlarged morphology and increased β-galactosidase activity. This hepaCAM-induced senescence in MCF7 cells was shown to be dependent on the p53/p21 pathway, as hepaCAM expression led to increased p53, p21 and p27 protein levels and reduced cyclin B1 and cdc2 levels. No significant effects of hepaCAM expression were observed on cdk4, cyclin D1 and cyclin E levels in MCF7 cells (Moh et al., 2008).

In U373 MG cells, the inhibition of proliferation upon hepaCAM expression was also associated with an increase in p21 levels and decrease in cyclin B1 and D1 levels, although no significant changes in cell cycle progression were observed. Interestingly, hepaCAM expression in U373 MG cells also significantly increased the expression of glial fibrillary acid protein (GFAP), a marker of astrocyte differentiation, and appeared to induce morphological changes that were characteristic of astrocytoma differentiation, i.e. from a polygonal morphology to a spindle-shaped morphology with long thin processes. The degree of differentiation was dependent on the levels of hepaCAM. The findings taken together, suggested that hepaCAM is able to induce differentiation of U373 MG cells (Lee et al., 2009).

In a study by another lab, the mechanism of hepaCAM-mediated tumour suppression was investigated in renal cell carcinoma. Consistent with previous findings in HepG2 and MCF7 cells, exogenous expression of hepaCAM in the renal cell carcinoma cell line 786-0 inhibited cell proliferation. It also caused arrest at the G1 phase of the cell cycle, with a concomitant downregulation of c-Myc at the post-transcriptional level. Expression of the c-Myc target gene and cell cycle protein, p21, was increased, while that of another target gene, cyclin D1, was decreased. Subsequent experiments demonstrated that hepaCAM expression reduced c-Myc protein stability, which could be rescued by treating cells with the proteasomal inhibitor MG132. Additionally, hepaCAM expression increased phosphorylation of c-Myc on T58, a signal for its ubiquitination. The authors thus concluded that hepaCAM expression induces ubiquitin-mediated c-Myc degradation in 786-0 cells, leading to G1 arrest caused by upregulation of p21 and downregulation of cyclin D1 (Zhang et al., 2011).

hepaCAM mRNA and protein expression was also shown to be downregulated in bladder transitional cell carcinoma, compared to adjacent normal tissues (Wang et al., 2013; Xu et al., 2012). Overexpression of hepaCAM in bladder cancer cell lines inhibited proliferation and this was correlated with a decrease in the levels of c-Myc, cyclin D1 and phosphorylated mTOR, and an increase in the levels of phosphorylated AMPK. The authors thus suggested that hepaCAM may regulate cell proliferation via the AMPK/mTOR pathway (Wang et al., 2013).

It should be noted however that while the studies by Moh et al. (2008), Zhang et al. (2011) and Wang et al. (2013) suggested pathways in which hepaCAM inhibits the proliferation of cancer cells, the experimental evidence only showed a correlation of hepaCAM expression with changes in the protein levels of the pathway mediators. No direct evidence has been provided to show that hepaCAM is upstream of or directly influences the signalling activities of these pathway proteins.

1.6.7.2. Effects on cell-ECM interaction

In the initial characterisation of hepaCAM, the adhesive properties of hepaCAM were verified by cell aggregation and spreading assays in HepG2 cells. Although hepaCAM did not influence cell-cell adhesion, it significantly augmented cell-ECM adhesion (Moh et al., 2005a). Expression of hepaCAM increased cell adhesion and spreading on the ECM component fibronectin in HepG2, MCF7 and U373 MG cells (Lee et al., 2009; Moh et al., 2005a; Moh et al., 2005b), and delayed cell detachment in MCF7 cells (Moh et al., 2005b). Furthermore, wound healing assays showed that hepaCAM increased cell motility in HepG2 and MCF7 cells (Moh et al., 2005a; Moh et al., 2005b). Expression of hepaCAM also increased the invasiveness of HepG2 cells as shown by the transwell Matrigel invasion assay (Moh et al., 2005a), although this was not observed in MCF7 cells due to their poorly invasive nature (Moh et al., 2005b). Intriguingly, in U373 MG cells, hepaCAM expression inhibited cell motility and invasion, indicating that hepaCAM may signal differently in different cell types (Lee et al., 2009), possibly due to different protein interactions or post-translational modifications.

1.6.7.3. Effects on vascular endothelial growth factor expression

Semi-quantitative RT-PCR showed that compared to adjacent normal tissues, *HEPACAM* mRNA expression was reduced in urothelial carcinoma tissues, and this was correlated with a significant increase in VEGF mRNA expression. *In vitro* experiments in 786-0 cells and the bladder carcinoma cell line T24 demonstrated that transfection of the *HEPACAM* gene was correlated with a significant decrease in VEGF protein levels (Yang et al., 2010; Zhang et al., 2013). In a subsequent study, human umbilical vein endothelial cells (HUVECs) treated with 786-0 cell-derived exosomes showed increased tube formation, which was correlated with increased VEGF expression in HUVECs and reduced hepaCAM expression (Zhang et al., 2013).

1.6.7.4. hepaCAM as a putative tumour suppressor

In summary, the frequent loss of *HEPACAM* in human HCC and the anti-proliferative effects of hepaCAM fulfil two important criteria as a tumour suppressor, as suggested by Moh et al. (2005a). Subsequent studies (Moh et al., 2008) also showed that hepaCAM expression is downregulated in diverse human cancers, further supporting that hepaCAM is a putative tumour suppressor.

1.6.8. The cytoplasmic domain of hepaCAM and its proteolytic cleavage

As mentioned in section 1.6.2, the cytoplasmic domain of hepaCAM is phosphorylated, suggesting that it may play a role in signalling cascades regulating cell adhesion and migration. To examine the importance of the cytoplasmic domain in the biological functions of hepaCAM, Moh et al. (2005b) constructed hCAM-tailless, a deletion mutant of hepaCAM lacking

the cytoplasmic domain (residues 264-416). MCF7 cells expressing hCAM-tailless displayed rates of wound healing comparable to mock-transfected cells, indicating that the hepaCAM cytoplasmic domain is essential for the functions of hepaCAM in cell motility. Deletion of the hepaCAM cytoplasmic domain also resulted in reduced cell adhesion to fibronectin, suggesting that the hepaCAM cytoplasmic domain is also important in mediating cell adhesion (Moh et al., 2009b; Moh et al., 2005b).

Moh et al. (2008) also showed that deletion of the cytoplasmic domain inhibited the tumour suppressor functions of hepaCAM. While expression of wild-type hepaCAM strongly inhibited proliferation and colony formation in MCF7 cells, expression of hCAM-tailless only resulted in a moderate inhibition. Unlike wild-type hepaCAM, the hCAM-tailless mutant also failed to cause cell cycle arrest in the G2/M phase and induce cellular senescence via the p53/p21 pathway. This suggests that growth inhibition and cell cycle regulation by hepaCAM are mediated by its cytoplasmic domain (Moh et al., 2008).

A later study by Zhang et al. (2010a) showed that hepaCAM undergoes proteolytic cleavage when exogenously expressed in MCF7 cells, generating a 25 kD fragment that consists mainly the cytoplasmic domain. To identify the molecular mechanisms of hepaCAM cleavage, the authors studied several signalling pathways known in regulating the cleavage of CAMs. Treatment with the phorbol ester PMA did not affect hepaCAM cleavage, while calcium influx promoted hepaCAM cleavage independent of the protein kinase C (PKC) pathway. On the other hand, treatment with the proteasome inhibitor

MG132, as well as with inhibitors of the cysteine proteases calpain-1 and cathepsin-B reduced hepaCAM cleavage. This suggested the possible involvement of the proteasome, calpain-1 and cathepsin-B in proteolytic cleavage of the hepaCAM cytoplasmic domain, and it is speculated that this may serve a regulatory role in the functions of hepaCAM in response to various cellular signals (Zhang et al., 2010a).

1.6.9. Identification of *HEPACAM* in the nervous system

HEPACAM was also identified and cloned in independent studies by other labs. In a study by Spiegel et al. (2006) to identify novel molecules expressed in peripheral myelinated nerves, *HEPACAM* was identified in cDNA libraries prepared from primary rat Schwann cells and rat sciatic nerves. Separately, using a structure-based genome-mining approach targeting VEGF and platelet derived growth factor (PDGF) Ig-like folds, Favre-Kontula et al. (2008) identified a sequence corresponding to a single-pass transmembrane protein containing two Ig-like domains. This sequence was cloned by exon assembly from a human brain genomic library and found to be identical to *HEPACAM*.

1.6.10. Role of *HEPACAM* in the nervous system

In addition to its function as a tumour suppressor gene in HCC and other human cancers, *HEPACAM* plays important roles in the central nervous system (CNS). In the study by Favre-Kontula et al. (2008), the hepaCAM protein was observed to be highly expressed in the human and mouse CNS, and was thus also named as GlialCAM. Its expression was upregulated during postnatal mouse brain development, in a coordinate manner with myelin basic protein. hepaCAM was also expressed in primary rat oligodendrocytes at

various stages of differentiation, where they could be detected in the cell body and cell processes, suggesting a potential role of hepaCAM in myelination and oligodendrocyte biology. Furthermore, hepaCAM expression was observed in primary rat astrocytes at the tip of cell processes in low-density cultures, and at cell-cell contact sites in confluent cultures, suggesting a role of hepaCAM in astrocyte-astrocyte interactions (Favre-Kontula et al., 2008).

1.6.11. Role of *HEPACAM* in the disease megalencephalic leukoencephalopathy with subcortical cysts

HEPACAM is the second gene involved in the hereditary disease megalencephalic leukoencephalopathy with subcortical cysts (MLC). MLC is a rare type of leukodystrophy and the classical phenotype is characterised by infantile-onset macrocephaly and delayed-onset neurological deterioration. Recessive mutations in the gene *MLC1* are observed in 75% of MLC patients. In identifying another MLC-related gene, hepaCAM was found to be a direct interacting partner of MLC1, a membrane protein with putative roles in ion transport. Subsequent genetic analysis of patients without *MLC1* mutations revealed that a large proportion had mutations in *HEPACAM* instead. Several different *HEPACAM* mutations were identified, and these mutations could be dominant or recessive (Lopez-Hernandez et al., 2011a). Mutations in *HEPACAM* and *MLC1* are believed to prevent proper ion and water homoeostasis of the brain, thus leading to a defect in brain volume regulation and chronic white matter oedema (van der Knaap et al., 2012).

Further molecular studies showed that hepaCAM interacts and co-localises with MLC1 in cell-cell junctions between astrocytes. Expression of hepaCAM

mutations in astrocytes and HeLa cells resulted in a diffused intracellular localisation of both hepaCAM and MLC1 with some enrichment in plasma membranes but not specifically at cell-cell junctions. This suggested that hepaCAM is required for the proper targeting of MLC1 to cell-cell junctions, and mutations in hepaCAM cause a mislocalisation of both molecules (Lopez-Hernandez et al., 2011a; Lopez-Hernandez et al., 2011b). These cell-cell junctions in which MLC1 was localised to were shown in another study to contain components typically found in tight junctions (occludin and ZO-1), adherens junctions (β-catenin) and gap junctions (connexin 43) (Duarri et al., 2011).

A later study identified hepaCAM as a binding partner of the chloride channel ClC-2 and showed that the two proteins co-localised in cell-cell junctions between astrocytes. hepaCAM also targets ClC-2 to these junctions and modifies ClC-2-mediated currents *in vitro* (Hoegg-Beiler et al., 2014; Jeworutzki et al., 2012).

1.6.12. Interactions of hepaCAM with other proteins

1.6.12.1.   Actin

hepaCAM has been shown to associate with the actin cytoskeleton. hepaCAM co-localised with F-actin predominantly at the cell-cell contacts of MCF7 cells, and the subcellular localisation of hepaCAM was dependent on the integrity of the actin cytoskeleton. A direct interaction between hepaCAM and F-actin was verified by co-immunoprecipitation and co-sedimentation assays. Deletion of the first or second Ig-like domains or the cytoplasmic domain of hepaCAM resulted in a loss of interaction, indicating that an intact hepaCAM

is required for its stable interaction with the actin cytoskeleton. This interaction is suggested to be important for the functions of hepaCAM in mediating cell adhesion and migration (Moh et al., 2009b).

1.6.12.2.   Caveolin-1

hepaCAM also associates with caveolin-1, a principal structural component of caveolae which are plasma membrane invaginations and a specialised type of lipid rafts. hepaCAM was shown to co-localise with caveolin-1 in the nucleus and punctuate structures in the cytoplasm. The two proteins could be co-immunoprecipitated and the association was shown to be dependent on the first Ig-like domain of hepaCAM. Since caveolae and caveolin-1 are involved in endocytosis and signal transduction, it is suggested that the association of hepaCAM with caveolin-1 may play a role in the signalling processes of hepaCAM. Furthermore, as caveolin-1 is downregulated in several cancers and has also been proposed to function as a tumour suppressor, its association with hepaCAM may contribute to the tumour suppressive activities of hepaCAM (Moh et al., 2009a).

1.7.   Connexin 43 and other connexins

As discussed in section 1.3.1, connexins are the major components of gap junctions. In this section, the synthesis and turnover of connexins, as well as the functions of connexins in tumourigenesis will be discussed further with an emphasis on connexin 43, which is of particular interest to this project.

Connexins are named according to their molecular weights. Connexin 43, encoded by the gene *GJA1* with a molecular weight of 43 kD, is the most ubiquitously expressed of the 21 human connexins. Found in almost all organ

systems, it is expressed in a broad spectrum of cell types including astrocytes, cardiomyocytes, keratinocytes and smooth muscle cells (Laird, 2006). Due to the diverse expression pattern of connexin 43, alterations in connexin 43 gap junction communication are associated with many pathologies including ischemic heart disease (Smith et al., 1991), the pleiotropic development disorder oculodentodigital dysplasia (Paznekas et al., 2003) and cancer (Cronier et al., 2009; Mesnil et al., 2005; Naus and Laird, 2010).

1.7.1. The life cycle of connexins

Similar to other transmembrane proteins, connexins are synthesised by endoplasmic reticulum (ER)-bound ribosomes and inserted co-translationally into the ER membrane. Oligomerisation of connexins into connexons occurs during their transport between the ER and the trans-Golgi network. Upon the completion of oligomerisation, connexons are packaged into vesicles and trafficked to the plasma membrane, where they can dock with connexons on adjacent cells to form gap junction channels which coalesce with other channels to form a gap junction plaque. Alternatively, connexons may remain undocked and function as hemichannels (Laird, 2006; Segretain and Falk, 2004).

Connexin proteins have a short half-life of only a few hours, which is surprisingly short for a structural membrane protein. Gap junction turnover has been widely shown to occur within several hours of their delivery to the cell surface, and involves the internalisation of gap junctions into annular junctions (also known as connexosomes). These gap junction complexes are subsequently disassembled and individual connexin proteins are targeted for

degradation in lysosomes, or an alternative pathway involving the proteasome (Berthoud et al., 2004; Laird, 2006; Segretain and Falk, 2004). The synthesis and degradation of connexins, in particular connexin 43, is summarised in Figure 5 below.
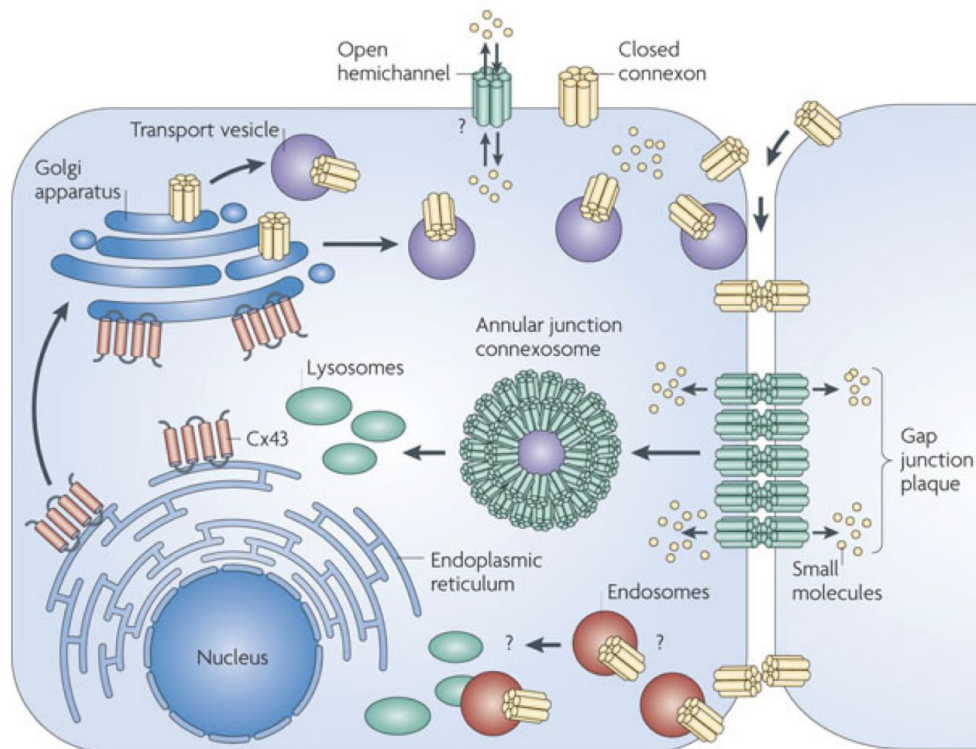
Figure 5. An overview of the life cycle of connexin 43. Connexin 43 undergoes a continuous renewal process in cells. From Naus and Laird (2010).

Though not well-understood, the continuous synthesis and turnover of connexins is believed to be another mechanism to regulate GJIC, in addition to the opening and closing of gap junction channels. This may facilitate the rapid up- or down-regulation of gap junction activity based on the physiological requirements of cells (Segretain and Falk, 2004).

1.7.2. Post-translational modification of connexins

Connexins undergo different types of post-translational modifications, including phosphorylation, hydroxylation, acetylation and palmitoylation. These modifications can regulate the functions of connexins in and outside of gap junctions, as well as the assembly and turnover of gap junctions. The most studied of these post-translational modifications is phosphorylation, which can occur on various residues on the cytoplasmic loop or C-terminal domain of connexins. Phosphorylation of connexins by kinases such as Src, PKC and MAPKs has been observed in at least nine connexins, including connexin 43. In the case of connexin 43, phosphorylation on different residues can either enhance or inhibit GJIC, as well as influence its functions independent of gap junctions (Dbouk et al., 2009; Solan and Lampe, 2009).

1.7.3. Role of connexins in tumourigenesis

1.7.3.1. Connexins as tumour suppressors

The role of gap junctions and connexins in tumorigenesis was first suggested by Loewenstein and Kanno (1966), when a lack of electrical coupling was observed in rat hepatomas. Since then, there has been a multitude of studies exploring the link between connexins and cancer. Firstly, it was observed that gap junctions and connexins are frequently downregulated or completely lost in human or rodent solid tumours, as well as in cell lines derived from various tumour types (Huang et al., 1998; Laird et al., 1999; Mesnil et al., 2005; Tsai et al., 1996). In several studies, an aberrant localisation of connexins in transformed cells has also been reported *in vivo* and *in vitro*, instead of a downregulation in connexin expression. While connexins are usually localised on the plasma membrane at cell-cell contacts, a cytoplasmic localisation of

connexins has been observed in transformed cells (Mesnil et al., 2005), including glioblastoma cells (Cottin et al., 2008; Cottin et al., 2011).

Secondly, the re-introduction of connexin expression in transformed cells inhibits cell proliferation and tumour growth (Eghbali et al., 1991; Huang et al., 1998). Connexin overexpression also causes partial re-differentiation of transformed cells and inhibits angiogenic processes (Hirschi et al., 1996; McLachlan et al., 2006).

Thirdly, the involvement of connexins in tumour suppression is also supported by studies involving the knockdown or knockout of connexins. Silencing of connexins has been reported to promote tumour cell growth and migration (Shao et al., 2005). In studies using connexin knockout (King and Lampe, 2004a, b; Temme et al., 1997) and heterozygous mice (Avanzo et al., 2004), as well as transgenic mice expressing dominant-negative mutants of connexins (Dagli et al., 2004), an increase in tumour incidence was observed upon exposure of the mice to carcinogens. The experimental evidence thus pointed to a role for the loss of connexin expression in tumourigenesis.

The tumour suppressive properties of connexins have been proposed to be GJIC-dependent, as well as GJIC-independent by interaction with other tumour suppressor molecules (reviewed in Cronier et al., 2009; Mesnil et al., 2005; Naus and Laird, 2010).

1.7.3.2. GJIC-dependent mechanisms of connexin-mediated tumour suppression

The loss of GJIC in tumourigenesis can be attributed to the loss of expression or aberrant localisation of connexins, resulting in the lack of functional gap junctions between cells. It is believed that the loss of GJIC between neighbouring cells facilitates cell dissociation in the invasive regions of the primary tumour (Mesnil et al., 2005). It has been proposed that the tumour suppressive roles of connexins are linked to GJIC-mediated homeostatic exchange of small molecules in normal healthy tissues (Naus and Laird, 2010). However, the nature of the molecules that need to be exchanged to prevent cells from transforming to a more invasive phenotype is not well-characterised. One of the molecules exchanged via GJIC is glutathione (Goldberg et al., 1999), and it has been suggested that the antioxidant properties of glutathione protect cells from reactive oxygen species, and thus DNA damage in the tumorigenic process (Naus and Laird, 2010).

The GJIC-mediated exchange of small molecules has also been explored as a mechanism of the "bystander effect" in cancer therapy. The bystander effect is a phenomenon in which the effects of a therapeutic agent are spread from the targeted cells to neighbouring non-targeted cells in a tumour mass, thereby achieving maximal killing of cancer cells (Prise and O'Sullivan, 2009). For example, a strategy that has been studied is the transfer of the toxic metabolites of the prodrug ganciclovir from targeted tumour cells to surrounding non-targeted cells via GJIC (Mesnil and Yamasaki, 2000).

1.7.3.3. GJIC-independent mechanisms of connexin-mediated tumour suppression

In addition to their roles in gap junctions and hemichannels, connexins are involved in various functions mediated by their interacting partners. These interactions lead to the modulation of gene expression in several processes including cell proliferation, cell migration and angiogenesis (Dbouk et al., 2009; Naus and Laird, 2010).

The re-introduction of connexins in cancer cell lines inhibits proliferation by regulating the expression of genes involved in the cell cycle. Overexpression of connexin 43 has been correlated with decreased expression of cyclin A, cyclin D1, cyclin D2, and various cyclin-dependent kinases (CDKs) (Chen et al., 1995). Connexin 43 also increases the levels of the CDK inhibitors p21 and p27 and inhibited cell cycle progression from G1 to S phase (Sanchez-Alvarez et al., 2006; Zhang et al., 2001).

In addition, connexin 43 has been shown to regulate the expression of molecules involved in angiogenesis. Silencing of connexin 43 downregulates the expression of the anti-angiogenic factor TSP-1 and upregulates the expression of the pro-angiogenic factor VEGF (Shao et al., 2005). In another study, connexin 43 overexpression results in decreased endothelial cell tubulogenesis and migration *in vitro*, and reduced blood vessel formation in xenoplant tumours, without re-establishing GJIC (McLachlan et al., 2006).

Connexin 43 has also been reported to interact with the tumour suppressor caveolin-1 in the lipid rafts of keratinocytes (Langlois et al., 2008), and this interaction is altered in keratinocyte transformation processes in vitro,

suggesting a role for this interaction in tumour suppression (Langlois et al., 2010). In a caveolin-1 positive keratinocyte cell line, connexin 43 knockdown leads to EMT features and increased cell invasion, while connexin 43 overexpression protects against the stimulation of cell invasion in a GJIC-independent mechanism (Langlois et al., 2010).

The interaction of connexin 43 with the matricellular protein NOV (CCN3) has also been documented as another GJIC-independent tumour suppression mechanism. Exogenous expression of connexin 43 in glioma and choriocarcinoma cells leads to an upregulation of NOV expression and a physical interaction of these two proteins is observed As NOV has been shown to inhibit cell proliferation and suppress tumourigenesis, it is suggested to be a putative downstream effector of connexin 43-mediated signalling cascades (Fu et al., 2004; Gellhaus et al., 2004; Gupta et al., 2001).

1.7.3.4. Connexins and metastasis

While the above sections have focused on the tumour suppressive roles of connexins, there is increasing evidence that connexins may instead facilitate invasion and metastasis. Connexin 43 expression has been shown to enhance the transendothelial migration or diapedesis of breast tumour cells. This suggested that the establishment of heterocellular GJIC between tumour cells and endothelial cells may be a key regulatory step during metastasis (Pollmann et al., 2005). Similarly, connexin 26 was proposed to facilitate the intravasation and extravasation of melanoma cells through heterologous gap junction formation with endothelial cells (Ito et al., 2000).

Furthermore, the formation of heterotypic gap junctions between a human breast carcinoma cell line and a human osteoblastic cell line was proposed as an explanation for the preferential metastasis of breast cancer cells to bones (Kapoor et al., 2004). Although there are limited studies on this aspect, the establishment of heterotypic GJIC between metastatic cells and cells of the colonised tissue may play an important role in metastasis (Cronier et al., 2009; Mesnil et al., 2005).

In summary, the seemingly contradictory roles of connexins in tumourigenesis may depend on the type of connexin being expressed and the cell or tumour type. Connexins may thus be better classified as conditional tumour suppressors due to their complex roles in mediating tumour suppression and progression (Mesnil et al., 2005; Naus and Laird, 2010).

1.8.   Objectives of the project

1.8.1. Current perspectives and aims of the project

hepaCAM is a novel Ig-CAM and putative tumour suppressor. Several studies (discussed in section 1.6.7.1) have shown a correlation of hepaCAM expression with changes in the protein levels of genes involved in regulating proliferation and the cell cycle. However, no direct evidence has been provided to show that hepaCAM interacts with and has a direct influence on the signalling activities of these regulatory proteins. Thus, the underlying mechanisms of hepaCAM-mediated tumour suppression are still not completely understood.

As discussed in section 1.6.11, in a separate area of research in neurobiology, hepaCAM has recently been shown to interact with MLC1, and MLC1 in turn

partially co-localises with the gap junction protein connexin 43 in astrocytic cell-cell junctions. Since connexin 43 has also been identified as a tumour suppressor protein, we hypothesise that hepaCAM may exert its tumour suppressive effects by influencing the activities of connexin 43. Thus, the first aim of this project is to characterise the interaction of hepaCAM with connexin 43 in cancer cells and understand whether this interaction contributes to hepaCAM's tumour suppressor activities.

In addition, as discussed in section 1.6.8, hepaCAM undergoes proteolytic cleavage in breast cancer cells to generate a 25 kD fragment containing mainly the cytoplasmic domain. However, the cellular signals which lead to hepaCAM cleavage and its biological significance have yet to be elucidated. As it has been proposed that the cytoplasmic domain of CAMs may support signalling in the absence of the extracellular domain (discussed in section 1.2.5), we hypothesise that proteolytic cleavage of the hepaCAM cytoplasmic domain occurs as part of its processing and signalling activities. Thus, the second aim of this project is to understand the upstream signals which lead to hepaCAM cytoplasmic domain cleavage, and investigate its functional significance in cancer cells.

1.8.2. Project approaches

To the first aim of the project, the human glioblastoma cell line U373 MG of astrocytic origin will be used. The U373 MG cell line does not endogenously express hepaCAM and our lab has established stable transfections of U373 MG cells expressing wild-type (WT) hepaCAM, as well as the empty vector as a control. In the initial stages of the project, I demonstrate that

U373 MG cells has an aberrant localisation of connexin 43 in the cytoplasm similar to previous reports in other glioblastoma cell lines, and that exogenous hepaCAM expression in U373 MG cells causes a re-localisation of connexin 43 to cell-cell junctions. To further characterise the relationship of hepaCAM with connexin 43, I will also utilise stable U373 MG cell lines established in our lab which express mutations of hepaCAM involved in the disease MLC.

In the second part of the project, the proteolytic cleavage of the hepaCAM cytoplasmic domain will be studied in U373 MG cells, the human breast adenocarcinoma cell line MCF7 and the human HCC cell line HepG2. MCF7 and HepG2 cells stably transfected with hepaCAM have been established previously and will be used in the project, along with the corresponding parental or vector-transfected cells. The stable U373 MG cells expressing WT and mutant hepaCAM will also be used in this part of the project to investigate whether mutations in hepaCAM have any effects on its proteolytic cleavage.

CHAPTER 2   MATERIALS AND METHODS

2.1.   Cell culture

2.1.1.   Cell lines and culture conditions

The human glioblastoma astrocytoma U373 MG cell line was a kind gift from Associate Professor Celestial Yap from the Department of Physiology, NUS. Cells were cultured in F-12 medium (Life Technologies, Carlsbad, CA, USA) supplemented with 10% fetal bovine serum (FBS; Biowest, Nuaille, France).

The human embryonic kidney 293 cell line containing the SV40 large T antigen (HEK293T) was a kind gift from Associate Professor Paul MacAry from the Department of Microbiology, NUS. Cells were cultured in high glucose Dulbecco's Modified Eagle Medium (DMEM; Sigma-Aldrich, St. Louis, MO, USA) supplemented with 10% FBS.

The human breast adenocarcinoma cell line MCF7 and the human hepatocellular carcinoma cell line HepG2 were cultured in high glucose DMEM supplemented with 10% FBS.

All cells were grown at 37°C in a humidified incubator supplied with 5% CO_2.

2.1.2.   Subculture of adherent cells

Cells were maintained in the log phase and passaged when they reached 80-100% confluence. The culture medium was aspirated and cells were rinsed once with phosphate-buffered saline (PBS). Cells were incubated with 1× trypsin-EDTA (Biowest) for 2-5 min at 37°C until they were detached.

Subsequently, cells were resuspended in fresh medium to inactivate trypsin and split 1:4 or to the required cell density.

2.1.3. Cryopreservation of cells

Cells were detached and spun down at $200 \times g$ for 5 min. The cell pellet was resuspended in freezing medium (consisting of culture medium with 10% FBS and 8% DMSO) to a minimum density of 1×10^6 cells/ ml. The cell suspension was transferred to a cryotube and stored at -80°C overnight, before transferring to liquid nitrogen for long term storage.

2.2. DNA constructs

The plasmids used for the transfection of U373 MG and HEK293T cells, GlialCAM-WT-3.1, GlialCAM-R92Q-3.1, GlialCAM-R92W-3.1 and the corresponding empty vector pcDNA3.1 were provided by Professor Raúl Estévez, University of Barcelona, Spain. WT hepaCAM (GlialCAM), hepaCAM-R92Q and hepaCAM-R92W were cloned into the pcDNA3.1 vector with a C-terminal 3×FLAG epitope (Lopez-Hernandez et al., 2011a).

The plasmids used for the transfection of MCF7 and HepG2 cells, hepaCAM-pcDNA6B/His and the corresponding empty vector pcDNA6B/His were provided by Dr Moh Mei Chung, NUS. hepaCAM was cloned into the pcDNA6B/V5-His vector with a C-terminal V5 epitope and poly-histidine tag (Moh et al., 2005a).

2.3.   Transformation of *Escherichia coli*

50-100 ng of plasmid DNA was mixed with 20-50 µl of competent *E. coli* DH5α cells (New England Biolabs, Ipswich, MA, USA) and incubated on ice for 30 min. The cells were then subjected to heat-shock at 42°C for 30 seconds and immediately cooled on ice for 2 min. 1 ml of Luria-Bertani (LB) broth was added to the cells and incubated at 37°C for 1 hour with shaking. After incubation, the cells were pelleted by centrifugation at 3,000 rpm for 3 min. The transformation mixtures were subsequently plated onto LB agar plates containing the appropriate antibiotic and incubated overnight at 37°C.

2.4.   Plasmid miniprep

A single *E. coli* colony was inoculated into 5 ml LB broth supplemented with the appropriate antibiotic and incubated overnight at 37°C with shaking. Plasmid DNA was purified from the *E. coli* culture using the Wizard Plus SV Minipreps DNA Purification System (Promega, Madison, WI, USA), according to the manufacturer's instructions. Using this kit based on the alkaline lysis method, the *E. coli* culture was pelleted by centrifugation at 13,000 rpm for 1 min and the pellet was resuspended completely in 250 µl Cell Resuspension Solution. Thereafter, *E. coli* cells were lysed in 250 µl Cell Lysis Solution. The lysate was incubated with 10 µl Alkaline Protease Solution for 5 min at room temperature to inactivate endonucleases and other proteins released during lysis which may affect the quality of the plasmid DNA. Subsequently, the lysate was mixed with 350 µl Neutralisation Solution and spun down at 13,000 rpm for 10 min to precipitate unwanted cellular debris containing chromosomal DNA and proteins. The cleared lysate containing the plasmid DNA was transferred to a spin column and centrifuged

at 13,000 rpm for 1 min. The immobilised DNA was washed with 750 μl and subsequently 250 μl of Column Wash Solution. Finally, the DNA was eluted with sterile nuclease-free water and the concentration was quantified using the NanoDrop spectrophotometer (Thermo Scientific, Rockford, IL, USA). The plasmid DNA was stored at -20°C until use.

2.5.   Transfection of cells

2.5.1. Stable transfection of U373 MG cells for overexpression of hepaCAM

U373 MG cells were stably transfected with pcDNA3.1, WT hepaCAM, hepaCAM-R92Q and hepaCAM-R92W by Dr Moh Mei Chung. Stable transfection of U373 MG cells was performed using Lipofectamine with PLUS reagent (Life Technologies) according to the manufacturer's instructions, and cells were selected in culture medium containing 800 μg/ml G418 (Sigma-Aldrich, St. Louis, MO, USA) for two weeks before cloning. After selection, stable clones were maintained in medium containing 100 μg/ml G418.

2.5.2. Stable transfection of MCF7 and HepG2 cells for overexpression of hepaCAM

MCF7 and HepG2 cells were stably transfected with pcDNA6B/V5-His and hepaCAM previously by Dr Moh Mei Chung (Moh et al., 2005a; Moh et al., 2005b). Stable transfection of MCF7 and HepG2 cells was performed using Lipofectamine with PLUS reagent according to the manufacturer's instructions, and stable clones were selected and maintained in medium containing 10 μg/ml blasticidin (Life Technologies).

2.5.3. Transient transfection of HEK293T cells for overexpression of hepaCAM

HEK293T cells were seeded one day before transfection such that they would be 70% confluent on the day of transfection. Cells were transfected with pcDNA3.1 and GlialCAM-WT-3.1 using Turbofect Transfection Reagent (Thermo Scientific), according to the manufacturer's instructions. For a 24-well plate, transfection complexes were prepared by mixing 1 μg of plasmid DNA with 2 μl transfection reagent in 100 μl Opti-MEM (Life Technologies) and added drop-wise to each well. Cells were incubated at 37°C in a CO_2 incubator and harvested 48 h post-transfection for western blot analysis.

2.5.4. Transient transfection of U373 MG cells for siRNA-mediated knockdown of connexin 43

U373 MG cells were seeded one day before transfection such that they would be 50% confluent on the day of transfection. Silencing of connexin 43 expression was performed using the GJA1 Trilencer-27 Human siRNA kit (OriGene, Rockville, MD, USA). Cells were transfected with 5 nM connexin 43 siRNA duplex (SR301801C) or universal scrambled siRNA duplex (SR30004) using Lipofectamine 2000 (Life Technologies), according to the manufacturer's instructions. For a 6-well plate, 4 μl Lipofectamine 2000 was diluted in 200 μl serum-free medium and incubated for 5 min. Appropriate amounts of the siRNA duplexes were diluted separately in 200 μl serum-free medium and mixed with the diluted Lipofectamine 2000. The mixture was then incubated for another 20 min to allow complex formation to occur. Thereafter, the transfection complexes were added drop-wise to each well and cells were incubated at 37°C in a CO_2 incubator. The knockdown of

connexin 43 was evaluated 48 h post-transfection by western blot analysis and immunofluorescent staining.

2.6. Preparation of whole cell extracts for western blot analysis

Cells grown as a monolayer were rinsed in PBS and scraped in radioimmunoprecipitation assay (RIPA) buffer supplemented with a protease inhibitor cocktail (1:100 dilution, Sigma-Aldrich). The cell lysate was further incubated on ice for 10 min with vortexing and centrifuged at 13,000 rpm for 10 min at 4°C to pellet the debris. The supernatant was retained and stored at -20°C or -80°C until use.

2.7. Determination of protein concentration by the Bradford assay

The concentration of protein in the cell lysates was quantified by the Bradford assay, a colorimetric protein assay based on the shift in absorbance of the Coomassie Brilliant Blue G-250 dye to 595 nm upon binding to protein. The working dye solution was prepared by diluting 1 part of the Dye Reagent Concentrate (Bio-Rad, Hercules, CA, USA) in 4 parts of deionised water. 10 μl of the protein sample diluted in PBS was mixed with 200 μl working dye solution, and the absorbance at 595 nm (A595) was measured with the Bio-Rad Model 680 microplate reader. A standard curve was also computed by measuring the A595 of bovine serum albumin (BSA; Biowest) at concentrations of 0-1 mg/ml. The concentration of protein in the samples was determined based on this standard curve.

2.8. Western blot analysis

2.8.1. SDS-polyacrylamide gel electrophoresis (SDS-PAGE)

Protein samples were resolved by SDS-PAGE using the Bio-Rad Mini-PROTEAN electrophoresis system. Equal protein amounts were mixed with an appropriate amount of 2× or 5× Laemmli sample buffer, and denatured by heating at 95°C for 5 min. The samples and a molecular weight reference, Precision Plus Protein Prestained Standards (Bio-Rad), were then loaded onto a 10% or 12% polyacrylamide gel and resolved at 150 V for 70 min in 1× SDS-PAGE running buffer (Life Technologies).

2.8.2. Protein transfer

Proteins were transferred from the polyacrylamide gel onto a PVDF membrane (Bio-Rad) using the Bio-Rad Mini Trans-Blot system. The PVDF membrane was first pre-wet with absolute ethanol until translucent. The membrane, gel, filter paper and fibre pads were then equilibrated in Towbin buffer for 15 min. The gel sandwich was assembled and proteins were transferred from the gel to the membrane at 100 V for 60 min in Towbin buffer containing 0.1% SDS. To maintain uniform conductivity and temperature during transfer, an ice pack was placed in the tank and the buffer was continuously stirred on a stir plate.

2.8.3. Antibody probing and detection

After protein transfer, the membrane was rinsed with Tris-buffered saline containing 0.1% Tween-20 (TBST), blocked with blocking buffer (5% skim milk in TBST) for 1 h at room temperature and probed with primary antibody overnight at 4°C. Table 1 lists the primary antibodies used for western blot

analysis and their dilutions in blocking buffer. Full-length hepaCAM was detected with a commercial antibody (clone 419305) raised against an immunogen derived from residues 34-242 of hepaCAM, which approximates the hepaCAM extracellular domain. Alternatively, full-length hepaCAM as well as the cleaved hepaCAM fragment containing the cytoplasmic domain could be detected with a custom-made antibody (clone 5A1F1) raised against an epitope comprising residues 357-389 in the hepaCAM cytoplasmic domain, or with HRP-conjugated antibodies against the C-terminal FLAG-tag or V5-tag on the hepaCAM cytoplasmic domain.

After incubation with primary antibody and washing three times in TBST, 5 min each, the blot was incubated with horseradish peroxidase (HRP)-conjugated secondary antibody (1:5,000 dilution in blocking buffer): goat anti-mouse IgG-HRP (Thermo Scientific, Rockford, IL, USA) or goat anti-rabbit IgG-HRP (Santa Cruz Biotechnology, Dallas, TX, USA) for 1-2 h at room temperature. The blot was then washed three times with TBST and protein bands were detected with SuperSignal West Pico or Femto Chemiluminescent Substrate (Thermo Scientific), and exposed to X-ray films (Thermo Scientific).

To re-probe with another antibody, the blot was stripped in a 15-min wash of stripping buffer and rinsed in TBST before blocking.

Table 1. List of primary antibodies used for western blot analysis.

Protein	Clonality	Clone / Catalog Number	Source	Dilution
hepaCAM (extracellular domain)	Mouse monoclonal	419305	R&D Systems, Minneapolis, MN, USA	1:500
hepaCAM (cytoplasmic domain)	Mouse monoclonal	5A1F1 (custom-made; hybridoma culture supernatant)	GenScript, Piscataway, NJ, USA	1:500
Connexin 43	Rabbit polyclonal	3512	Cell Signaling Technology, Danvers, MA, USA	1:2,000
FLAG-HRP	Mouse monoclonal	5A8E5	GenScript	1:5,000
V5-HRP	Mouse monoclonal	R961-25	Life Technologies	1:5,000
GAPDH	Mouse monoclonal	6C5	Santa Cruz Biotechnology	1:5,000
EGFR	Mouse monoclonal	0.N.268	Santa Cruz Biotechnology	1:1,000
HDAC2	Mouse monoclonal	3F3	Santa Cruz Biotechnology	1:5,000

2.9. Immunofluorescence staining and confocal microscopy

Cells were grown on round glass coverslips in 6-well plates to 70-90% confluence and fixed in 4% paraformaldehyde for 10 min at 37°C. They were then washed twice with PBS and permeabilised with 0.2% Triton X-100 in PBS for 5 min. After another wash with PBS twice, cells were blocked with 1% BSA in PBS for 1 h at room temperature and incubated with primary antibody overnight at 4°C. Table 2 lists the primary antibodies used for immunofluorescence staining and their dilutions in 1% BSA. Detection of full-length hepaCAM was performed with either an antibody against the hepaCAM extracellular domain (clone 419305) or with an antibody against the hepaCAM cytoplasmic domain (clone 5A1F1).

Excess primary antibody was removed the next day by washing cells twice with PBS. Thereafter, cells were incubated with the secondary antibodies Alexa Fluor 488 goat anti-mouse IgG and Alexa Fluor 594 goat anti-rabbit IgG (Life Technologies; both 1:100 dilution in 1% BSA) for 1-2 h at room temperature. Cells were subsequently washed twice with PBS and counterstained with DAPI for 30 min at 37°C. The coverslips were mounted onto glass slides with FluorSave Reagent (Merck Millipore, Billerica, MA, USA). Images were captured with an Olympus FluoView FV1000 confocal laser scanning microscope (Olympus, Tokyo, Japan) and analysed with FV1000 Viewer version 4.1. For confocal z-stack scans, three-dimensional images were reconstructed with Imaris version 7.6.4 (Bitplane, Zurich, Switzerland).

Table 2. List of primary antibodies used for immunofluorescence.

Protein	Clonality	Clone / Catalog Number	Source	Dilution
hepaCAM (extracellular domain)	Mouse monoclonal	419305	R&D Systems	1:100
hepaCAM (cytoplasmic domain)	Mouse monoclonal	5A1F1 (custom-made; hybridoma culture supernatant)	GenScript	1:2
Connexin 43	Rabbit polyclonal	3512	Cell Signaling Technology	1:100
EEA1	Rabbit monoclonal	C45B10	Cell Signaling Technology	1:100
PDI	Rabbit monoclonal	C81H6	Cell Signaling Technology	1:100
EBAG9 (RCAS1)	Rabbit monoclonal	D2B6N	Cell Signaling Technology	1:100

2.10. Treatment of cells with hepaCAM antibody

Cells expressing hepaCAM were treated overnight with a monoclonal antibody against the hepaCAM extracellular domain (clone 419305) at a concentration of 10 μg/ml. Mouse IgG1 (clone MOPC-21; Sigma-Aldrich) was included as an isotype control.

2.11. Co-immunoprecipitation assay

Co-immunoprecipitation (co-IP) assays were performed to determine whether connexin 43 could be co-immunoprecipitated together with WT hepaCAM, hepaCAM-R92Q or hepaCAM-R92W. The assays were carried out with or without *in vivo* cross-linking of proteins with dithiobis[succinimidyl propionate] (DSP; Thermo Scientific), which stabilises weak or transient protein interactions prior to cell lysis. Where cross-linking was performed,

cells grown as a monolayer were rinsed twice with PBS and incubated with 2 mM DSP for 30 min at room temperature. As DSP is water-insoluble, 4 mg of DSP was first dissolved in 0.4 ml DMSO and topped up with 4.6 ml PBS, and 5 ml of 2 mM DSP was used for a cell culture flask of area 75 cm^2. The cross-linking reaction was quenched by the addition of 20 mM Tris, pH 7.4 for 15 min. Thereafter, cells were washed twice with PBS and lysed in a non-denaturing lysis buffer (1% NP-40 in PBS) supplemented with a protease inhibitor cocktail. The protein concentration of the lysates were quantified by the Bradford assay as described in section 2.7. Equal protein amounts were pre-cleared with Protein G agarose beads (Thermo Scientific) for 1 h at 4°C to remove proteins that bind non-specifically to the beads. The pre-cleared lysates were then incubated with fresh Protein G agarose beads and 2 μg of hepaCAM antibody (clone 419305) or the isotype control (clone MOPC-21) overnight at 4°C with agitation. The beads were spun down the next day and washed four times with non-denaturing lysis buffer. Subsequently, the beads were boiled in 2× Laemmli sample buffer for 10 min to elute bound proteins and cleave DSP cross-links. The samples were then analysed by western blot to detect co-IP of connexin 43 with hepaCAM.

2.12. Subcellular fractionation

Subcellular fractionation of cell lines was performed with the Subcellular Protein Fractionation Kit for Cultured Cells (Thermo Scientific), according to the manufacturer's instructions. The kit enables the sequential separation of cytoplasmic, membrane, soluble nuclear, chromatin-bound and cytoskeletal fractions from cell cultures.

Cells were harvested with 1× trypsin-EDTA and washed with ice-cold PBS. All subsequent incubations and centrifugations were performed at 4°C, and the samples and extraction buffers were kept on ice at all times, unless otherwise stated. For a cell pellet with a packed volume of approximately 20 µl, 200 µl Cytoplasmic Extraction Buffer containing protease inhibitors was added and mixed gently for 10 min on a rotary shaker to selectively permeabilise the plasma membrane and release soluble cytoplasmic contents. After centrifugation at 500 × g for 5 min, the supernatant was retained as the cytoplasmic extract. The pellet was then lysed with 200 µl Membrane Extraction Buffer containing protease inhibitors by vortexing for 5 s at the maximum speed, and further incubation for 10 min with gentle mixing. The Membrane Extraction Buffer solubilises the contents of the plasma, mitochondria, ER and Golgi membranes, but not the nuclear membranes. The sample was then centrifuged at 3,000 × g for 5 min and the supernatant was retained as the membrane extract. Next, the pellet containing intact nuclei was lysed with 100 µl Nuclear Extraction Buffer (NEB) supplemented with protease inhibitors. The sample was vortexed for 15 s at the maximum speed, and further incubated for 30 min with gentle mixing. The lysate was then centrifuged at 5,000 × g for 5 min and the supernatant was retained as the soluble nuclear extract. To release chromatin-bound nuclear proteins, 100 µl room temperature NEB containing protease inhibitors, $CaCl_2$ and micrococcal nuclease was added to the recovered pellet and vortexed for 15 s at the maximum speed. After further incubation at 37°C for 5 min and vortexing for another 15 s, the lysate was centrifuged at 16,000 × g for 5 min and the supernatant was retained as the chromatin-bound nuclear extract. 100 µl room

temperature Pellet Extraction Buffer containing protease inhibitors was then added to the remaining insoluble pellet, vortexed for 15 s at the maximum speed and incubated at room temperature for 10 min. Finally, the lysate was centrifuged at $16,000 \times g$ for 5 min, and the supernatant retained as the cytoskeletal extract. The fractions were stored at -80°C until use. 20 μg of each fraction was loaded onto a gel for western blot analysis.

For experiments involving only cytoplasmic and membrane protein extraction, the cytoplasmic and membrane extracts were prepared as described above and analysed by western blot, together with the remaining pellet containing the un-separated nuclear and cytoskeletal contents.

2.13. Isolation of total RNA from cells

Total RNA was extracted from cell cultures with the RNeasy Mini Kit (Qiagen, Hilden, Germany) as per the manufacturer's instructions. Cells were lysed in 350 μl Buffer RLT with β-mercaptoethanol and homogenised by vigorous pipetting. An equal volume of 70% ethanol was added to the cell lysate and mixed. The cell lysate was transferred to an RNeasy spin column and centrifuged. The immobilised RNA was then washed with 350 μl Buffer RW1 and subjected to on-column DNase digestion with the RNase-Free DNase Set (Qiagen) to remove trace genomic DNA contamination. DNase I mix containing 10 μl DNase I stock solution and 70 μl Buffer RDD was added directly to the column and incubated for 15 min at room temperature. Thereafter, the column was washed once with 350 μl Buffer RW1 and twice with 500 μl Buffer RPE. The RNA was eluted with RNase-free water and the

concentration was quantified using the NanoDrop spectrophotometer (Thermo Scientific). The RNA was stored at -80°C until use.

2.14. Semi-quantitative reverse-transcription-PCR (RT-PCR)

Connexin 43 expression at the mRNA level was determined semi-quantitatively with the OneStep RT-PCR Kit (Qiagen). The enzyme mix in the kit contains reverse transcriptases and a hot-start Taq DNA polymerase, thus enabling both reverse transcription and PCR to be performed sequentially in a single reaction setup. 0.5 μg of total RNA and gene-specific primers were used for first-strand cDNA synthesis and subsequent PCR amplification. Table 3 shows the sequences of the primers used for amplifying connexin 43 and the internal control gene GAPDH. The primers for amplifying connexin 43 had been described in a previous study by Eugenin et al. (2003). Each reaction was set up on ice as described in Table 4 and the RT-PCR was performed under the conditions described in Table 5.

Table 3. Sequences of primers used in this study.

Primer	Sequence
Connexin 43	
Cx43-F	5'-GGG TTA AGG GAA AGA GCG ACC-3'
Cx43-R	5'-CCC CAT TCG ATT TTG TTC TGC-3'
GAPDH	
GAPDH-F	5'-CGG ATT TGG TCG TAT TGG GC-3'
GAPDH-R	5'-GGC AGA GAT GAT GAC CCT TTT G-3'

Table 4. Semi-quantitative RT-PCR reaction components.

Component	Volume (µl)
Master mix	
RNase-free water	$15 - x$
5× RT-PCR buffer	5
dNTP mix (10 mM)	1
Forward primer (10 µM)	1.5
Reverse primer (10 µM)	1.5
RT-PCR enzyme mix	1
Template RNA	x
Total volume	25

Table 5. Semi-quantitative RT-PCR conditions.

	Temperature	Time	Cycles
Reverse transcription	50°C	30 min	1
Initial PCR activation	95°C	15 min	1
Denaturation	94°C	30 s	
Annealing	50°C	30 s	34
Extension	72°C	1 min	
Final extension	72°C	10 min	1

2.15. Agarose gel electrophoresis

The products of RT-PCR were resolved in a 1.5% agarose gel. To prepare the gel, 0.6 g of agarose was dissolved completely in 40 ml of 1× Tris-acetate-EDTA (TAE) buffer (Vivantis, Malaysia) by microwaving. A 1:10,000 dilution of GelGreen (Biotium, Hayward, CA, USA) was added to the cooled agarose mixture before casting the gel. Once set, the gel was submerged in an electrophoresis tank filled with 1× TAE buffer. Samples and 1 kb DNA Ladder (Promega) were mixed with an appropriate amount of 6× Blue/Orange Loading Dye (Promega) and loaded onto the gel. The gel was electrophoresed at 100 V for 40 min and viewed with a UV transilluminator.

2.16. Cycloheximide chase assay

To determine the stability of connexin 43 protein, cells were treated with 50 μg/ml cycloheximide (CHX; Sigma-Aldrich), a potent inhibitor of protein synthesis. At each time-point (0, 30, 60 and 90 min), cells were lysed in RIPA buffer supplemented with a protease inhibitor cocktail. Equal protein amounts were analysed by western blot and GAPDH was used as a loading control.

2.17. Quantification of western blot using ImageJ

The densities of western blot bands were quantified using the gel analysis method in ImageJ (National Institutes of Health, Bethesda, MD, USA). For the CHX chase assay, the densities of the connexin 43 bands were normalised to the densities of the respective GAPDH bands at each time-point.

2.18. Cell adhesion assay

The attachment of hepaCAM-expressing cells to fibronectin was quantitated as detailed below, with reference to the methods described by Humphries (2001) and Akiyama (2002).

2.18.1. Preparation of fibronectin-coated plates

Glass coverslips or cell culture plates were coated with 10 μg/ml fibronectin from bovine plasma (Sigma-Aldrich) overnight at 4°C. Any remaining uncoated sites in the fibronectin-coated wells were blocked with 1% BSA for 30-60 min prior to the assay.

Separate coverslips or wells were coated with 0.1% poly-L-lysine (Sigma-Aldrich) as a non-integrin ligand control.

2.18.2. Adhesion of cells to fibronectin

Prior to performing the adhesion assay, cells were starved in serum-free medium overnight to remove extracellular and exogenous stimulatory factors present in FBS, thus ensuring that their adhesion to fibronectin is solely due to integrin-mediated signalling. The next day, serum starved cells were gently detached with StemPro Accutase cell dissociation reagent (Life Technologies) and resuspended in serum-free medium to a density of 2×10^5 cells/ml. Cells were then allowed to adhere to fibronectin-coated wells at 37°C for 5 min, or longer where indicated. Unattached or loosely adherent cells were removed by gently washing wells three times with PBS. Attached cells were subsequently fixed in 4% paraformaldehyde and analysed by immunofluorescence staining or quantitated by crystal violet staining.

2.18.3. Crystal violet staining

To quantitate the attachment to fibronectin, cells were stained with 0.1% crystal violet for 60 min. Excess dye was removed by washing the wells three times with water. The bound dye was subsequently solubilised with 10% acetic acid and the A595 was measured with the Bio-Rad Model 680 microplate reader. Background crystal violet staining was determined from blank wells that had been coated with 1% BSA, and was subtracted from all experimental results. A standard curve correlating A595 values and cell numbers was computed by allowing known numbers of cells to fully adhere to poly-L-lysine-coated wells. The percentage of cells adhering to fibronectin was subsequently calculated from the A595 measurements with reference to the standard curve.

2.19.   Wound healing assay

Cell migration was assessed by wound healing assays. Cells were grown to confluence in 6-well plates and transfected with connexin 43 siRNA or scrambled siRNA. At 24 h post-transfection, confluent monolayers were scratched with a sterile plastic 200 μl micropipette tip to generate wounds. The scratch wounds were viewed using the Axiovert 40 inverted microscope (Carl Zeiss, Jena, Germany) and three representative wound sites were marked out on the plate. Microscopic images of these wound sites were taken at 0, 24 and 48 h. The percentage wound closure was determined by measuring the width of the remaining unfilled spaces of the wounds.

2.20. ^{3}H-thymidine incorporation assay

Cell proliferation was quantified by the incorporation of ^{3}H-thymidine. Cells were transfected with connexin 43 siRNA or scrambled siRNA. At 24 h post-transfection, cells were detached and seeded in replicate wells of a 96-well plate at 10% confluence. After culturing for another 24 h, cells were pulsed with 0.5 µCi ^{3}H-thymidine (Perkin Elmer, Waltham, MA, USA) and incubated at 37°C in a CO_2 incubator overnight. The next days, cells were lysed by freezing and harvested onto a Packard Unifilter Plate using the MicroMate 196 Cell Harvester (Packard Instruments, Meridien, CT, USA). The plate was dried at 56°C for 1-2 h, after which 20 µl MicroScint solution (Perkin Elmer) was added to each well. Radioactivity was measured using the TopCount liquid scintillation analyser (Packard Instruments).

2.21. Cell aggregation and anoikis assay

Cells were grown as aggregates under anchorage-independent conditions and assayed for anoikis, with reference to the methods described by Weng et al. (2002) and Zhang et al. (2010b).

2.21.1. Culture of cells under anchorage-independent conditions

Anchorage-independent culture conditions were created by coating 60 mm culture dishes twice with 2.5 ml polyhydroxyethylmethacrylate (poly-HEMA; Sigma-Aldrich) solution (12 mg/ml in 95% ethanol) and drying overnight at 50-60°C. Prior to use, the dishes were rinsed twice with PBS to remove residual ethanol. Cells grown as a monolayer were subsequently detached with StemPro Accutase and resuspended in culture medium as a single-cell suspension. They were then seeded onto the poly-HEMA-coated culture

dishes at a density of 1×10^5 cells/ml and incubated at 37°C in a CO_2 incubator overnight. Under these anchorage-independent conditions, cells will tend to cluster together and grow as aggregates.

2.21.2. Determination of cell aggregate volume

Cells were stained with 1.5 μM calcein-AM (Life Technologies) for 20 min at 37°C, detached and seeded onto poly-HEMA-coated culture dishes as described above. After incubation at 37°C overnight, the aggregates were visualised by confocal microscopy and confocal z-stacks were analysed as described in section 2.9. Three-dimensional rendering of the aggregates was performed and the volume of each individual aggregate was determined. The spheroid volume threshold was set at 100,000 μm^3 and values below this threshold were excluded from statistical analysis as they tended to be single cells or loose clumps of cells.

2.21.3. Determination of anoikis by flow cytometry

Anoikis is a form of apoptosis induced in anchorage-dependent cells when there is a loss of attachment to the ECM. To determine anoikis, cells were grown under anchorage-independent conditions as described above. After incubation at 37°C overnight, the aggregates were harvested and dissociated with StemPro Accutase into a single-cell suspension. Anoikis was determined by the annexin V/7-AAD apoptosis assay described in section 2.22.2. Cells grown as monolayer cultures were included as controls to determine the baseline apoptosis rates.

2.22. Flow cytometry

2.22.1. Detection of binding to fibronectin

To detect binding of hepaCAM to fibronectin by fluorescence activated cell sorting (FACS), serum starved cells were gently detached with StemPro Accutase cell dissociation reagent, washed and blocked in 1% BSA for 10 min. Cells were subsequently incubated with 50 μg/ml HiLyte Fluor 488-labeled fibronectin from bovine plasma (Cytoskeleton Inc., Denver, CO, USA) diluted in 1% BSA for 15 min at room temperature. No fibronectin was added for the negative control. Flow cytometry was performed on a CyAn ADP Analyser (Beckman Coulter, Brea, CA, USA). Data were analysed using Summit version 4.3.1 (Beckman Coulter).

2.22.2. Annexin V/7-AAD apoptosis assay

Apoptosis was determined by annexin V/7-AAD staining. Briefly, cells were washed twice with cold PBS and resuspended in 1× Binding Buffer (eBioscience, San Diego, CA, USA). For a 100 μl cell suspension, 2.5 μl Annexin V-Alexa Fluor 647 (BioLegend, San Diego, CA, USA) and 5 μl 7-AAD (eBioscience) were added and incubated in the dark for 15 min at room temperature. Thereafter, 400 μl 1× Binding Buffer was added to each sample and flow cytometry was performed as described above.

2.23. Calcein-AM transfer assay

Gap junction activity or intercellular communication was quantified using a well-established method described by Kiang et al. (1994) and Czyz et al. (2000). In this method, cells are labelled with two dyes: DiI (red), a fluorescent lipophilic dye that binds to cell membranes, and calcein-AM, the

acetoxymethyl ester derivative of calcein (green). Calcein-AM is non-fluorescent until hydrolysed in the cytoplasm by esterases to calcein, which is small enough to be transferred between cells via gap junctions. Cells labelled with DiI and calcein-AM ("donor cells") are co-cultured with unstained cells ("recipient cells") from the same cell line. Recipient cells that have taken up calcein via GJIC will be stained green only, and can be distinguished from donor cells which will be stained both red and green. The amount of gap junction activity can be correlated to the percentage of cells in which calcein-AM transfer has occurred, as measured by flow cytometry.

In this study, donor cells and recipient cells were seeded separately into a 12-well plate and 100 mm culture dish respectively, and cultured overnight. Donor cells were labelled with 1 μM Vybrant DiI (Life Technologies) and 5 μM calcein-AM (Life Technologies) for 20 min at 37°C, and washed twice with PBS to remove excess dye. Both donor and recipient cells were dissociated with 0.2× trypsin-EDTA, mixed at a ratio of 1:40 (donor:recipient) and co-cultured overnight (15 h) at 37°C in a 100 mm dish. The next day, cells were harvested with 0.2× trypsin-EDTA and fixed in 1% paraformaldehyde. Flow cytometry was performed on a Fortessa Cell Analyser (BD Biosciences, San Jose, CA, USA). Data were analysed using FlowJo version 7.6.1 (FlowJo LLC, Ashland, OR, USA).

2.24. Statistical analysis

Statistical analyses for all experimental data were performed using GraphPad Prism version 5.01 (La Jolla, CA, USA). Statistical significance was determined by a two-tailed unpaired Student's t-test, or one-way analysis of

variance (ANOVA) with Tukey's multiple comparisons test. Values of p < 0.05 were considered significant.

CHAPTER 3   RESULTS

3.1   Interaction of hepaCAM with connexin 43

This section discusses the experiments to study the functions of hepaCAM in relation to the gap junction protein connexin 43 in U373 MG glioblastoma cells.

3.1.1.   hepaCAM co-localises with connexin 43 at the cell-cell contacts of U373 MG cells

Several studies have shown an abnormal localisation of connexin 43 in the cytoplasm of tumour cells, instead of the cell membrane (reviewed in Mesnil et al., 2005). In glioblastoma, previous studies had found a predominant localisation of connexin 43 in the cytoplasmic perinuclear region in three different glioblastoma cell lines (Cottin et al., 2008), as well as in four out of eight primary glioblastoma cultures established from clinical cases (Cottin et al., 2011). Conversely in non-neoplastic brain tissues, connexin 43 was localised to regions of cell-cell contact, characteristic of gap junctions between astrocytes (Cottin et al., 2011).

To investigate whether the expression of hepaCAM influences connexin 43 localisation in glioblastoma cells, the U373 MG cell line, which does not endogenously express hepaCAM, was stably transfected with WT hepaCAM and the corresponding empty vector and stained for connexin 43. Similar to previous findings in glioblastoma cells (Cottin et al., 2008), connexin 43 in vector-transfected U373 MG cells had a diffused staining in the cytoplasm and perinuclear region, and there was little staining for connexin 43 at the cell

membrane and at cell-cell contacts (Figure 6). On the other hand, in U373 MG cells expressing WT hepaCAM, connexin 43 was redistributed to the cell membrane, particularly at sites of cell-cell contacts, where strong co-localisation of connexin 43 with hepaCAM could be observed. Connexin 43 also co-localised with hepaCAM in distinct punctuate structures scattered throughout the cytoplasm, and there was comparatively less staining for connexin 43 in the perinuclear region compared to control cells. These punctuate structures are reminiscent of vesicles of the endomembrane system, and thus suggested that hepaCAM may play a role in the vesicular transport of connexin 43 to cellular junctions.

As mentioned previously, mutations in hepaCAM can cause the disease MLC. We next examined the effects of these mutations on connexin 43 localisation in U373 MG cells. We selected two naturally occurring mutations in which the arginine residue in the 92nd amino acid position had been replaced with glutamine (R92Q) or with tryptophan (R92W) (Lopez-Hernandez et al., 2011a). These single amino acid substitutions occur in the hepaCAM extracellular domain, specifically the first Ig-like domain.

As shown in Figure 6, the subcellular distribution of connexin 43 in U373 MG cells expressing hepaCAM-R92Q or hepaCAM-R92W was similar to the vector-transfected cells as connexin 43 was localised mainly in the cytoplasm and perinuclear region. Compared to cells expressing WT hepaCAM, there was reduced localisation of both connexin 43 and mutant hepaCAM at cell-cell contacts. Although co-localisation of connexin 43 with mutant hepaCAM could still be observed, it occurred mainly in intracellular compartments and

not at cell-cell contacts, which suggested that the R92Q and R92W mutations

may inhibit the ability of hepaCAM to target connexin 43 to cellular junctions,

as well as interfere with the localisation of hepaCAM itself at these regions.
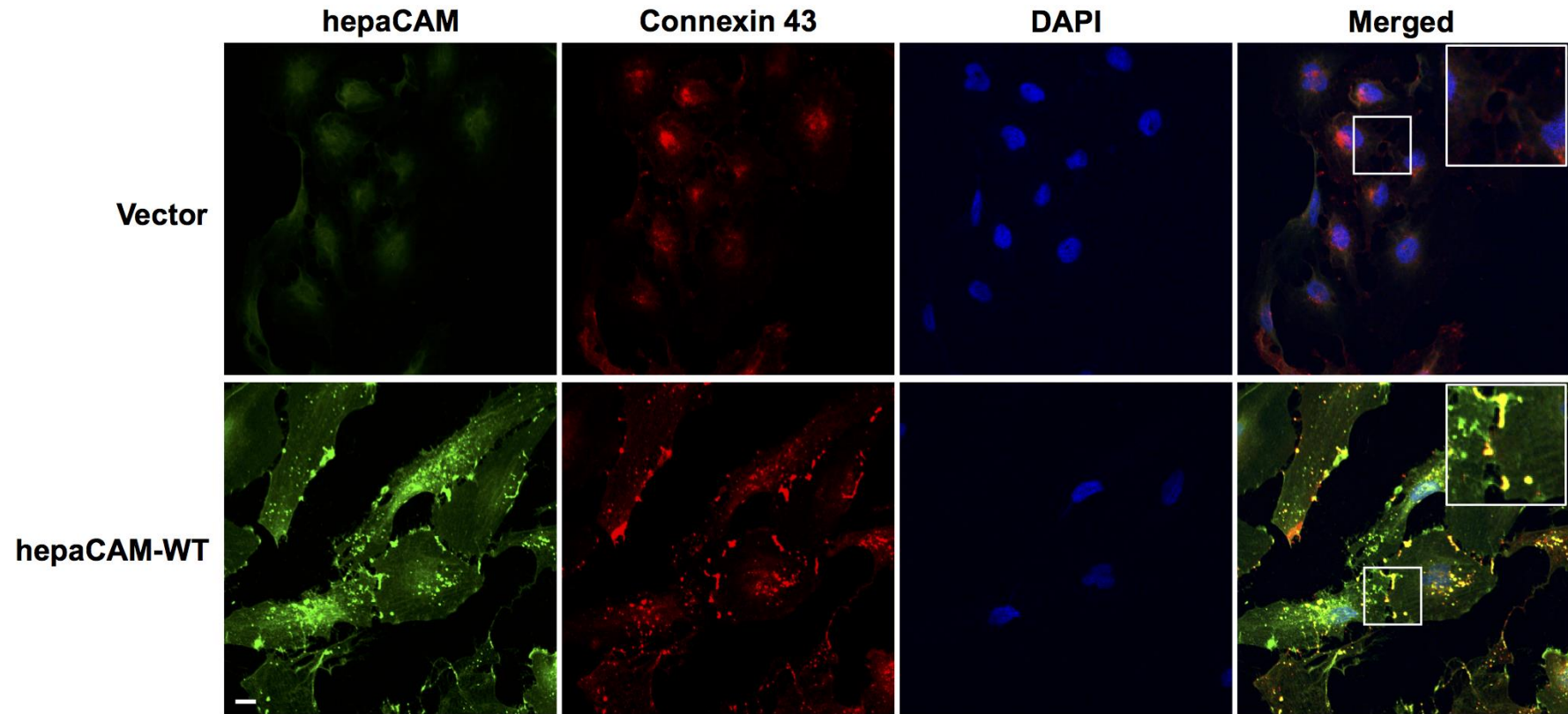
Figure 6. hepaCAM co-localises with connexin 43 at the cell-cell contacts of U373 MG cells, and mutations in the hepaCAM extracellular domain prevent its association with connexin 43 at the cell-cell contacts. Cells were stably transfected with pcDNA3.1 vector, wild-type hepaCAM, hepaCAM-R92Q (next page) and hepaCAM-R92W (next page). Immunofluorescent staining was performed with antibodies against the hepaCAM cytoplasmic domain (green) and connexin 43 (red). Co-localisation of hepaCAM and connexin 43 is indicated by yellow fluorescence. Nuclei were stained with DAPI (blue). Insets show a higher magnification of sites of cell-cell contacts. Cells were visualised by confocal microscopy under a 60× objective. The images presented are representative of images taken from at least six different fields. Scale bar: 10 μm.
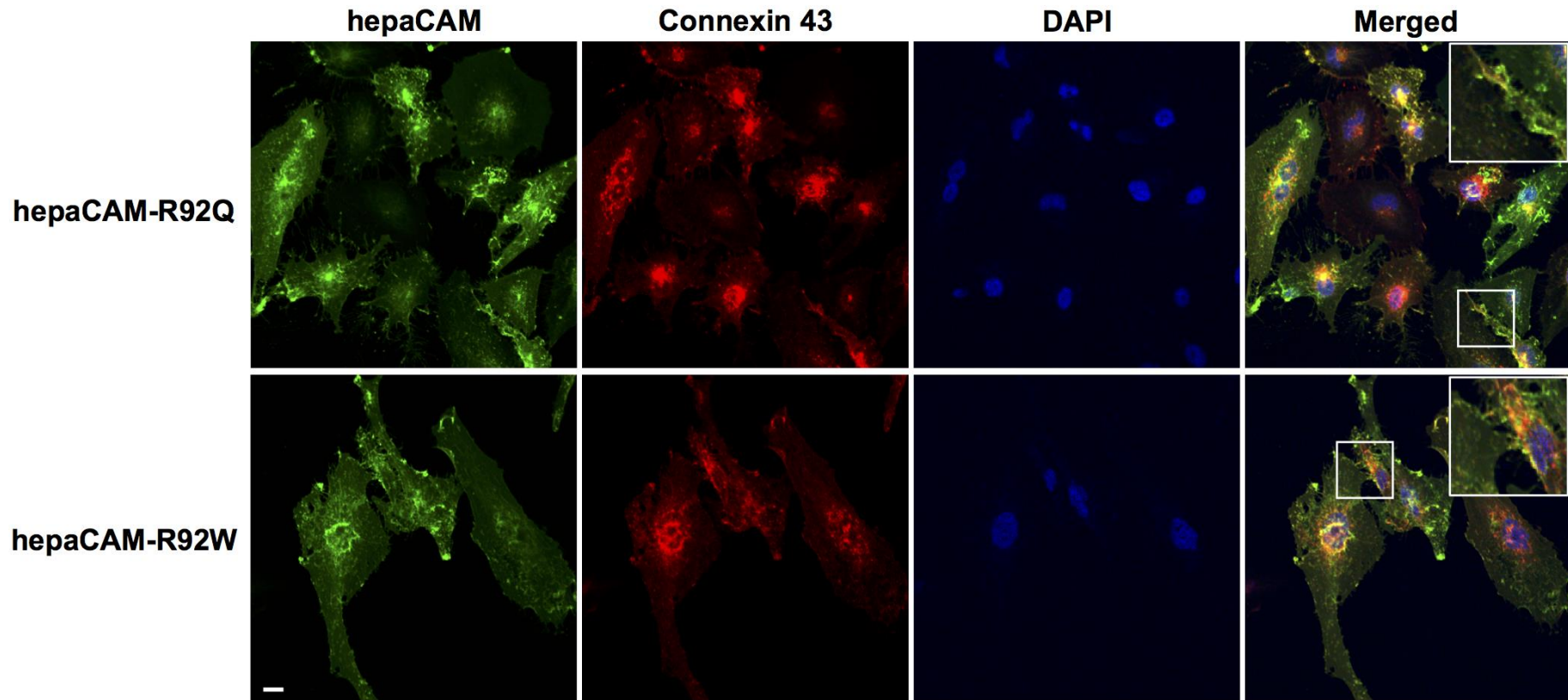
Figure 6 (continued). hepaCAM co-localises with connexin 43 at the cell-cell contacts of U373 MG cells, and mutations in the hepaCAM extracellular domain prevent its association with connexin 43 at the cell-cell contacts. Cells were stably transfected with pcDNA3.1 vector (previous page), wild-type hepaCAM (previous page), hepaCAM-R92Q and hepaCAM-R92W. Immunofluorescent staining was performed with antibodies against the hepaCAM cytoplasmic domain (green) and connexin 43 (red). Co-localisation of hepaCAM and connexin 43 is indicated by yellow fluorescence. Nuclei were stained with DAPI (blue). Insets show a higher magnification of sites of cell-cell contacts. Cells were visualised by confocal microscopy under a 60× objective. The images presented are representative of images taken from at least six different fields. Scale bar: 10 μm.

3.1.2. hepaCAM can be co-immunoprecipitated with connexin 43

As immunofluorescent studies showed an association of WT hepaCAM with connexin 43 at the cell-cell contacts of U373 MG cells, we next verified the physical interaction of these two proteins by a co-IP assay. Protein lysates were prepared from U373 MG cells stably transfected with WT hepaCAM, and WT hepaCAM was precipitated using an antibody against the hepaCAM extracellular domain. As shown in Figure 7, connexin 43 could be co-precipitated together with WT hepaCAM, indicating that hepaCAM co-localises and interacts with connexin 43.
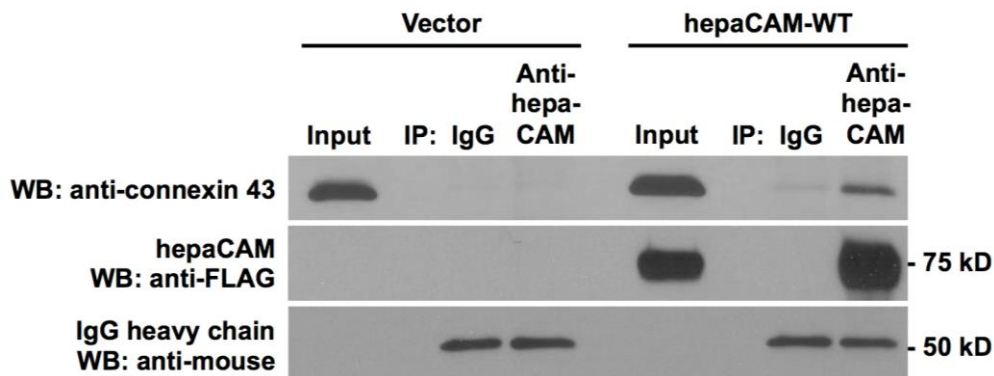
Figure 7. Co-immunoprecipitatation of connexin 43 and hepaCAM. Cell lysates were prepared from U373 MG cells stably transfected with pcDNA3.1 vector and wild-type hepaCAM (fused to a C-terminal 3×FLAG epitope), and immunoprecipitated with antibody against the hepaCAM extracellular domain (IP hepaCAM). Immunoprecipitation with mouse IgG1 (IP IgG) was included as a negative control. Western blot analysis was performed on the immunoprecipitates and input (3%) using connexin 43 antibody. The efficiency of hepaCAM immunoprecipitation was evaluated with an HRP-conjugated FLAG antibody. The IgG heavy chain detected with an HRP-conjugated anti-mouse antibody is shown as a loading control for the IP antibodies. The result presented is a representative experiment of two independent experiments with similar results.

3.1.3. Mutations in hepaCAM weaken the interaction of hepaCAM with connexin 43

We next examined whether the R92Q and R92W mutations in the hepaCAM extracellular domain affect the physical interaction of hepaCAM with connexin 43 in U373 MG cells. WT hepaCAM and hepaCAM containing the R92Q and R92W mutations were precipitated from the protein lysates using an antibody against the hepaCAM extracellular domain. Interestingly, connexin 43 could be co-precipitated to a higher extent with WT hepaCAM than with hepaCAM-R92Q or hepaCAM-R92W (Figure 8A). This was not due to less precipitation of hepaCAM-R92Q and hepaCAM-R92W, since the levels of hepaCAM precipitated were comparable across all three samples when the blot was re-probed with an antibody against the FLAG-epitope on hepaCAM. Hence, the results suggested that connexin 43 had a lower affinity with these mutations of hepaCAM than with WT hepaCAM.

The co-IP assay was also repeated with *in vivo* cross-linking of proteins with DSP prior to cell lysis to stabilise low-affinity or transient protein interactions. As DSP is lipophilic and membrane-permeable, it is able to cross-link protein molecules within the cell, as well as on the cell surface. It was observed that connexin 43 could be co-precipitated effectively with WT hepaCAM or with hepaCAM containing the R92Q or R92W mutations (Figure 8B). The results thus indicated that the binding affinity of hepaCAM for connexin 43 is weakened by the R92Q and R92W mutations in the hepaCAM extracellular domain, and that connexin 43 could not be co-precipitated effectively with mutant hepaCAM unless the physical interaction of the two proteins had been stabilised by prior cross-linking.

(A) Without cross-linking of proteins:
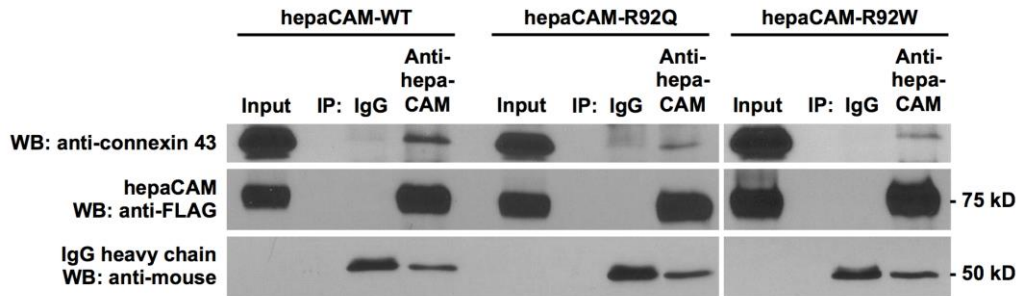
(B) Cross-linking of proteins with DSP:
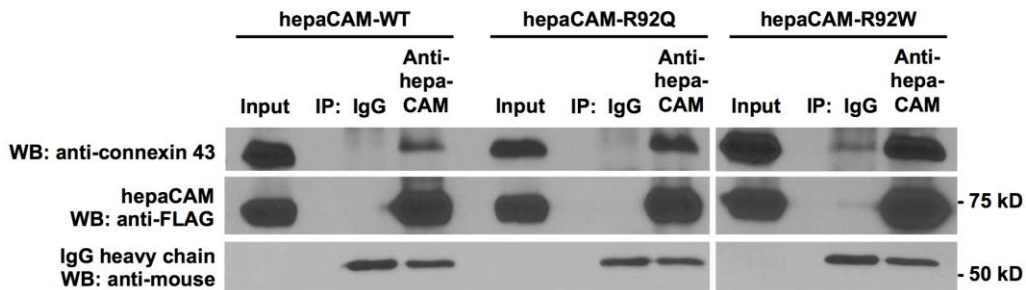
Figure 8. Co-immunoprecipitation of wild-type and mutant hepaCAM with connexin 43. Mutations in the hepaCAM extracellular domain weaken the interaction of hepaCAM with connexin 43. (A) Cell lysates were prepared from U373 MG cells stably transfected with wild-type hepaCAM, hepaCAM-R92Q and hepaCAM-R92W (fused to a C-terminal 3×FLAG epitope). (B) Cellular proteins were cross-linked with dithiobis[succinimidyl propionate] (DSP) prior to cell lysis. hepaCAM was immunoprecipitated using antibody against the hepaCAM extracellular domain (IP hepaCAM). Immunoprecipitation with mouse IgG1 (IP IgG) was included as a negative control. Western blot analysis was performed on the immunoprecipitates and input (2%) using connexin 43 antibody. Efficiency of hepaCAM immunoprecipitation was evaluated with an HRP-conjugated FLAG antibody. The IgG heavy chain detected with an HRP-conjugated anti-mouse antibody is shown as a loading control for the IP antibodies. The result presented is a representative experiment of at least four independent experiments with similar results.

3.1.4. Connexin 43 protein expression is increased in hepaCAM-expressing U373 MG cells

Immunofluorescent staining of connexin 43 in WT hepaCAM-expressing U373 MG cells (Figure 6) indicated not only a cellular redistribution of connexin 43 by hepaCAM but also an increase in connexin 43 expression levels. This was confirmed by western blot analysis, which showed a significant two-fold increase in connexin 43 protein levels by WT hepaCAM compared to vector-transfected control cells (Figure 9A, B). On the other hand, the two hepaCAM mutations, especially R92Q, were less effective in enhancing connexin 43 expression, as no significant difference in connexin 43 protein levels was observed between control cells and cells expressing hepaCAM-R92Q or hepaCAM-R92W (Figure 9A, B).
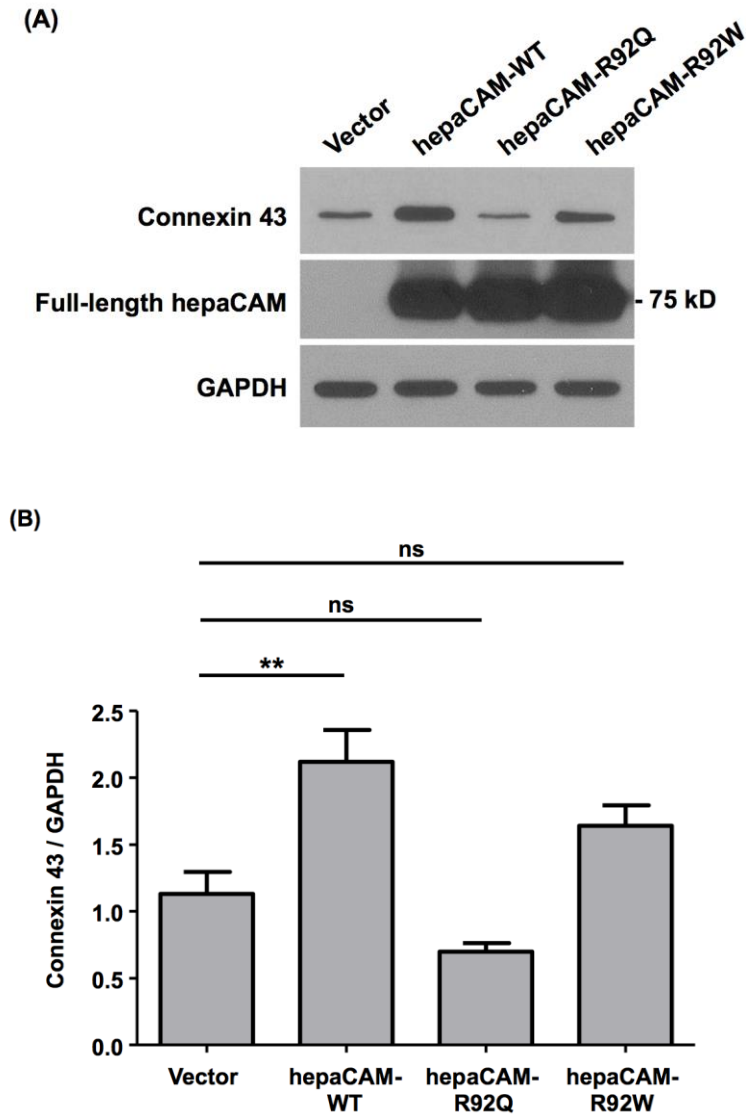
Figure 9. Expression of wild-type hepaCAM in U373 MG cells increases connexin 43 protein levels. (A) Cell lysates were prepared from U373 MG cells stably transfected with pcDNA3.1 vector, wild-type hepaCAM, hepaCAM-R92Q and hepaCAM-R92W. 20 μg of cell lysates were subjected to western blot analysis using antibodies against connexin 43 and the FLAG-tag on the hepaCAM cytoplasmic domain. GAPDH was used as a loading control. The result presented is a representative experiment of four independent experiments with similar results. (B) Quantification of connexin 43 protein levels in all four independent western blot analyses. Using ImageJ, the densities of the connexin 43 bands were normalised to the densities of the respective GAPDH bands for each sample, and the mean relative density over the four experiments was calculated. The data presented are the means ± SE (n = 4), ** $p < 0.01$ as assessed by one-way ANOVA with Tukey's multiple comparisons test.

76

3.1.5. Increased connexin 43 protein expression in hepaCAM-expressing cells is not due to upregulation at the transcriptional level

As western blot analysis showed that connexin 43 protein expression is upregulated in WT hepaCAM-expressing U373 MG cells compared to control cells, we next sought to understand whether this upregulation occurs at the transcriptional or post-transcriptional level. Using primers to amplify a 248-bp fragment of connexin 43 mRNA as previously described by Eugenin et al. (2003), semi-quantitative RT-PCR was performed to determine connexin 43 mRNA expression in vector-transfected, WT and mutant hepaCAM-expressing U373 MG cells (Figure 10).
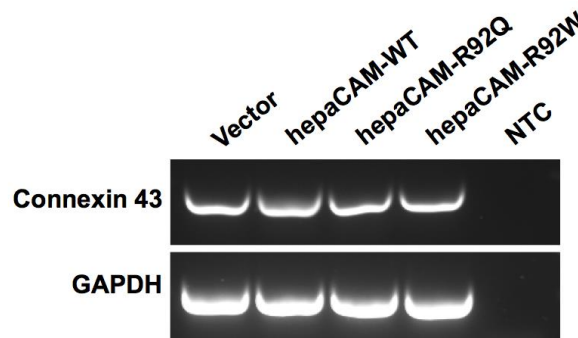
Figure 10. Evaluation of connexin 43 mRNA expression by semi-quantitative RT-PCR. Total RNA was isolated from U373 MG cells stably transfected with pcDNA3.1 vector, wild-type hepaCAM, hepaCAM-R92Q and hepaCAM-R92W. GAPDH was included as a housekeeping gene control, while RT-PCR reactions without an RNA template were included as no template controls (NTC). The result presented is a representative experiment of two independent experiments with similar results.

The results showed that connexin 43 mRNA levels were similar across all four cell lines. This indicated that the increased connexin 43 protein levels in WT hepaCAM-expressing U373 MG cells are due to an upregulation at the post-transcriptional level, instead of the transcriptional level.

3.1.6. hepaCAM enhances connexin 43 protein stability

Connexin 43 has been reported to undergo rapid turnover with a short half-life of 1-5 h (Beardslee et al., 1998; Laird et al., 1991). We thus hypothesised that the increased levels of connexin 43 protein in WT hepaCAM-expressing U373 MG cells are due to a slower rate of turnover compared to control cells. To assess whether hepaCAM influences connexin 43 protein stability in U373 MG cells, the kinetics of connexin 43 degradation were determined by a cycloheximide chase assay. Cycloheximide is a potent inhibitor of translational elongation and is commonly used to investigate the stability of a target protein without confounding contributions from newly synthesised proteins. Control and WT hepaCAM-expressing U373 MG cells were treated with cycloheximide in a time-course experiment of up to 90 min and harvested at intervals of 30 min to determine the amounts of connexin 43 protein remaining.

Compared to vector-transfected cells, cells expressing WT hepaCAM had increased stability of connexin 43 as shown by its slower rate of degradation. Upon 90 min of inhibition with cycloheximide, the percentage of connexin 43 protein remaining in vector-transfected U373 MG cells was 27% while that remaining in WT hepaCAM-expressing U373 MG cells was 81% (Figure 11A, B). The results suggested that the binding of hepaCAM to connexin 43 slows down its rate of degradation and increases its half-life. Thus, the increased levels of connexin 43 protein observed in WT-hepaCAM-expressing U373 MG cells is due to enhanced connexin 43 protein stability.
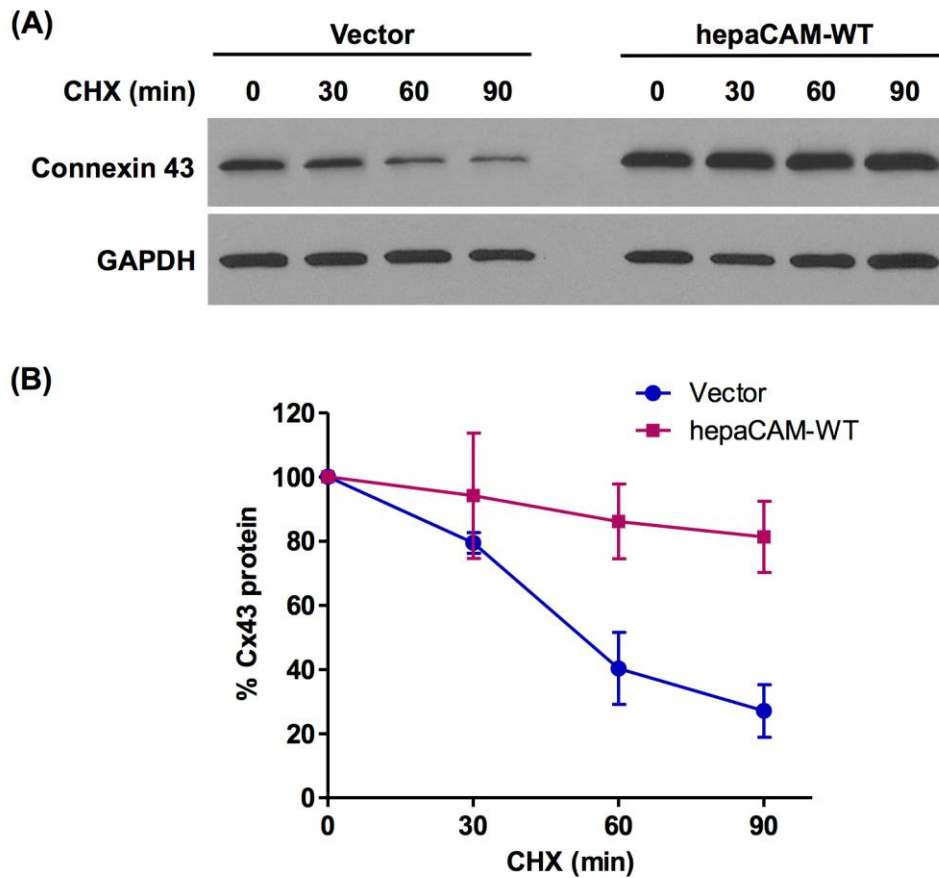
Figure 11. Evaluation of connexin 43 protein stability by cycloheximide chase assay. (A) U373 MG cells stably transfected with pcDNA3.1 vector or wild-type hepaCAM were treated with cycloheximide (CHX) (50 μg/ml) for the times indicated. At each time-point, cells were lysed and 30 μg of cell lysates were subjected to western blot analysis using connexin 43 antibody. GAPDH was used as a loading control. The result presented is a representative experiment of three independent experiments with similar results. (B) Summary of the quantification of all three independent CHX chase experiments using ImageJ. The densities of the connexin 43 bands were normalised to the densities of the respective GAPDH bands at each time-point. The level of connexin 43 remaining at each time-point was calculated as a percentage of the initial connexin 43 level (time 0 of CHX treatment). The data presented are the means ± SE (n = 3).

3.1.7. Expression of hepaCAM in HEK293T cells leads to increased connexin 43 protein levels

To determine whether hepaCAM also regulates connexin 43 protein levels in other cell lines, we transiently transfected WT hepaCAM in human embryonic kidney HEK293T cells, which have a high transfection efficiency of 85% (Supplementary Figure 1) and low levels of endogenous connexin 43 expression. Exogenous expression of hepaCAM in HEK293T cells led to a significant 1.5-fold increase in connexin 43 protein levels (Figure 12A, B), further supporting our previous observation that hepaCAM enhances connexin 43 protein stability. It should be noted that connexin 43 was detected as two bands in the HEK293T cells, as connexin 43 is well-known to undergo post-translational modifications such as phosphorylation, giving rise to shifts in the electrophoretic mobility. Based on these results, it is observed that hepaCAM acts as a general regulator of connexin 43 stability in different cell types.
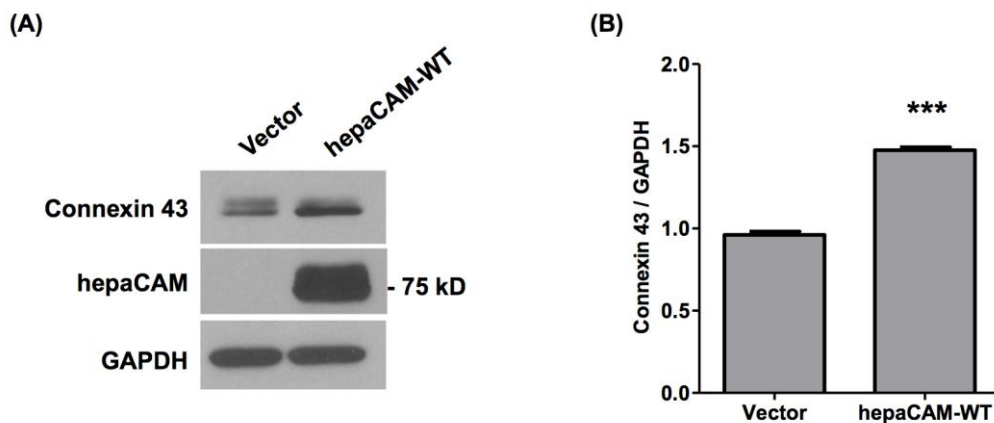
Figure 12. Expression of hepaCAM in HEK293T cells increases connexin 43 protein levels. (A) HEK293T cells were transiently transfected with pcDNA3.1 vector or wild-type hepaCAM. Two days after transfection, cells were lysed and 60 μg of cell lysates were subjected to Western blot analysis using antibodies against connexin 43 and the hepaCAM extracellular domain. GAPDH was used as a loading control. The result presented is a representative experiment of three independent experiments with similar results. (B) Summary of the quantification of all three experiments using ImageJ. The densities of the connexin 43 bands were normalised to the densities of the respective GAPDH bands for each sample, and the mean relative density over the three experiments was calculated. The data presented are the means ± SE (n = 3), *** $p < 0.0001$ as assessed by t-test.

3.1.8. Treatment with an antibody against the hepaCAM extracellular domain affects connexin 43 localisation at cell-cell contacts

As observed previously in Figure 6, the R92Q and R92W mutations in the hepaCAM extracellular domain appear to impair the targeting of connexin 43 to the cell-cell contacts of U373 MG cells. We next sought to understand whether neutralisation of hepaCAM with an antibody would also have similar effects on connexin 43 localisation.

U373 MG cells expressing WT hepaCAM were treated overnight with an antibody against the hepaCAM extracellular domain, and stained for connexin 43 (Figure 13). In cells treated with the IgG control, connexin 43 was localised mainly to cell junctions, where co-localisation with hepaCAM was also observed, in accordance with previous findings. On the other hand, treatment of cells with the hepaCAM antibody significantly reduced connexin 43 localisation at cell-cell contacts. Diffused staining of connexin 43 in the cytoplasm and perinuclear region of the cells was observed, and the overall expression of connexin 43 appeared to be diminished. Treatment of cells with the hepaCAM antibody also abrogated connexin 43 co-localisation with hepaCAM.

Hence, similar to the mutations in the hepaCAM extracellular domain, neutralisation of hepaCAM with an antibody against its extracellular domain disrupts connexin 43 targeting to the junctions of U373 MG cells. Taken together, the data suggest that it is the extracellular domain of hepaCAM which interacts with connexin 43, and that the physical interaction of hepaCAM with connexin 43 aids in targeting connexin 43 to cell-cell contacts.

Neutralisation of hepaCAM with the antibody disrupts the interaction with connexin 43, resulting in an intracellular accumulation of connexin 43 and reduced targeting to the plasma membrane.

Figure 13. Treatment of hepaCAM-expressing U373 MG cells with an antibody against the hepaCAM extracellular domain prevents the association of hepaCAM with connexin 43 at cell-cell contacts. Wild-type hepaCAM-expressing U373 MG cells were treated overnight with antibody against the hepaCAM extracellular domain in soluble form (10 μg/ml). Cells were also treated with the isotype mouse IgG1 as a control. The next day, cells were fixed and immunofluorescent staining was performed with antibodies against the hepaCAM extracellular domain (green) and connexin 43 (red). Co-localisation of hepaCAM and connexin 43 is indicated by yellow fluorescence. Nuclei were stained with DAPI (blue). Cells were visualised by confocal microscopy under a 60× objective. The images presented here are representative of images taken from at least six different fields. Scale bar: 10 μm.

3.1.9. Treatment with an antibody against the hepaCAM extracellular domain downregulates connexin 43 expression

As immunofluorescent staining of connexin 43 in hepaCAM antibody-treated cells also suggested an overall reduction in connexin 43 expression, we next determined connexin 43 protein levels in WT hepaCAM-expressing U373 MG cells upon overnight treatment with hepaCAM antibody. In cells treated with the hepaCAM antibody, connexin 43 expression was downregulated compared to cells treated with the IgG control (Figure 14). The results suggested that hepaCAM antibody treatment of the cells disrupts the interaction of hepaCAM with connexin 43 and destabilises connexin 43. Hence, the results further lend support to the conclusion that the hepaCAM-connexin 43 interaction enhances the stability of connexin 43 protein.
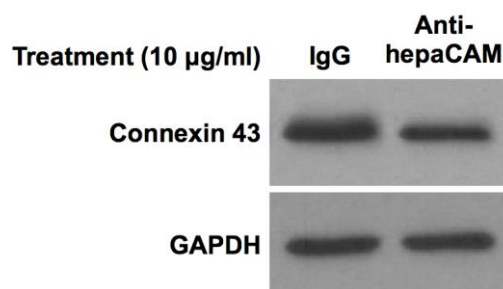
Figure 14. Treatment of hepaCAM-expressing U373 MG cells with an antibody against the hepaCAM extracellular domain causes a downregulation of connexin 43 expression. Wild-type hepaCAM-expressing U373 MG cells were treated overnight with antibody against the hepaCAM extracellular domain in soluble form (10 µg/ml). Cells were also treated with the isotype mouse IgG1 as a control. The next day, cells were lysed and 20 µg of cell lysates were subjected to western blot analysis using connexin 43 antibody. GAPDH was used as a loading control. The result presented is a representative experiment of two independent experiments with similar results.

Since western blot analysis showed an overall decrease in connexin 43 expression upon treatment with hepaCAM antibody, we next wanted to determine whether the downregulation occurred in the cytoplasmic and membrane compartments. Subcellular protein fractionation to isolate the cytoplasmic and membrane extracts was performed on WT hepaCAM-expressing U373 MG cells upon overnight treatment with hepaCAM antibody. The membrane extract obtained from subcellular fractionation is a mixture of the contents of the plasma, mitochondria, ER and Golgi membranes. As shown in Figure 15, compared to IgG-treated cells, connexin 43 levels were reduced in both the cytoplasmic and membrane fractions from hepaCAM antibody-treated cells. This corroborates the results in Figure 14 which showed an overall decrease in connexin 43 expression upon hepaCAM antibody treatment and confirms that connexin 43 is destabilised when its interaction with hepaCAM is disrupted.

It should also be noted that while immunofluorescent staining showed a marked reduction in connexin 43 expression at the plasma membrane upon hepaCAM antibody treatment (Figure 13), there was only a moderate decrease in connexin 43 protein levels in the membrane fraction, which contains the contents of the endomembrane system in addition to the plasma membrane (Figure 15). As a diffused intracellular localisation of connexin 43 was also observed upon hepaCAM antibody treatment (Figure 13), the results taken together suggested that hepaCAM antibody treatment may also cause an accumulation of connexin 43 in the compartments of the endomembrane system, for example the ER and Golgi membranes due to impaired targeting to the plasma membrane. Alternatively, connexin 43 may accumulate in

endosomal and lysosomal compartments due to its decreased stability and

increased rate of turnover upon hepaCAM antibody treatment.

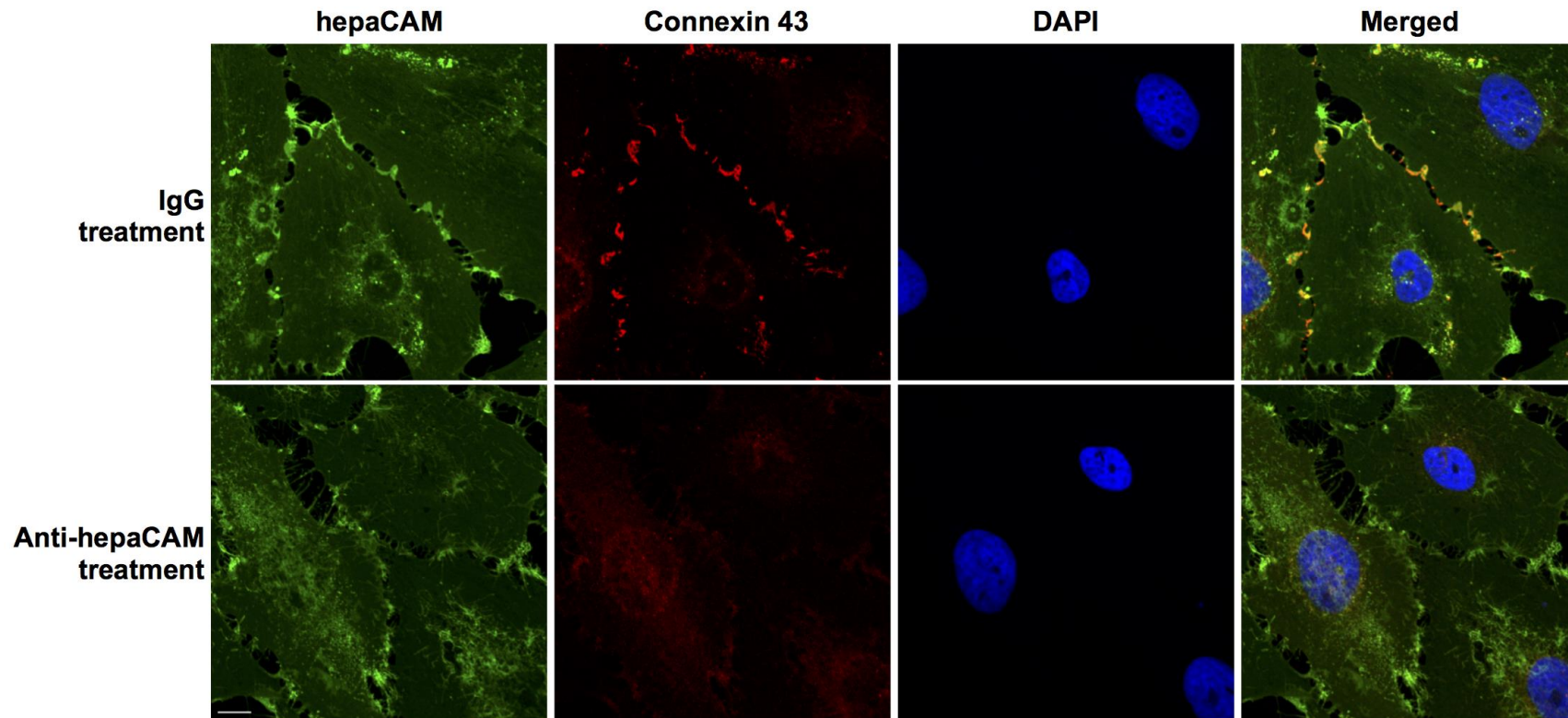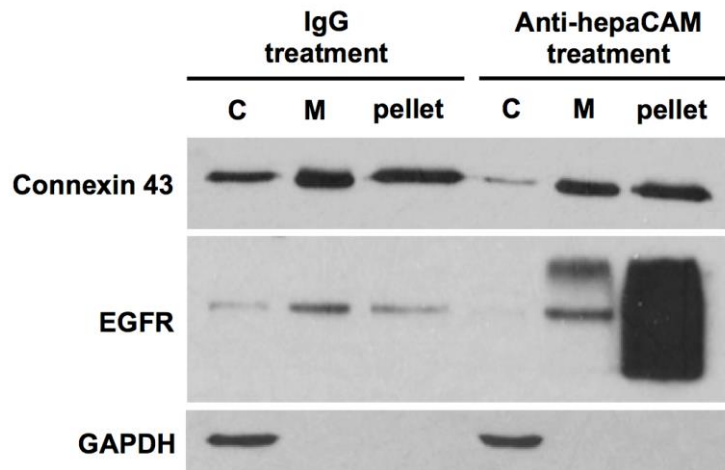**Figure 15. Treatment of hepaCAM-expressing U373 MG cells with an antibody against the hepaCAM extracellular domain causes a downregulation of connexin 43 expression in both cytoplasmic and membrane fractions.** Wild-type hepaCAM-expressing U373 MG cells were treated overnight with antibody against the hepaCAM extracellular domain in soluble form (10 μg/ml). Cells were also treated with the isotype mouse IgG1 as a control. The next day, cells were detached and subjected to subcellular fractionation to isolate the cytoplasmic (C) and membrane (M) fractions. The membrane fraction contains the contents of the plasma, mitochondria, ER and Golgi membranes. The pellet refers to the residue after extraction of the cytoplasmic and membrane fractions. 20 μg of each fraction and the pellet were subjected to western blot analysis using connexin 43 antibody. EGFR and GAPDH were used as loading controls for the membrane and cytoplasmic fractions respectively.

3.1.10. Connexin 43 knockdown does not affect hepaCAM localisation

Since hepaCAM expression in U373 MG cells targets connexin 43 to cellular junctions, we wanted to determine whether the converse was true, i.e. whether the presence of connexin 43 influences hepaCAM localisation at cell-cell contacts. WT hepaCAM-expressing U373 MG cells were subjected to siRNA-mediated silencing of connexin 43 expression to determine hepaCAM localisation in the absence of connexin 43. The siRNA duplex used and its concentration were first optimised (Supplementary Figure 2).

The efficiency of connexin 43 knockdown in WT hepaCAM-expressing U373 MG cells was verified by western blot analysis (Figure 16) and the subcellular localisation of hepaCAM and connexin 43 was analysed by confocal microscopy (Figure 17). As shown by western blot analysis, connexin 43 protein expression could be effectively silenced in WT hepaCAM-expressing U373 MG cells 48 h after transfection with connexin 43 siRNA. The knockdown of connexin 43 expression did not affect the overexpression of WT hepaCAM in U373 MG cells, as their levels were comparable between connexin 43 siRNA-transfected cells and scrambled siRNA-transfected cells (Figure 16). In addition, immunofluorescent staining showed that silencing of connexin 43 in WT hepaCAM-expressing U373 MG cells also did not affect the subcellular localisation of hepaCAM, as well as the overall morphology of the cells (Figure 17). This indicates that connexin 43 is not necessary for the targeting of hepaCAM to cellular junctions and suggests that hepaCAM can function independently of connexin 43. These results also parallel the findings by previous studies that MLC1 is not necessary for hepaCAM targeting to cellular junctions (Lopez-Hernandez et al., 2011b).
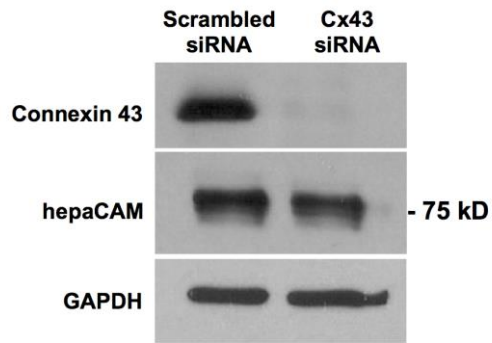
Figure 16. siRNA-mediated knockdown of connexin 43 in hepaCAM-expressing U373-MG cells. Wild-type hepaCAM-expressing U373 MG cells were transfected with 5 nM connexin 43 siRNA or scrambled siRNA and lysed 48 h post-transfection. 20 μg of cell lysates were subjected to western blot analysis using connexin 43 antibody. Full-length hepaCAM was detected with an antibody against the hepaCAM cytoplasmic domain. GAPDH was used as a loading control. The result presented is a representative experiment of three independent experiments with similar results.
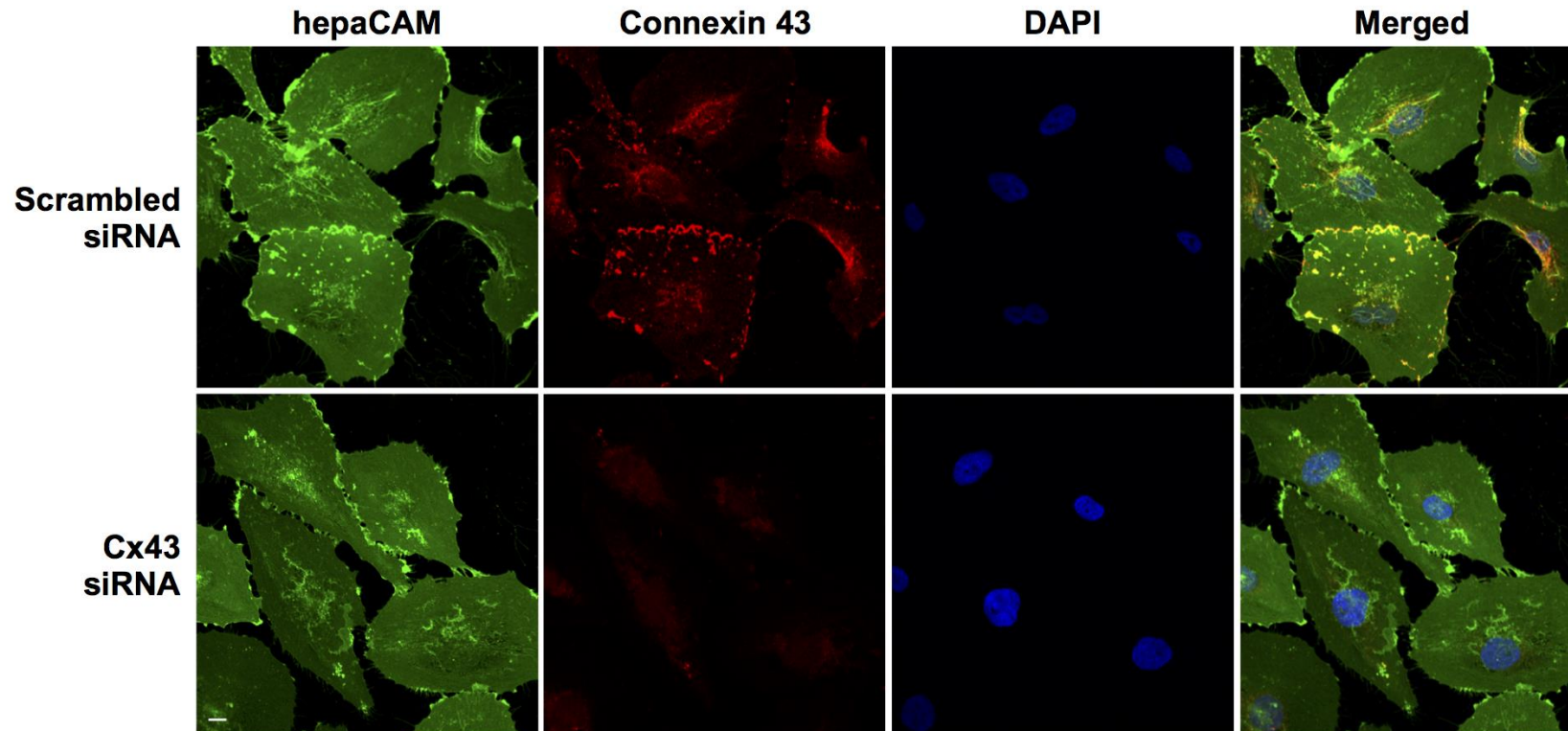
Figure 17. Silencing of connexin 43 does not affect hepaCAM localisation in U373 MG cells. Wild-type hepaCAM-expressing U373 MG cells were transfected with 5 nM scrambled siRNA or connexin 43 siRNA. Cells were fixed 48 h post-transfection and immunofluorescent staining was performed with antibodies against the hepaCAM extracellular domain (green) and connexin 43 (red). Co-localisation of hepaCAM and connexin 43 is indicated by yellow fluorescence. Nuclei were stained with DAPI (blue). Cells were visualised by confocal microscopy under a 60× objective. The images presented here are representative of images taken from at least six different fields. Scale bar: 10 μm.

3.1.11. Connexin 43 knockdown does not affect the functions of hepaCAM in cell adhesion, migration and proliferation

Since hepaCAM interacts with and stabilises connexin 43, we postulated that connexin 43 may be involved in the functions of hepaCAM in U373 MG cells. Since hepaCAM expression in U373 MG cells has been shown to increase adhesion, reduce migration and inhibit proliferation (Lee et al., 2009), we investigated whether the depletion of connexin 43 in WT hepaCAM-expressing U373 MG cells influenced these functions of hepaCAM.

Connexin 43 expression in vector-transfected and WT-hepaCAM U373 MG cells was silenced by siRNA-mediated knockdown, and their adhesion to fibronectin-coated culture plates was quantified by crystal violet staining (Figure 18). The expression of WT hepaCAM led to a significant two-fold increase in adhesion to fibronectin compared to vector-transfected cells, in accordance with previous findings in U373 MG cells. However, no significant difference in adhesion was observed upon connexin 43 knockdown in both vector-transfected and WT-hepaCAM-expressing cells.
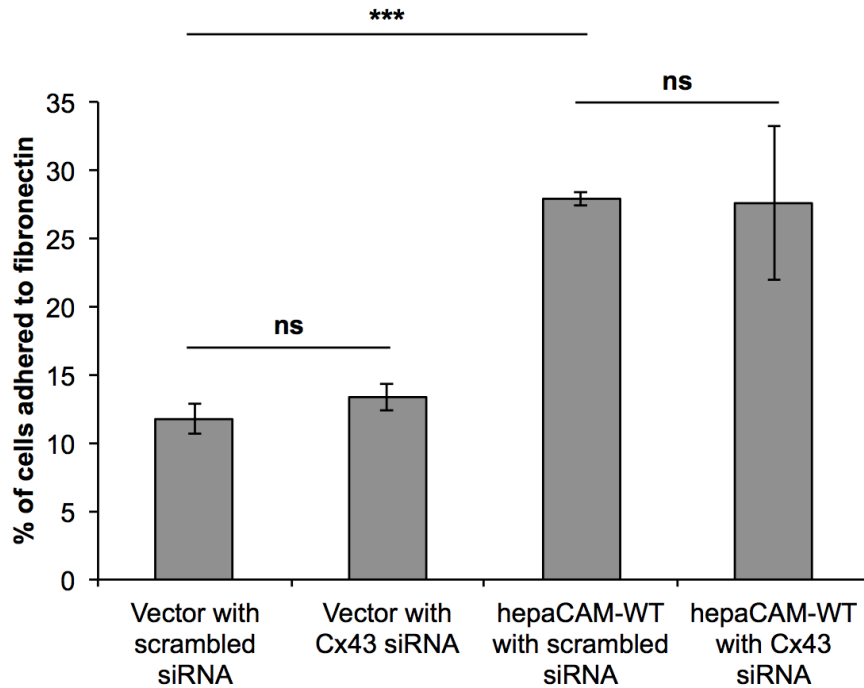
Figure 18. Silencing of connexin 43 does not affect the increased adhesion of hepaCAM-expressing U373 MG cells to fibronectin. Vector-transfected and wild-type hepaCAM-expressing U373 MG cells were transfected with 5 nM scrambled siRNA or connexin 43 siRNA and serum-starved 24 h post-transfection. After an overnight starvation, cells were detached and allowed to adhere to fibronectin-coated plates for 5 min. After 5 min, unattached or loosely adherent cells were washed away, and attached cells were fixed and stained with crystal violet. The crystal violet stain was subsequently solubilised and the A595 measured. The number of cells adhering to fibronectin was determined from the A595 measurements with reference to a standard curve plotted using A595 values from known numbers of cells, and calculated as a percentage of the total number of cells seeded. The data represent means ± SD (n = 3), *** $p < 0.0001$ as assessed by one-way ANOVA with Tukey's multiple comparisons test. The results presented are representative of three independent experiments with similar results.

The migration of vector-transfected and WT-hepaCAM U373 MG cells upon connexin 43 knockdown was assessed by the wound healing assay (Figure 19). In accordance with previous findings, hepaCAM expression in U373 MG cells significantly reduced cell migration at 24 and 48 h, compared to vector-transfected cells. Silencing of connexin 43 significantly reduced migration of vector-transfected U373 MG cells only at 48 h, and had no significant effects on the migration of hepaCAM-expressing U373 MG cells. Thus, the inhibitory effects of hepaCAM on cell migration were not reversed or further enhanced by connexin 43 knockdown.
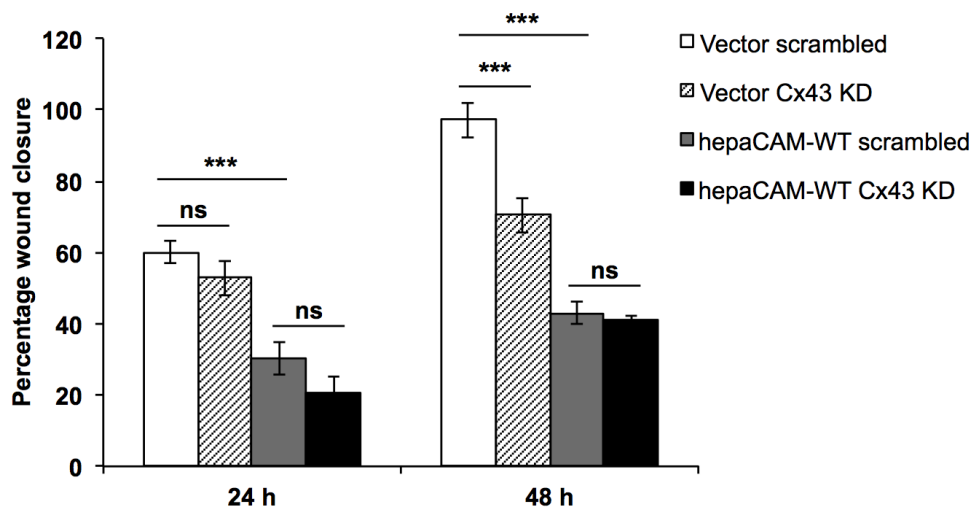
Figure 19. Silencing of connexin 43 does not affect the reduced migration of hepaCAM-expressing U373 MG cells. Vector-transfected and wild-type hepaCAM-expressing U373 MG cells were transfected with 5 nM scrambled siRNA or connexin 43 siRNA (Cx43 KD), and cell migration was assessed by the wound healing assay 24h post-transfection. Confluent monolayers were scratched with a pipette tip and the wounds were imaged at 0, 24 and 48 h. The sizes of the wounds were measured on the microscopic images to calculate the percentage wound closure (mean ± SD, n = 3). *** $p < 0.0001$ as assessed by one-way ANOVA with Tukey's multiple comparisons test. The results presented are representative of three independent experiments with similar results.

We next quantified the proliferation of vector-transfected and WT-hepaCAM U373 MG cells upon connexin 43 knockdown by the incorporation of radioactive ^{3}H-thymidine into newly synthesised DNA. While the proliferation of WT-hepaCAM-expressing U373 MG cells was significantly inhibited compared to vector-transfected cells consistent with previous findings, no significant difference in proliferation was observed in both cell lines upon connexin 43 knockdown (Figure 20).
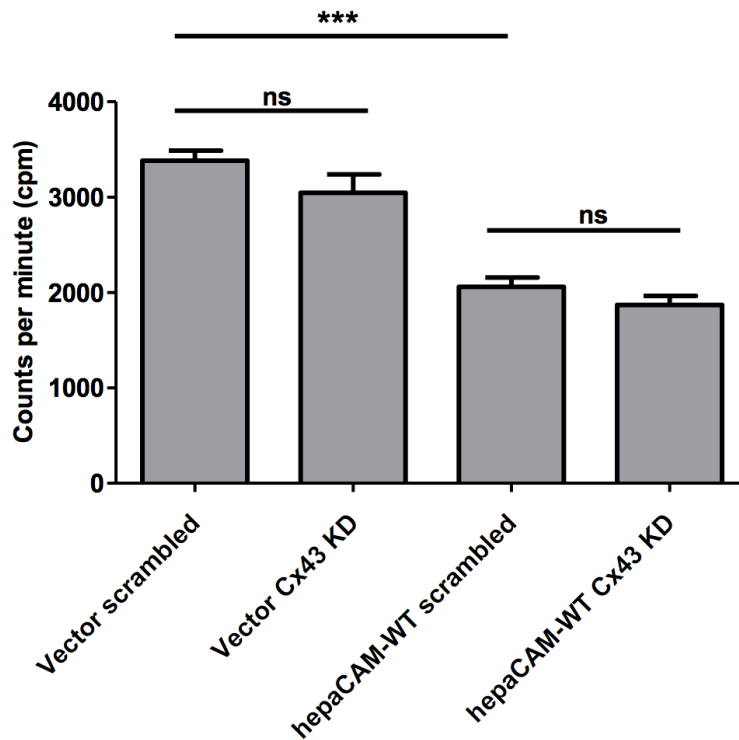
Figure 20. Silencing of connexin 43 does not affect the anti-proliferative effects of hepaCAM in U373 MG cells. Vector-transfected and wild-type hepaCAM-expressing U373 MG cells were transfected with 5 nM scrambled siRNA or connexin 43 siRNA (Cx43 KD). Cell proliferation was quantified 48 h post-transfection by the incorporation of ^{3}H-thymidine. Proliferation is indicated by counts per minute (cpm). The data represent means ± SE, n = 8. *** p < 0.0001 as assessed by one-way ANOVA with Tukey's multiple comparisons test. The results presented are representative of two independent experiments with similar results.

Thus, the results indicated that connexin 43 in U373 MG cells is not directly involved in the functions of hepaCAM in increasing cell adhesion, reducing migration and inhibiting proliferation.

3.1.12. hepaCAM increases gap junction activity in U373 MG cells

Since hepaCAM expression caused a re-distribution of connexin 43 to the cell surface at cell-cell contacts and the main function of connexin 43 is in gap junctions, we hypothesised that the hepaCAM-connexin 43 interaction may promote gap junction activity. Hence, we investigated gap junction activity in hepaCAM-expressing U373 MG cells by the calcein-AM transfer assay as described in detail in section 2.23. In this assay, donor cells stained with calcein-AM were co-cultured with unstained recipient cells of the same cell line and the percentage of recipient cells that have taken up calcein by gap junction transfer was measured by flow cytometry (Figure 21A). The percentage of control U373 MG cells in which calcein transfer occurred was 11%, and this was increased to about 23% in hepaCAM-expressing U373 MG cells (Figure 21B, C). Thus, the results indicated a two-fold increase in gap junction activity upon hepaCAM expression in U373 MG cells.

The calcein-AM transfer assay was also performed on control and hepaCAM-expressing MCF7 (Figure 21D, E) and HepG2 cells (Figure 21F, G). However, compared to U373 MG cells, the percentage of cells in which calcein transfer occurred was much lower at 1-2% in control and hepaCAM-expressing MCF7 and HepG2 cells. There was slight or no increase in the percentage calcein transfer upon hepaCAM expression in MCF7 and HepG2 cells. The minimal gap junction activity observed can be explained by the lack

of endogenous connexin 43 expression in control and hepaCAM-expressing MCF7 and HepG2 cells, as shown by a prolonged exposure in western blot analysis (Figure 21H). The results taken together indicate that hepaCAM specifically increases gap junction activity mediated by connexin 43.

Additionally, from the prolonged western blot exposure, hepaCAM-expressing U373 MG cells appear to have higher levels of post-translationally modified connexin 43, as observed by the stronger intensity for the slower-migrating bands of connexin 43 (Figure 21H). As discussed in section 1.7.2, connexin 43 is frequently phosphorylated. Thus, it is likely that these bands are for phosphorylated forms of connexin 43 which promote gap junction activity, as suggested by the higher gap junction activity in hepaCAM-expressing U373 MG cells.
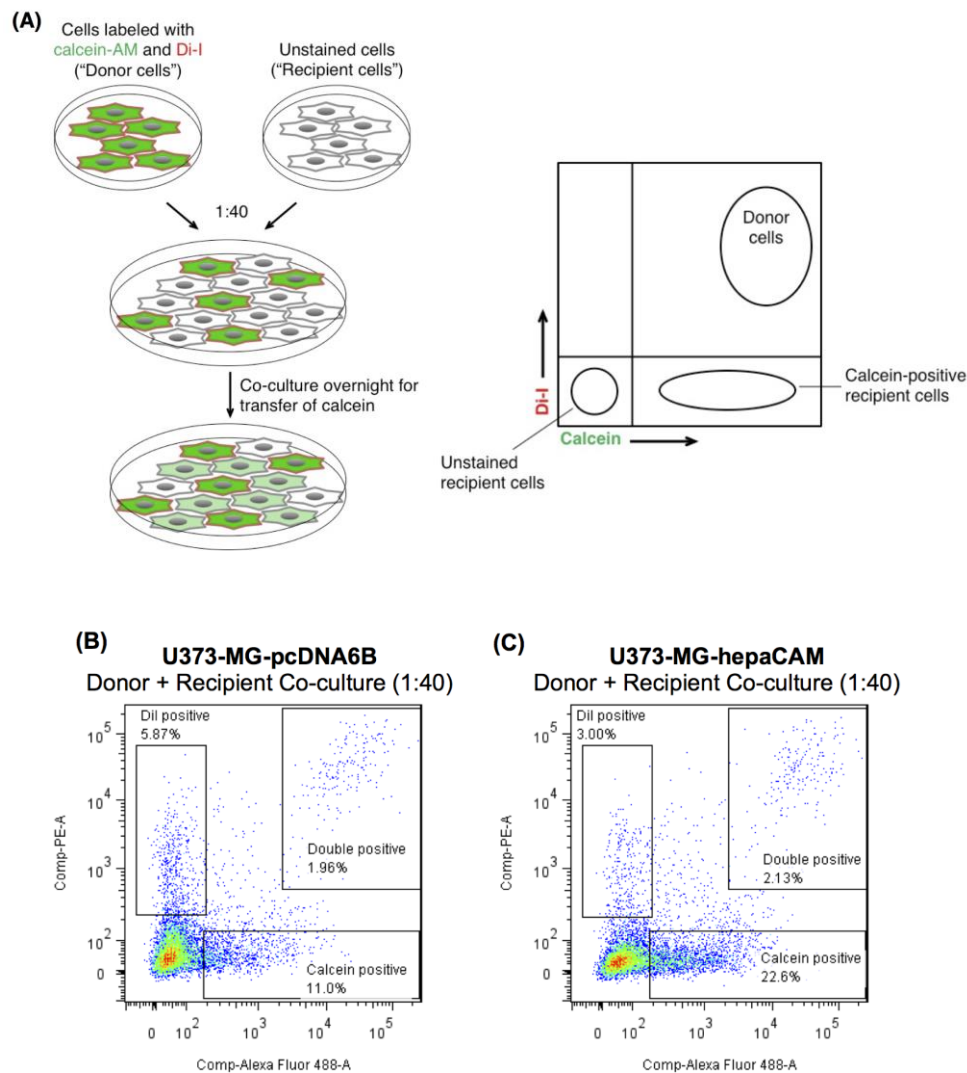
Figure 21. Expression of hepaCAM increases gap junction activity in U373 MG cells, but not in MCF7 and HepG2 cells. (A) Schematic for the quantification of gap junction activity by the calcein-AM transfer assay. Cells labelled with calcein-AM and DiI (donor) were co-cultured overnight with unlabelled cells (recipient) at a ratio of 1:40 (donor:recipient) and assayed by flow cytometry the next day. Gap junction activity is correlated to the percentage of calcein-positive recipient cells in (B) U373 MG cells stably transfected with the pcDNA6B/V5-His empty vector and (C) U373 MG cells stably transfected with hepaCAM. The results presented are representative of two independent experiments with similar results.
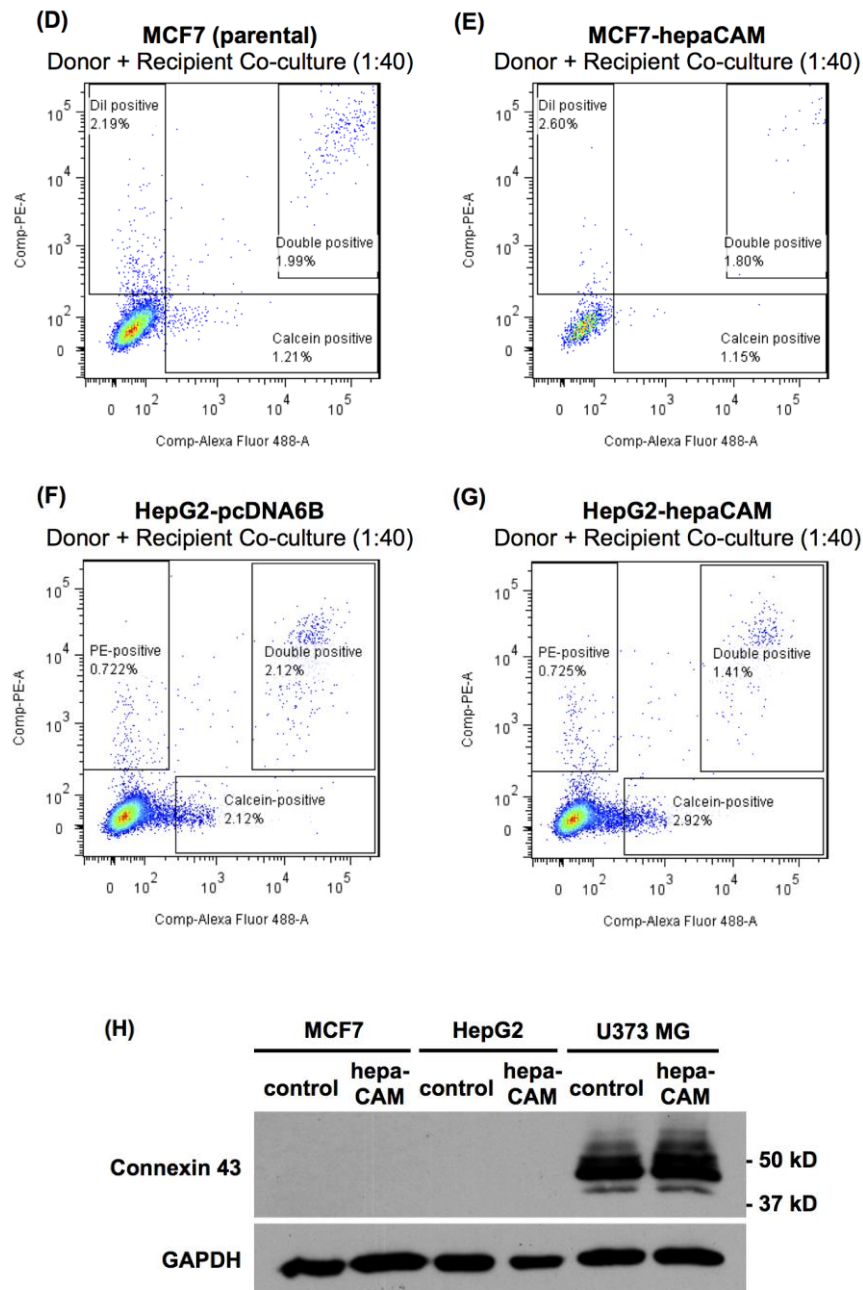
Figure 21 (continued). Expression of hepaCAM increases gap junction activity in U373 MG cells, but not in MCF7 and HepG2 cells. Gap junction activity is correlated to the percentage of calcein-positive recipient cells in (D) parental MCF7 cells, (E) MCF7 cells stably transfected with hepaCAM, (F) HepG2 cells stably transfected with the pcDNA6B/V5-His empty vector and (G) HepG2 cells stably transfected with hepaCAM. The results presented are representative of two independent experiments with similar results. (H) Connexin 43 expression in hepaCAM-expressing cancer cells. Cell lysates were prepared from control and hepaCAM-expressing MCF7, HepG2 and U373 MG cells. 50 μg of cell lysates were subjected to western blot analysis using connexin 43 antibody. GAPDH was used as a loading control. The result presented is a representative experiment of two independent experiments with similar results.

3.2 hepaCAM expression promotes cell death by anoikis

The previously published studies on hepaCAM have mainly focused on its functions in inhibiting proliferation and mediating cell-ECM adhesion and migration. We wanted to investigate whether hepaCAM has unpublished roles in cell-cell adhesion and cell survival. As discussed briefly in the introduction, cellular adhesion to the ECM mediated by CAMs transmits cell survival signals. When anchorage-dependent cells are detached from the ECM, anoikis, a form of programmed cell death, is induced. Thus, anoikis is a mechanism to maintain normal tissue organisation and prevent dysplasia by eliminating cells that have managed to escape from their environment (Frisch and Screaton, 2001). On the other hand, tumour cells tend to form multicellular aggregates or spheroids in the absence of attachment to the ECM. The formation of aggregates when tumour cells are grown under anchorage-independent conditions is proposed to suppress anoikis, facilitating their survival and metastasis (Kang et al., 2007; Zhang et al., 2004).

Since hepaCAM expression in U373 MG cells targets connexin 43 to cell-cell contacts and promotes gap junction activity, we wanted to study whether it also influences anoikis and the aggregation of U373 MG cells into spheroids. Vector-transfected and WT hepaCAM-expressing U373 MG cells were detached into a single-cell suspension and cultured overnight on dishes coated with poly-HEMA, which will prevent attachment and create anchorage-independent conditions. The sizes of the cellular aggregates formed were quantified by confocal microscopy (Figure 22), and the percentage anoikis was determined by annexin V/7-AAD staining (Figure 23). Interestingly, WT hepaCAM-expressing U373 MG cells tended to form significantly smaller

aggregates compared to vector-transfected U373 MG cells (Figure 22A, B). In addition, WT hepaCAM-expressing U373 MG cells grown under anchorage-independent conditions had a higher rate of apoptosis at 22.0% (7.1% higher than the baseline apoptosis of 14.9% in the monolayer culture), compared to vector-transfected U373 MG cells at 11.9% (4.5% higher than the baseline apoptosis of 7.4% in the monolayer culture) (Figure 23), suggesting that hepaCAM expression slightly increases the susceptibility of U373 MG cells to anoikis.
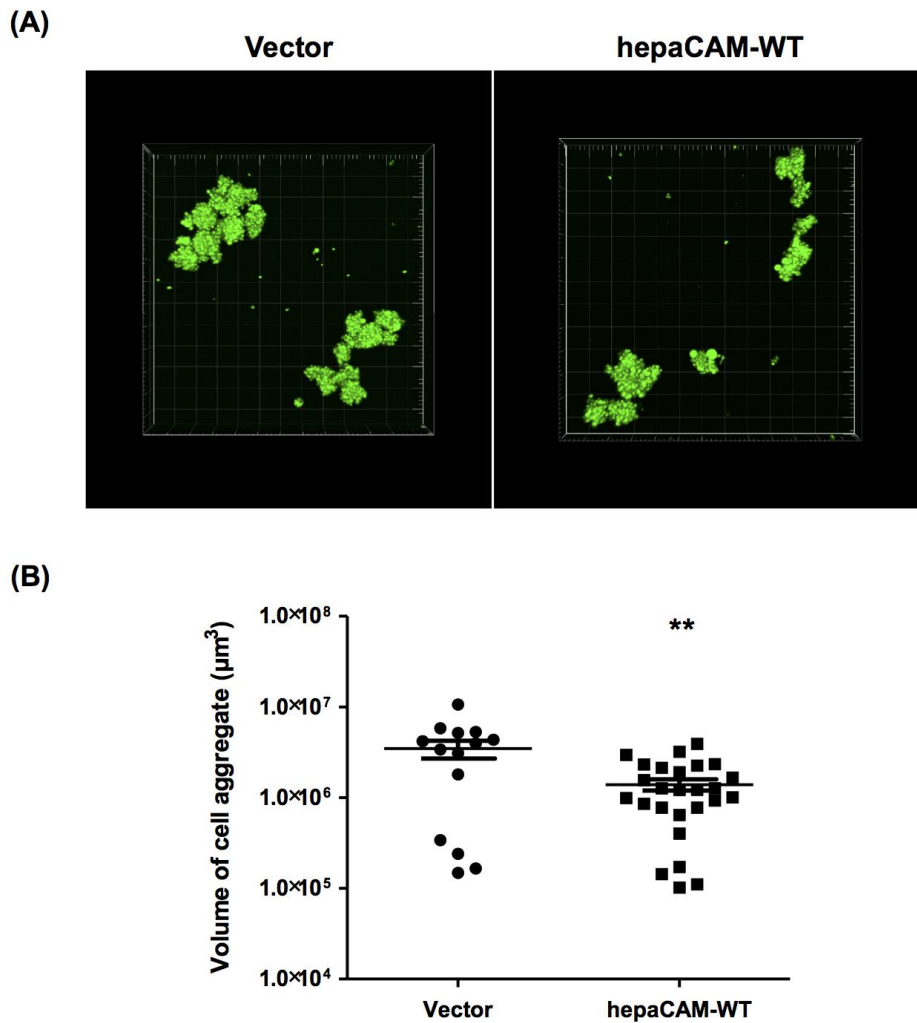
Figure 22. hepaCAM-expressing U373 MG cells form smaller aggregates when grown under anchorage-independent conditions. Vector-transfected and wild-type hepaCAM-expressing U373 MG cells were stained with calcein-AM, detached into a single-cell suspension and seeded onto poly-HEMA-coated culture dishes. After culturing overnight, the aggregates were visualised by confocal microscopy under a 10× objective. (A) Confocal z-stacks of the scans were reconstructed. The images presented here are representative of images taken from at least six different fields. (B) The volume of each aggregate was determined for vector-transfected (n = 14) and wild-type hepaCAM-expressing (n = 26) U373 MG cells. ** $p < 0.01$ as assessed by t-test.
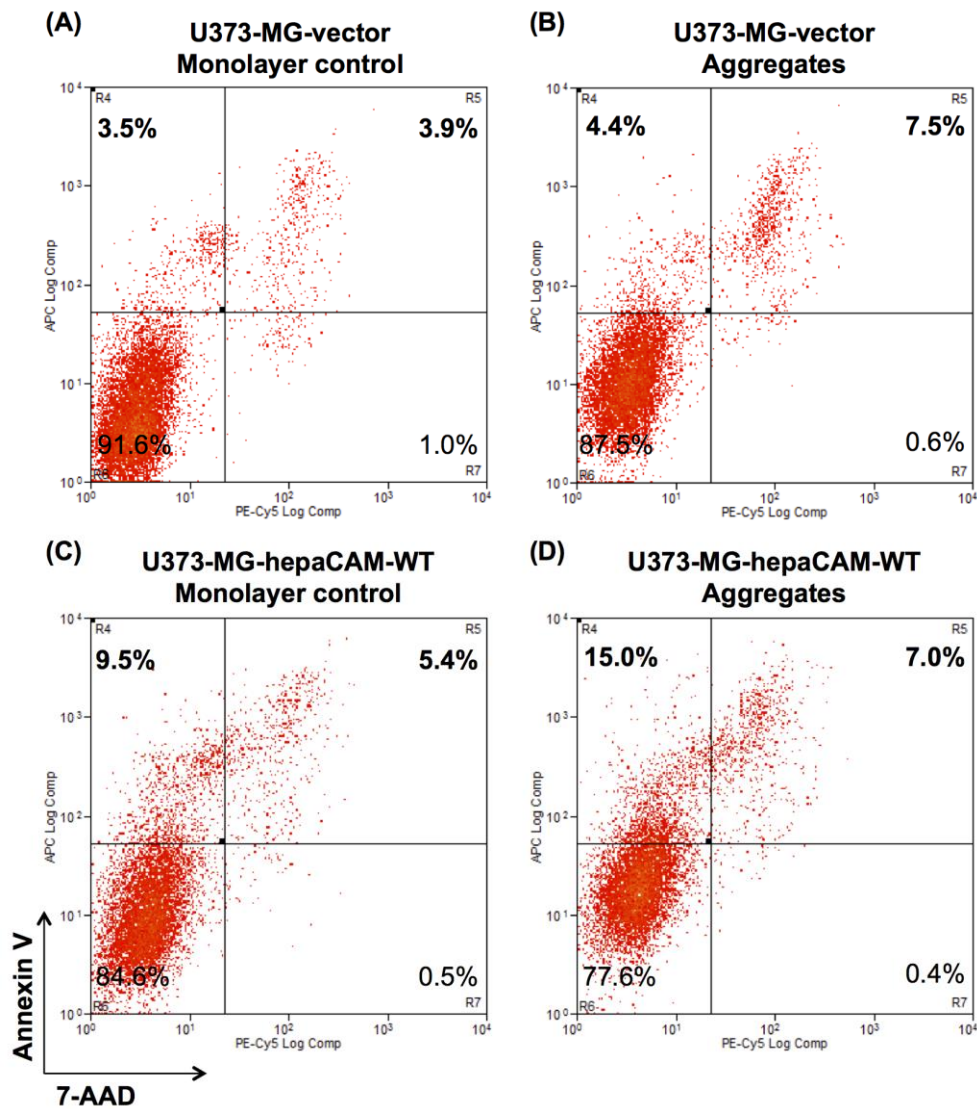
Figure 23. hepaCAM-expressing U373 MG cells are more susceptible to anoikis when grown under anchorage-independent conditions. Vector-transfected and wild-type hepaCAM-expressing U373 MG cells were detached into a single-cell suspension and seeded onto poly-HEMA-coated culture dishes. After culturing overnight, the aggregates were harvested, dissociated and assayed for anoikis by annexin V/7-AAD staining. Cells grown as monolayer cultures were included as controls to determine the baseline apoptosis. (A) The percentage total apoptosis in vector-transfected U373 MG cells grown as a monolayer is 7.4%. (B) The percentage total apoptosis in vector-transfected U373 MG cells grown under anchorage-independent conditions is 11.9%. (C) The percentage total apoptosis in wild-type hepaCAM-expressing U373 MG cells grown as a monolayer is 14.9%. (D) The percentage total apoptosis in wild-type hepaCAM-expressing U373 MG cells grown under anchorage-independent conditions is 22.0%.

3.3   hepaCAM signalling and proteolytic cleavage of the hepaCAM cytoplasmic domain

This section discusses the experiments to study the signals that lead to hepaCAM cytoplasmic domain cleavage in cancer cells exogenously expressing hepaCAM.

3.3.1. Mutations in hepaCAM affect cleavage of the hepaCAM cytoplasmic domain in U373 MG cells

As mentioned in section 1.6.8, hepaCAM expressed exogenously in MCF7 breast cancer cells undergoes proteolytic cleavage to generate a 25 kD fragment containing mainly the cytoplasmic domain (Zhang et al., 2010a). We wanted to study whether this phenomenon could also be observed in U373 MG glioblastoma cells stably transfected with WT hepaCAM. To detect the cleaved hepaCAM fragment by western blot, a custom-made antibody against the hepaCAM cytoplasmic domain was utilised. Western blot analysis showed that in addition to full-length hepaCAM at 75 kD, a band at approximately 25 kD could be detected in WT hepaCAM-expressing U373 MG cells. Since the 25 kD band was not detected in vector-transfected U373 MG cells, it indicates that it is specific for the cleaved hepaCAM fragment (Figure 24). Thus, the results suggest that proteolytic cleavage of the hepaCAM cytoplasmic domain is a ubiquitous event in the processing of hepaCAM in different cancer cell lines.
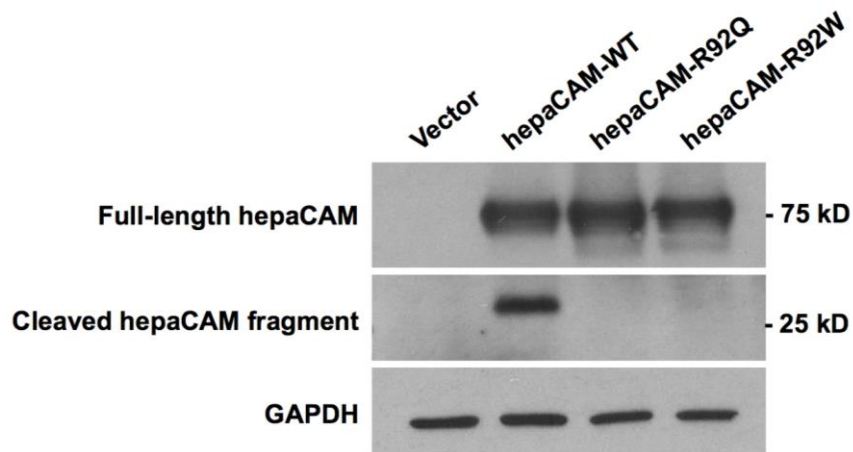
Figure 24. Mutations in the hepaCAM extracellular domain prevent proteolytic cleavage of the hepaCAM cytoplasmic domain in U373 MG cells. Cell lysates were prepared from U373 MG cells stably transfected with pcDNA3.1 vector, wild-type hepaCAM, hepaCAM-R92Q and hepaCAM-R92W. 20 µg of cell lysates were subjected to western blot analysis. Full-length hepaCAM was detected with an antibody against the hepaCAM extracellular domain. The 25 kD cleaved hepaCAM fragment was detected with an antibody against the hepaCAM cytoplasmic domain. GAPDH was used as a loading control. The result presented is a representative experiment of at least four independent experiments with similar results.

Since we were also interested in studying the signalling mechanisms which lead to hepaCAM cytoplasmic domain cleavage, we next determined whether the R92Q and R92W mutations in hepaCAM had any effects on the levels of the 25 kD cleaved hepaCAM fragment. Interestingly, the cleaved hepaCAM cytoplasmic domain was not detected in cells expressing hepaCAM-R92Q or hepaCAM-R92W (Figure 24). As these mutations occur in the hepaCAM extracellular domain, it suggested that signalling through the extracellular domain leads to proteolytic cleavage of the cytoplasmic domain.

3.3.2. Treatment with an antibody against the hepaCAM extracellular domain blocks cleavage of the hepaCAM cytoplasmic domain

To test the hypothesis that signalling through the hepaCAM extracellular domain leads to proteolytic cleavage of the cytoplasmic domain, we next determined the levels of the 25 kD cleaved fragment in WT hepaCAM-expressing U373 MG cells upon overnight treatment with an antibody against the hepaCAM extracellular domain. As observed in Figure 25, the levels of the cleaved hepaCAM cytoplasmic domain fragment were markedly reduced in cells treated with the hepaCAM antibody, compared to cells treated with the IgG control, indicating that the binding of the antibody to the hepaCAM extracellular domain inhibits proteolytic cleavage of the hepaCAM cytoplasmic domain in U373 MG cells. Thus, this antibody likely has antagonistic activities against the functions of hepaCAM.

The levels of the 25 kD cleaved hepaCAM fragment were also determined in in hepaCAM-expressing MCF7 and HepG2 cells upon overnight treatment with an antibody against the hepaCAM extracellular domain. Proteolytic cleavage of the hepaCAM cytoplasmic domain was observed in control IgG-treated MCF7 and HepG2 cells. However, upon treatment with the hepaCAM antibody, hepaCAM cytoplasmic domain cleavage was significantly inhibited in both MCF7 and HepG2 cells (Figure 26), similar to the observations in U373 MG cells and confirming the ubiquity of hepaCAM cytoplasmic domain processing in diverse cancer cell lines. The results also suggested a possibility that the signalling mechanisms leading to hepaCAM proteolytic cleavage are similar across different cell lines.

It should also be noted that the inhibition of hepaCAM cytoplasmic domain proteolytic cleavage occurred at comparable levels when cells were treated with hepaCAM antibody in immobilised or soluble form (Supplementary Figure 3).
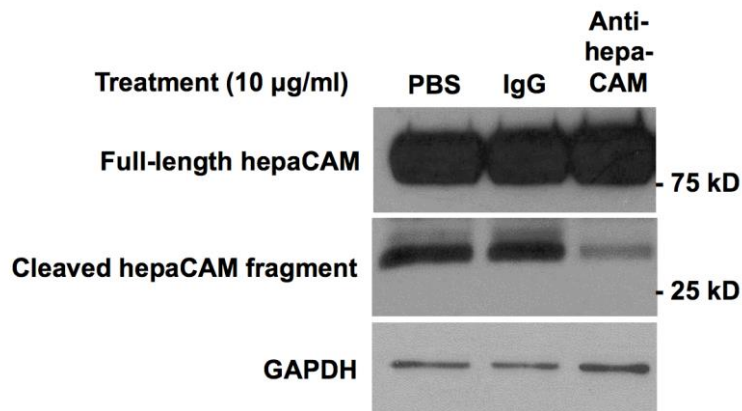
Figure 25. Treatment of hepaCAM-expressing U373 MG cells with an antibody against the hepaCAM extracellular domain prevents proteolytic cleavage of the hepaCAM cytoplasmic domain. Wild-type hepaCAM-expressing U373 MG cells were treated overnight with antibody against the hepaCAM extracellular domain in soluble form (10 μg/ml). Cells were also treated with PBS or the isotype mouse IgG1 as controls. The next day, cells were lysed and 20 μg of cell lysates were subjected to western blot analysis. Full-length hepaCAM (75 kD) and the cleaved hepaCAM fragment (25 kD) were detected using an antibody against the FLAG-tag on the hepaCAM cytoplasmic domain. GAPDH was used as a loading control. The result presented is a representative experiment of two independent experiments with similar results.
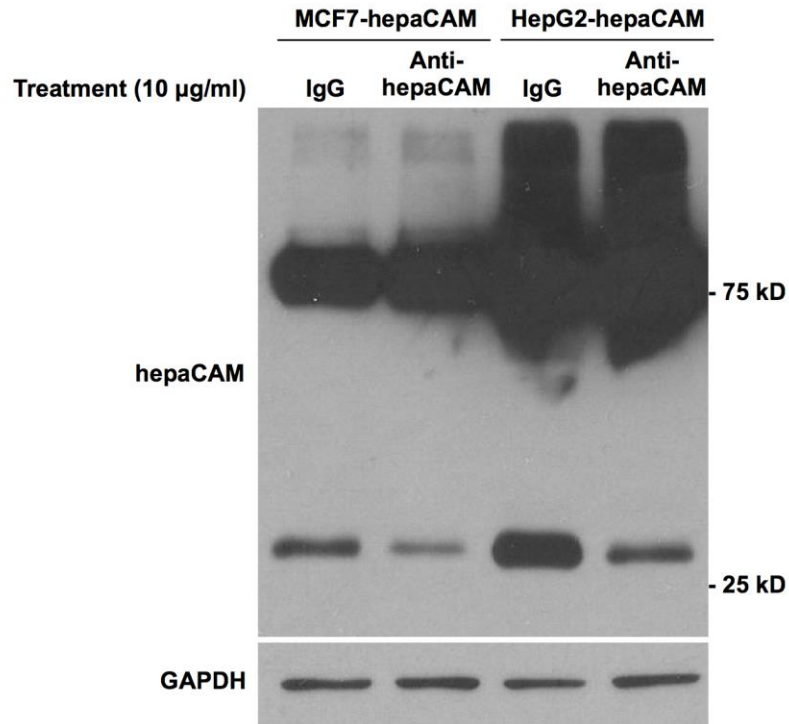
Figure 26. Treatment of hepaCAM-expressing MCF7 and HepG2 cells with an antibody against the hepaCAM extracellular domain prevents proteolytic cleavage of the hepaCAM cytoplasmic domain. MCF7 and HepG2 cells were stably transfected with hepaCAM and treated overnight with antibody against the hepaCAM extracellular domain in soluble form (10 μg/ml). Cells were also treated with the isotype mouse IgG1 as a control. The next day, cells were lysed and 20 μg of cell lysates were subjected to western blot analysis using antibodies against the V5-tag on the hepaCAM cytoplasmic domain. GAPDH was used as a loading control. The result presented is a representative experiment of two independent experiments with similar results.

3.3.3. Connexin 43 knockdown does not affect the cleavage of the hepaCAM cytoplasmic domain in U373 MG cells

As shown in section 3.1, the extracellular domain of hepaCAM interacts with connexin 43. Since treatment of U373 MG cells with an antibody against the hepaCAM extracellular domain inhibited hepaCAM cytoplasmic domain cleavage and concomitantly downregulated connexin 43 expression, we wanted to investigate the possibility that these two events may be interconnected in U373 MG cells. Such a possibility was also suggested by the observation that hepaCAM cytoplasmic domain cleavage is inhibited in the mutant hepaCAM-expressing U373 MG cells which also have reduced connexin 43 expression. To determine whether connexin 43 expression had any effects on hepaCAM cytoplasmic domain cleavage, silencing of connexin 43 expression was performed in WT hepaCAM-expressing U373 MG cells by transfection with connexin 43 siRNA, and the levels of the 25 kD cleaved hepaCAM fragment were evaluated 48 h post-transfection by western blot.
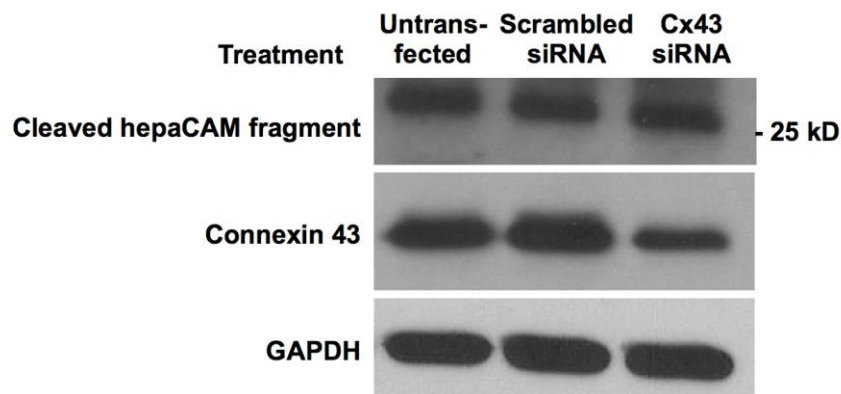
Figure 27. Silencing of connexin 43 does not affect proteolytic cleavage of the hepaCAM cytoplasmic domain in U373 MG cells. Wild-type hepaCAM-expressing U373 MG cells were transfected with 5 nM connexin 43 siRNA or scrambled siRNA and lysed 48 h post-transfection. 20 μg of cell lysates were subjected to western blot analysis using an antibody against the hepaCAM cytoplasmic domain to detect the 25 kD cleaved hepaCAM fragment, and connexin 43 antibody. GAPDH was used as a loading control.

Silencing of connexin 43 did not affect hepaCAM cytoplasmic domain cleavage, as the levels of 25 kD cleaved hepaCAM fragment were comparable in scrambled and connexin 43 siRNA-transfected cells (Figure 27). The results thus indicated that while neutralisation of hepaCAM with an antibody both inhibited hepaCAM cytoplasmic domain cleavage and downregulated connexin 43 expression, these two downstream events were regulated independently of each other in U373 MG cells.

3.3.4. The cleaved hepaCAM cytoplasmic domain fragment is localised to the endomembrane system and the nucleus

To further understand the functions of the cleaved hepaCAM cytoplasmic domain fragment, subcellular fractionation was performed to determine its localisation in hepaCAM-expressing cells. The cytoplasmic, membrane (containing the contents of the plasma, mitochondria, ER and Golgi membranes), soluble nuclear and chromatin-bound nuclear fractions were isolated from hepaCAM-expressing HepG2 cells and analysed by western blot using the antibody against the hepaCAM cytoplasmic domain.
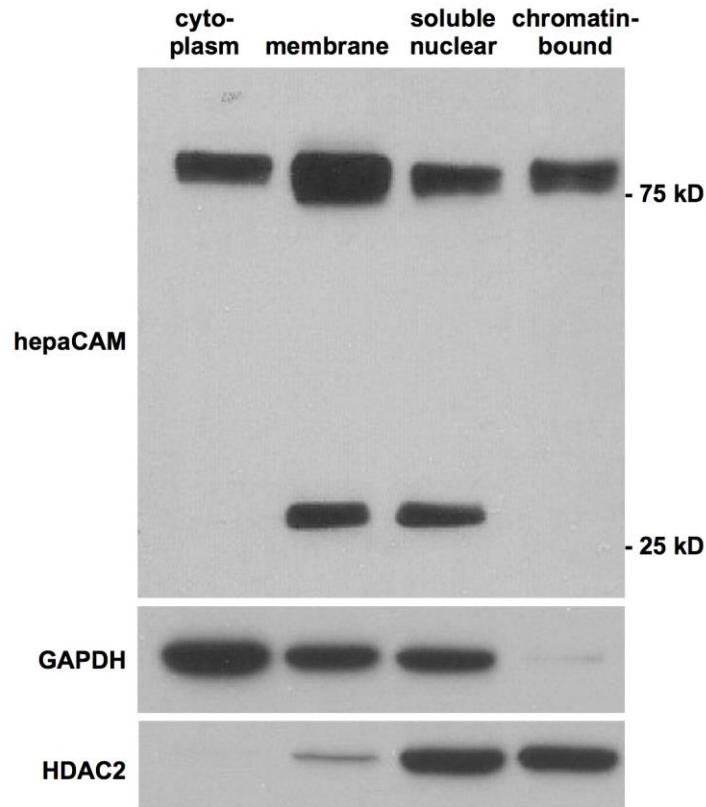
Figure 28. The cleaved hepaCAM cytoplasmic domain fragment is localised to the membrane and soluble nuclear fractions. HepG2 cells stably transfected with hepaCAM were subjected to subcellular fractionation to isolate the cytoplasmic, membrane, soluble nuclear and chromatin-bound nuclear fractions. The membrane fraction contains the contents of the plasma, mitochondria, ER and Golgi membranes. 20 μg of each fraction was subjected to western blot analysis. Full-length hepaCAM and the cleaved hepaCAM fragment were detected with an antibody against the hepaCAM cytoplasmic domain. GAPDH and HDAC2 were used as loading controls for the cytoplasmic and soluble nuclear fractions respectively.

As shown in Figure 28, full-length hepaCAM was detected in all fractions, with the highest levels found in the membrane fraction. The 25 kD cleaved hepaCAM fragment was detected in both the membrane and soluble nuclear fractions. Similar localisation of full-length hepaCAM and the cleaved hepaCAM fragment was also observed in U373 MG cells (data not shown). The presence of the cleaved hepaCAM fragment in the membrane fraction suggests two possibilities: (1) the cytoplasmic domain of hepaCAM may be cleaved post-translationally by proteases in the ER and Golgi compartments while it is trafficked to the plasma membrane; (2) hepaCAM may undergo proteolytic cleavage in the endosomal vesicles upon its internalisation. Furthermore, its presence in the soluble nuclear fraction and its absence in the chromatin-bound nuclear fraction indicate that it may have functions in the regulation of gene expression but does not directly bind to DNA sequences as a transcription factor. The origin of the cleaved hepaCAM fragment in the soluble nuclear fraction is not known at this point, as full-length hepaCAM could also be detected in the same fraction. Hence, it could have arisen from its translocation to the nucleus or proteolytic cleavage of hepaCAM present in the nucleus itself.

3.3.5. hepaCAM undergoes proteolytic cleavage upon binding to the integrin ligand fibronectin

The proteolytic cleavage of the hepaCAM cytoplasmic domain was inhibited by the R92Q and R92W mutations in the hepaCAM extracellular domain, and by the neutralising antibody which also binds to the hepaCAM extracellular domain. These two observations led us to postulate that the binding of hepaCAM to an extracellular ligand provides the signal for the cleavage of the cytoplasmic domain.

Expression of hepaCAM has been previously shown to increase cell adhesion and spreading on the ECM component fibronectin in the three cancer cell lines, HepG2, MCF7 and U373 MG (Lee et al., 2009; Moh et al., 2005a; Moh et al., 2005b). Since proteolytic cleavage of the hepaCAM cytoplasmic domain was also observed in these three cell lines, and was similarly inhibited by the antibody against the hepaCAM extracellular domain, we hypothesised that the interaction of hepaCAM with fibronectin may lead to proteolytic cleavage of the hepaCAM cytoplasmic domain. To verify the interaction of hepaCAM with fibronectin, the binding of fluorescently labelled fibronectin to WT hepaCAM-expressing U373 MG cells was measured by flow cytometry. As shown in Figure 29, binding to fibronectin was observed in 5.7% of vector-transfected U373 MG cells and was increased to 22.0% for WT-hepaCAM-expressing cells. These results confirmed that hepaCAM interacts with fibronectin, although it remains to be seen whether the interaction is direct or indirect.
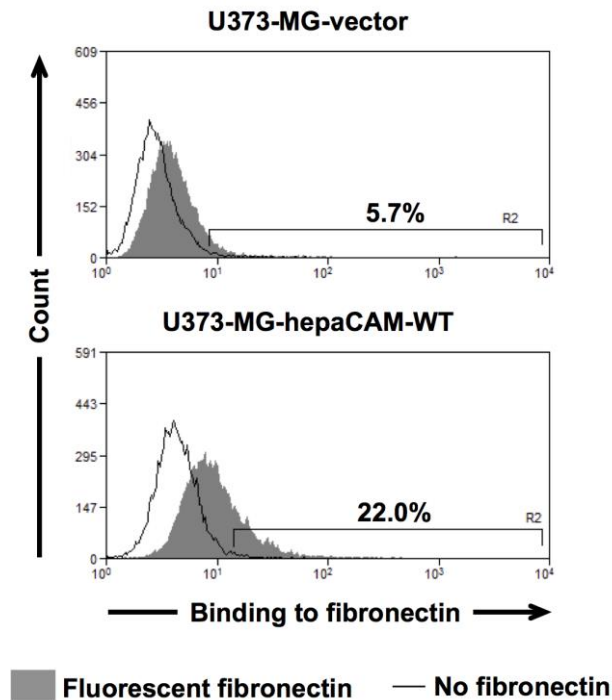
Figure 29. hepaCAM binds to fibronectin. U373 MG cells stably transfected with pcDNA3.1 vector or wild-type hepaCAM were dissociated and incubated with fluorescently labelled fibronectin (50 μg/ml) for 15 min, washed and analysed by flow cytometry. Indicated are the percentages of cells bound to fluorescently labelled fibronectin as compared to the background signal. The results presented are representative of four independent experiments with similar results.

To test the hypothesis that binding to the integrin ligand fibronectin induces proteolytic cleavage of the hepaCAM cytoplasmic domain, WT hepaCAM-expressing U373 MG cells were detached from a cell culture flask and seeded onto fibronectin-coated plates in a short time-course experiment of up to 60 min. As a control, cells were also seeded onto plates coated with the non-integrin ligand poly-L-lysine. In contrast to ECM proteins such as fibronectin, poly-L-lysine promotes cell attachment non-specifically and does not promote morphological spreading of cells (Akiyama, 2002). After allowing the cells to attach, they were harvested at the time-points 10, 30 and 60 min and western

blot analysis was performed to determine the levels of the 25 kD cleaved hepaCAM fragment upon adhesion to fibronectin (Figure 30).
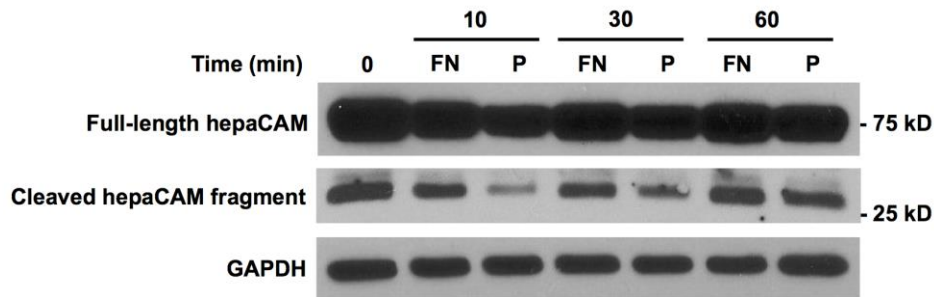
Figure 30. The hepaCAM cytoplasmic domain is proteolytically cleaved upon adhesion of hepaCAM-expressing U373 MG cells on fibronectin. U373 MG cells stably transfected with wild-type hepaCAM were detached and allowed to adhere to fibronectin-coated plates (FN). Plates coated with poly-L-lysine (P), a non-integrin ligand, were included as controls. An aliquot of the detached cells was retained as a control for time-point 0. At the respective time-points (10, 30 and 60 min), all cells were harvested and lysed. 20 μg of cell lysates were subjected to western blot analysis using an HRP-conjugated FLAG antibody to detect the FLAG-tag on the hepaCAM cytoplasmic domain. The result presented is a representative experiment of three independent experiments with similar results.

As shown in Figure 30, there was increased proteolytic cleavage of the hepaCAM cytoplasmic domain in cells adhered to the fibronectin-coated plates compared to cells adhered to the poly-L-lysine control at 10 and 30 min, suggesting that integrin-mediated adhesion of cells to fibronectin induces hepaCAM cleavage. The gradual increase in hepaCAM proteolytic cleavage across time in cells adhered to the poly-L-lysine could be due to the eventual secretion of ECM proteins by U373 MG cells themselves.

3.3.6. hepaCAM is internalised upon adhesion and spreading of cells on fibronectin

In U373 MG cells, hepaCAM can be detected in intracellular punctuate structures which suggested its presence in vesicles of the endomembrane system (Figure 6). Furthermore, subcellular fractionation showed that the cleaved hepaCAM fragment was detected in the membrane fraction, which contains components of the endomembrane system (Figure 28). Thus, we hypothesised that hepaCAM may be internalised upon the adhesion and spreading of cells on fibronectin, leading to its proteolytic cleavage.

We first determined the subcellular localisation of hepaCAM in well-spread U373 MG cells grown on untreated cell culture plates. Cells were co-stained with the organelle markers: early endosome antigen 1 (EEA1), protein disulfide isomerase (PDI) and estrogen receptor-binding fragment-associated gene 9 (EBAG9, also known as RCAS1), which are markers for the endosomes, ER and the Golgi apparatus respectively.
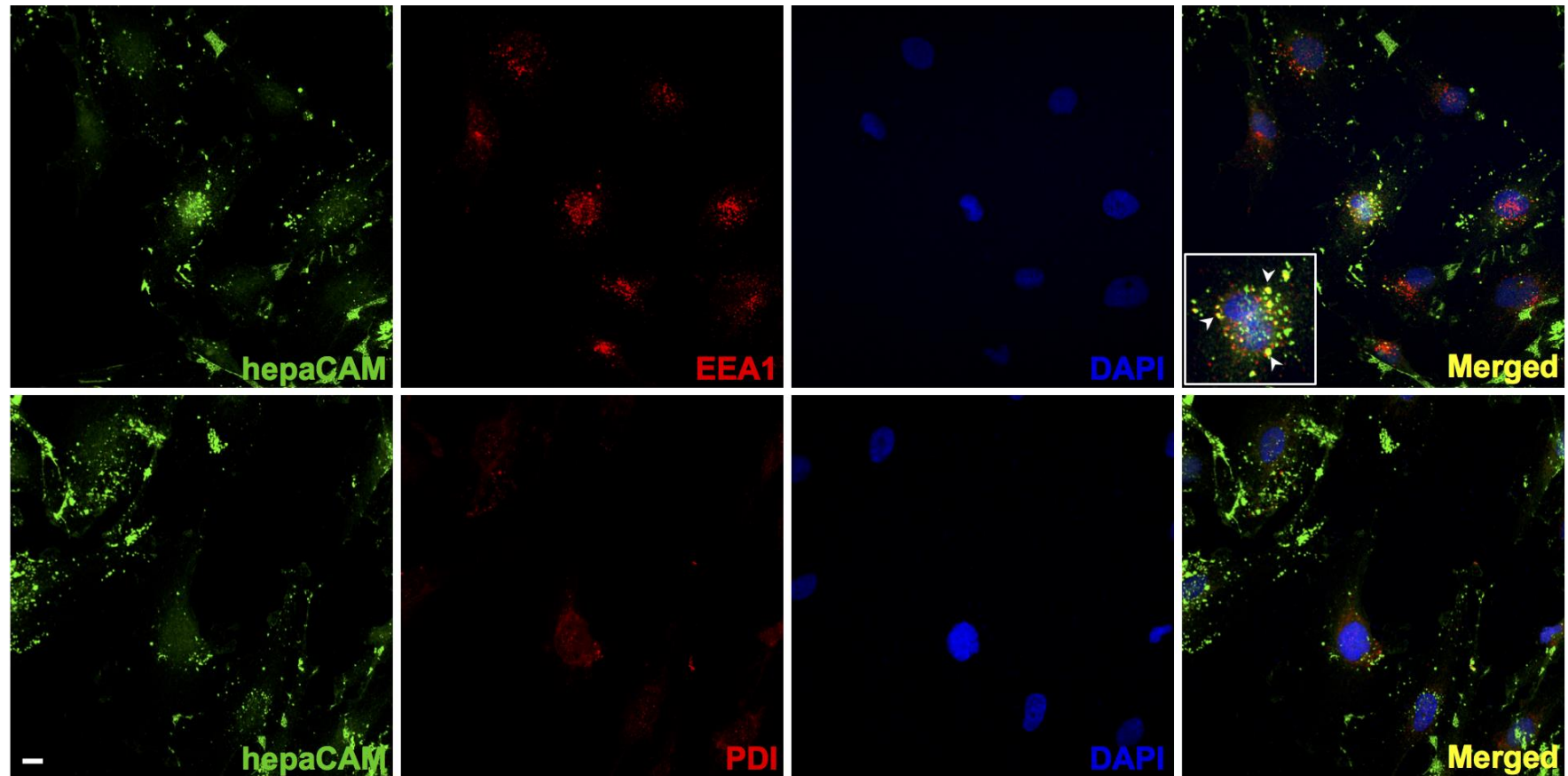
Figure 31. hepaCAM is localised in the early endosomes. U373 MG cells stably transfected with wild-type hepaCAM were stained with antibodies against the hepaCAM cytoplasmic domain (green) and one of the indicated organelle markers (red). The organelle markers were EEA1 (early endosomes), PDI (endoplasmic reticulum) and EBAG9 (Golgi apparatus) (next page). Co-localisation is indicated by yellow fluorescence. hepaCAM staining co-localised with EEA1 is shown by white arrows in the inset. Nuclei were stained with DAPI (blue). Cells were visualised by confocal microscopy under a 60× objective. The images presented here are representative of images taken from at least six different fields. Scale bar: 10 μm.
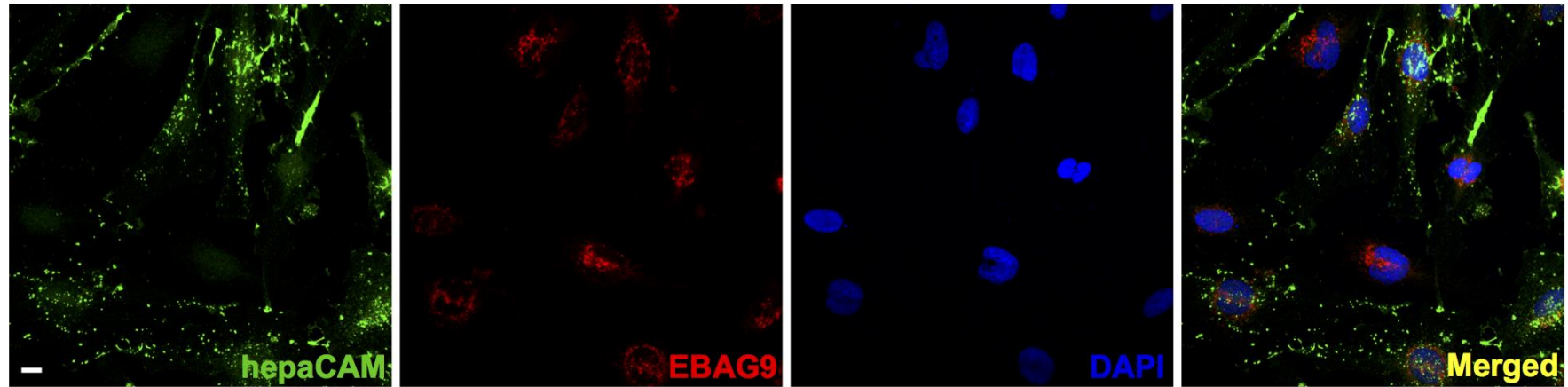
Figure 31 (continued). hepaCAM is localised in the early endosomes. U373 MG cells stably transfected with wild-type hepaCAM were stained with antibodies against the hepaCAM cytoplasmic domain (green) and one of the indicated organelle markers (red). The organelle markers were EEA1 (early endosomes) (previous page), PDI (endoplasmic reticulum) (previous page) and EBAG9 (Golgi apparatus). Co-localisation is indicated by yellow fluorescence. hepaCAM staining co-localised with EEA1 is shown by white arrows in the inset. Nuclei were stained with DAPI (blue). Cells were visualised by confocal microscopy under a 60× objective. The images presented here are representative of images taken from at least six different fields. Scale bar: 10 μm.

Immunofluorescent staining showed a partial co-localisation of hepaCAM with EEA1 in the early endosomes and no significant co-localisation of hepaCAM with PDI in the ER and with EBAG9 in the Golgi apparatus (Figure 31). In addition, there were intracellular punctuate structures containing hepaCAM but not co-stained with EEA1, and we postulate these may be staining for hepaCAM in secretory vesicles and/or endosomes at later stages. The results suggested that hepaCAM in untreated U373 MG cells undergoes internalisation as part of its normal turnover or signal transduction, and we hypothesise that this occurs prior to proteolytic cleavage of the hepaCAM cytoplasmic domain.

Since integrin-mediated adhesion of cells to fibronectin induces cleavage of the hepaCAM cytoplasmic domain, we wanted to determine whether this also induces the internalisation of hepaCAM. WT hepaCAM-expressing U373 MG cells were detached from a cell culture flask and seeded onto fibronectin-coated and poly-L-lysine-coated culture plates. Cells were allowed to adhere to the plates for 1 and 7 h before they were fixed and stained for hepaCAM and EEA1 (Figure 32).
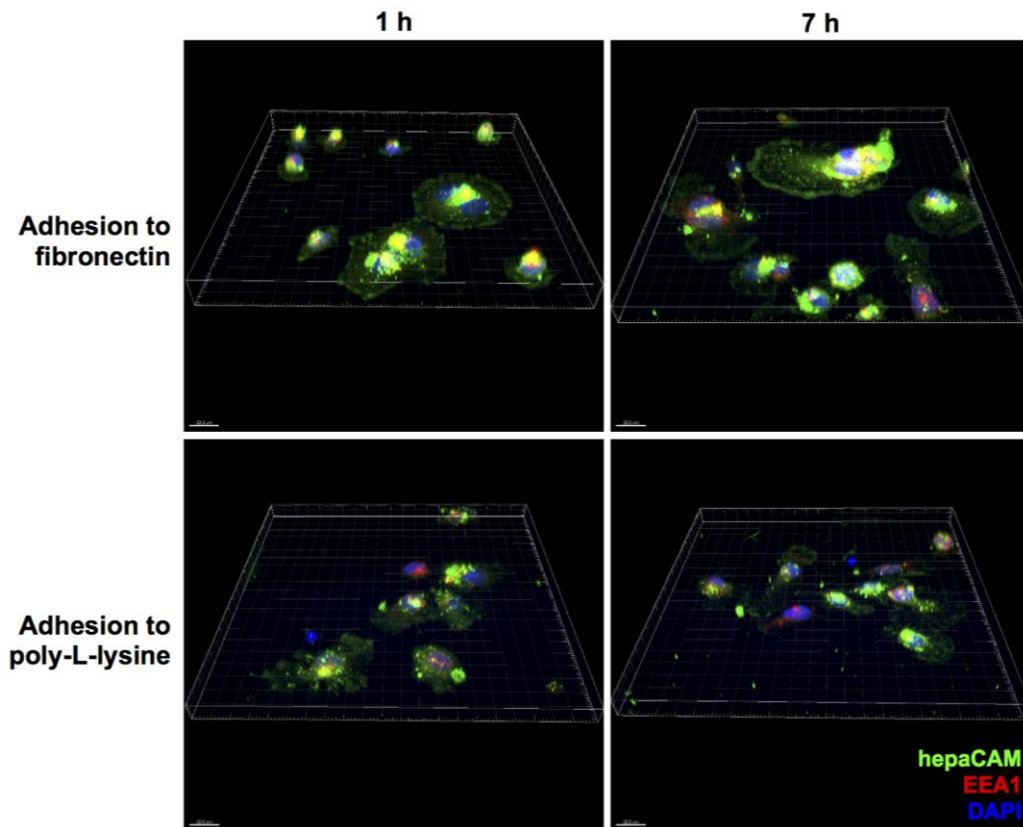
Figure 32. hepaCAM is internalised upon the adhesion and spreading of hepaCAM-expressing U373 MG cells on fibronectin. U373 MG cells stably transfected with pcDNA3.1 vector or wild-type hepaCAM were detached and allowed to adhere to fibronectin-coated plates. Plates coated with poly-L-lysine, a non-integrin ligand, were included as a control. After 1 and 7 h, unattached or loosely adherent cells were washed away, and attached cells were fixed and stained with antibodies against the hepaCAM cytoplasmic domain (green) and EEA1 (red). Co-localisation of hepaCAM and EEA1 is indicated by yellow fluorescence. Nuclei were stained with DAPI (blue). Cells were visualised by confocal microscopy under a 60× objective and confocal z-stacks of the scans were reconstructed. The images presented here are representative of images taken from at least six different fields. Scale bar: 20 μm.

As shown in Figure 32, upon the adhesion and spreading of cells on fibronectin for 1 h, there was significant co-localisation of hepaCAM with EEA1, indicating an internalisation of hepaCAM. The co-localisation persisted when cells were incubated for 7 h. In contrast, there was minimal co-localisation of hepaCAM with EEA1 in cells adhered to poly-L-lysine at 1 and 7 h. Furthermore, cells adhered to poly-L-lysine did not appear morphologically well-spread compared to cells adhered to fibronectin. Thus, the results suggested that hepaCAM is internalised upon integrin-mediated adhesion to and spreading of cells on fibronectin, and this concomitantly promotes hepaCAM proteolytic cleavage (Figure 30).

CHAPTER 4   DISCUSSION

4.1.   Interaction of hepaCAM with connexin 43

hepaCAM has been previously shown to interact with the membrane protein MLC1 and the chloride channel ClC-2 at the cell-cell junctions of astrocytes (Jeworutzki et al., 2012; Lopez-Hernandez et al., 2011a). In this present study, co-localisation and co-IP assays revealed a novel physical interaction of hepaCAM with the gap junction protein connexin 43 at cell-cell junctions of U373 MG human glioblastoma cells of astrocytic origin (Figure 33A). This interaction is not entirely unexpected, as MLC1 has been previously found to partially co-localise with connexin 43 at the astrocytic junctions (Duarri et al., 2011). The hepaCAM-connexin 43 interaction is also the first interaction of hepaCAM with a junctional protein to be observed in cancer cells. In MCF7 human breast cancer cells, no physical interaction of hepaCAM with the adherens junction protein E-cadherin was observed in co-IP assays, although the two proteins appeared to co-localise (Moh et al., 2005b).

It was observed that the R92Q and R92W mutations which occur in the extracellular domain of hepaCAM, and the antibody which binds to the hepaCAM extracellular domain both disrupt the interaction of hepaCAM with connexin 43 at cell-cell contacts (Figure 33B, C). This suggested that the interaction of hepaCAM and connexin 43 occurs via the hepaCAM extracellular domain. The hepaCAM extracellular domain, specifically the first Ig-like domain, has been previously shown to be essential in its interaction with the lipid raft protein caveolin-1 (Moh et al., 2009a). Since the R92Q and R92W mutations in hepaCAM occur in the first Ig-like domain, we

postulate that the interaction of hepaCAM with connexin 43 also occurs via this domain. The association of hepaCAM with F-actin, on the other hand, was suggested to be dependent on its cytoplasmic domain, but require an intact hepaCAM containing the extracellular domain (Moh et al., 2009b). As discussed in section 1.2.1, Ig-CAMs can establish heterophilic *cis*-interactions with other transmembrane proteins, as well as interact with cytoskeletal proteins and adaptor proteins. Thus similar to other Ig-CAMs, hepaCAM exhibits *cis*-interactions with the transmembrane proteins connexin 43 and caveolin-1 via its extracellular domain and associates with the actin cytoskeleton via its cytoplasmic domain.
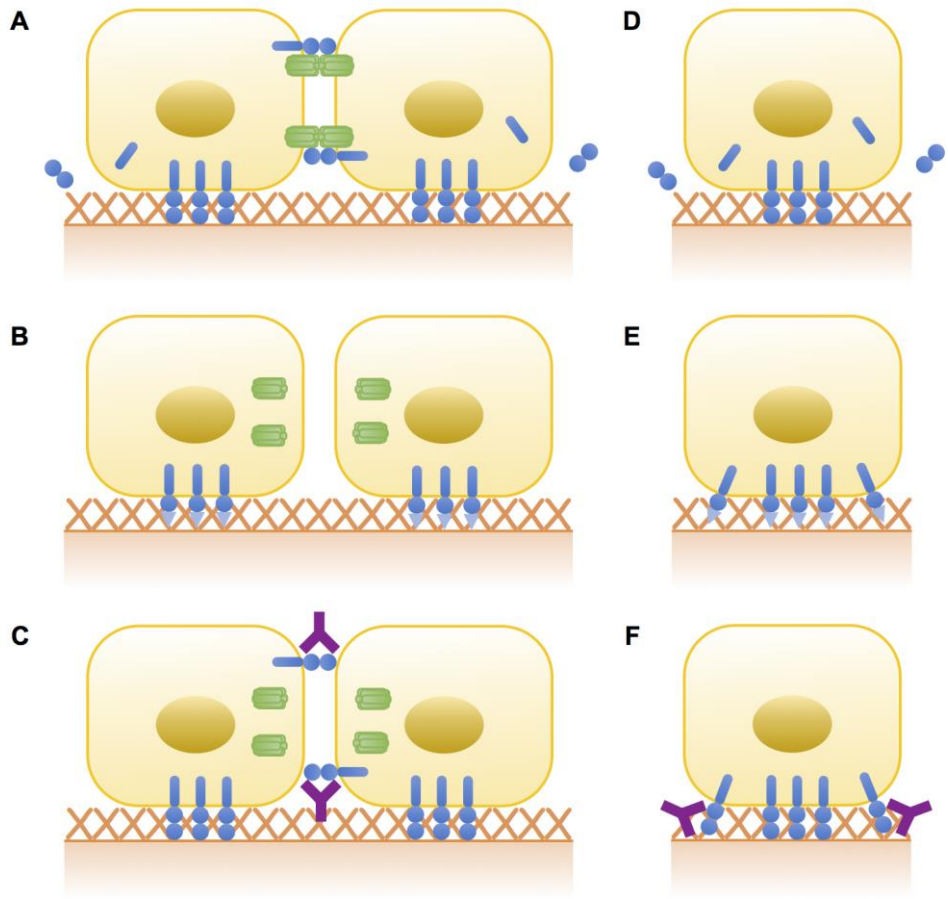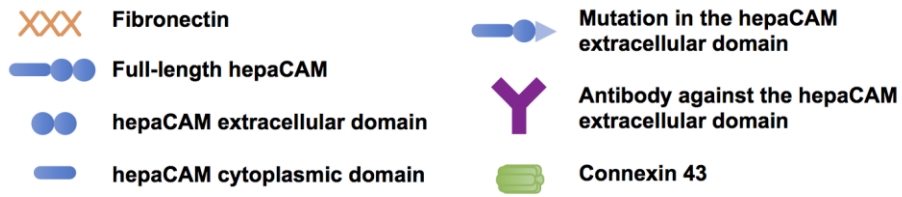
Figure 33. Schematic depiction of hepaCAM activities in U373 MG cells. (A) hepaCAM associates with connexin 43 at cell-cell contacts. (B) The R92Q and R92W mutations in the hepaCAM extracellular domain prevent association of hepaCAM with connexin 43 at cell-cell contacts. (C) Treatment of cells with antibody against the hepaCAM extracellular domain prevents association of hepaCAM with connexin 43 at cell-cell contacts and downregulates cell surface expression of connexin 43. (D) The hepaCAM cytoplasmic domain undergoes proteolytic cleavage under normal culture conditions or upon adhesion to the integrin ligand fibronectin. (E) The R92Q and R92W mutations in the hepaCAM extracellular domain block proteolytic cleavage of the cytoplasmic domain. (F) Treatment of cells with antibody against the hepaCAM extracellular domain blocks proteolytic cleavage of the cytoplasmic domain.

As shown by co-IP assays without prior cross-linking of proteins, connexin 43 was weakly co-immunoprecipitated with hepaCAM-R92Q or hepaCAM-R92W, compared to WT hepaCAM. However upon cross-linking, connexin 43 could be co-immunoprecipitated effectively with WT hepaCAM and mutant hepaCAM. This suggested that the binding site of hepaCAM to connexin 43 involves arginine (residue 92) in the first Ig-like domain, and that the R92Q and R92W mutations in hepaCAM both reduce the stability of its interaction with connexin 43. In the study by Lopez-Hernandez et al. (2011b), split-TEV assays showed that hepaCAM-R92Q had a decrease in its ability to hetero-oligomerise with MLC1, while hepaCAM-R92W still retained the ability to oligomerise with MLC1 at similar levels as WT hepaCAM. Thus, the R92Q and R92W mutations in hepaCAM appear to have differing effects on its interaction with connexin 43 and MLC1. For the R92Q mutation, the positively-charged (or basic) arginine is mutated to the polar uncharged glutamine, while for the R92W mutation, arginine is mutated to the non-polar tryptophan, which has a large hydrophobic side chain. The chemical bonds underlying hepaCAM's interactions with connexin 43 and MLC1 may be different, and hence the mutations may affect the binding affinity differently. It would be interesting to determine whether the other MLC-causing mutations in hepaCAM also affect its interaction with connexin 43, and this will also aid in further delineating the hepaCAM residues involved in the binding site. It would also be interesting to determine how the MLC-causing mutations in hepaCAM, including R92Q and R92W, affect its interaction with caveolin-1.

The cytoplasmic tail on the C-terminal end of connexin 43 contains several protein-protein interaction motifs, and has been shown to interact with various

proteins including the tight junction protein ZO-1 (Giepmans, 2004, 2006). As our findings indicate that it is the extracellular domain of hepaCAM which interacts with connexin 43, it is likely that this *cis*-interaction involves the extracellular loops of connexin 43. The docking of two apposing connexons to form a gap junction channel is dependent on the *trans*-interactions of the extracellular loops of connexins (Segretain and Falk, 2004). However, not much is currently known about the *cis*-interactions of the extracellular loops of connexin 43 with other proteins.

Although we have shown a physical interaction of hepaCAM and connexin 43 by co-IP assays, it is not completely known at this point whether the interaction is direct or indirect. While hepaCAM has also been shown to interact with caveolin-1 by co-IP assays, sequence analysis failed to identify consensus caveolin-binding motifs in hepaCAM (Moh et al., 2009a), raising the possibility that its interaction with caveolin-1 may be indirect. Thus, it still remains an open question whether hepaCAM interacts with connexin 43 as part of a complex containing other proteins. Since hepaCAM interacts with MLC1 and MLC1 partially co-localises with connexin 43, we also tried to determine MLC1 expression in vector-transfected and WT hepaCAM-expressing U373 MG cells by western blot analysis. However, despite using an anti-MLC1 antiserum (Lopez-Hernandez et al., 2011a) and two different commercial anti-MLC1 polyclonal antibodies, multiple non-specific bands were obtained and no distinct band for MLC1 was observed at the expected size of 41 kD (data not shown). As MLC1 could not be unambiguously detected in U373 MG cells, this aspect of the study was not further pursued.

4.2. hepaCAM is involved in the targeting of connexin 43 to cell-cell contacts

An aberrant localisation of connexin 43 in the cytoplasm of cancer cells instead of the cell membrane has been observed in chemically-induced tumours and the invasive parts of carcinomas, suggesting this may be a general phenomenon in tumourigenesis. The mechanisms leading to the aberrant localisation of connexin 43 are not completely understood (Mesnil et al., 2005). In some cases, the cytoplasmic localisation of connexin 43 has been attributed to its impaired trafficking to the membrane, resulting in a loss of GJIC (Govindarajan et al., 2002). In other cases, the intracellular accumulation of connexin 43 has been reported to be due to its internalisation in endosomes (Guan and Ruch, 1996; Mograbi et al., 2003).

In this study, we observed an intracellular accumulation of connexin 43 in U373 MG cells, with little staining at the cell membrane, similar to previous studies in glioblastoma cells (Cottin et al., 2008). Exogenous expression of WT hepaCAM in U373 MG cells caused a relocalisation of connexin 43 to the cell membrane at sites of cell-cell contacts, as well as increased its protein expression. This parallels previous observations that knockdown of hepaCAM expression in primary rat astrocytes led to an intracellular accumulation and reduced expression of MLC1 on the plasma membrane at cell-cell junctions (Capdevila-Nortes et al., 2013). Similarly, co-expression of hepaCAM with ClC-2 in HeLa cells led to a re-distribution of ClC-2 at cell-cell contacts (Jeworutzki et al., 2012). These findings taken together imply that hepaCAM plays a general role in the targeting of its interacting partners to cell-cell contacts. It should be noted that Jeworutzki et al. (2012) had reported no

126

changes in connexin 43 expression and localisation upon overexpression of hepaCAM in rat astrocytes; however, this may be explained by the fact that these astrocytes already express endogenous hepaCAM and some connexin 43 could be detected at astrocyte processes even without overexpression of hepaCAM.

The R92Q and R92W mutations in hepaCAM inhibited the functions of hepaCAM in targeting connexin 43 to the cellular junctions of U373 MG cells. These mutants of hepaCAM also showed a reduced localisation themselves at cellular junctions and tended to co-localise with connexin 43 intracellularly. This correlates with previous observations that MLC1 and ClC-2 in rat astrocytes are mis-localised when co-expressed with hepaCAM-R92Q, hepaCAM-R92W or other MLC-causing mutants of hepaCAM. These hepaCAM mutants, MLC1 and ClC-2 had a diffused intracellular localisation with partial enrichment in the plasma membrane, but not particularly at cellular junctions (Jeworutzki et al., 2012; Lopez-Hernandez et al., 2011a). Thus, it can be implied that MLC-causing mutations inhibit the general activities of hepaCAM in targeting itself and its interacting proteins to cell-cell contacts.

The silencing of connexin 43 in WT hepaCAM-expressing U373 MG cells did not affect hepaCAM localisation at cell-cell contacts. Similarly, hepaCAM localisation in astrocyte-astrocyte processes was not affected in ClC-2 knockout mice (Hoegg-Beiler et al., 2014) or by the knockdown of MLC1 (Lopez-Hernandez et al., 2011b), suggesting that hepaCAM is not obligatorily associated with MLC1 and ClC-2. Hence, the localisation of hepaCAM at the

cell-cell contacts of U373 MG cells is independent of its interaction with connexin 43.

4.3. hepaCAM increases the stability of connexin 43

Connexin 43 is known to undergo rapid turnover. In this study, connexin 43 expression is increased in U373 MG and HEK293T cells expressing WT hepaCAM, not due to an increase in its transcription, but due to its slower rate of turnover. The increased stability of connexin 43 protein is due to its interaction with hepaCAM, as treatment of cells with an antibody against the hepaCAM extracellular domain disrupts this interaction and causes a downregulation in connexin 43 expression. Similarly, the R92Q and R92W mutations in hepaCAM, which lead to a weaker interaction with connexin 43, did not enhance connexin 43 protein levels in U373 MG cells, unlike WT hepaCAM. These results parallel previous observations that the interaction of hepaCAM with MLC1 in rat astrocytes increases the protein stability of MLC1 (Capdevila-Nortes et al., 2013).

4.4. Functional significance of the interaction of hepaCAM with connexin 43 in U373 MG cells

4.4.1. hepaCAM increases connexin 43-mediated gap junction activity

After characterisation of the hepaCAM-connexin 43 interaction, we subsequently found that hepaCAM caused a two-fold increase in gap junction activity in U373 MG cells. Since the R92Q and R92W mutations in hepaCAM, as well as treatment of hepaCAM-expressing cells with an antibody against the hepaCAM extracellular domain both disrupted hepaCAM localisation at cellular junctions, it suggested that hepaCAM plays a role in

gap junction assembly and turnover. Thus, the increased gap junction activity in hepaCAM-expressing U373 MG cells is due to a slower rate of gap junction and connexin 43 turnover, resulting in more functional gap junction plaques on the cell surface. It should be noted that some gap junction activity could still be observed in the vector-transfected U373 MG cells despite a predominant intracellular accumulation of connexin 43. Cottin et al. (2008) had also shown that functional gap junction transfer could still occur in glioblastoma cell lines which had only a few gap junction plaques on the cell surface and mainly intracellular localisation of connexin 43. However, our findings indicate that hepaCAM expression in U373 MG cells significantly enhances gap junction transfer, implying a role of hepaCAM in promoting cell-cell communication in glioblastoma cells.

Presently, we also show that the exogenous expression of hepaCAM specifically increases gap junction activity mediated by connexin 43, as hepaCAM expression did not increase gap junction activity in cell lines which lack endogenous connexin 43 expression, MCF7 and HepG2. It would also be ideal to repeat the calcein-AM transfer assay using hepaCAM-expressing U373 MG cells in which connexin 43 expression had been silenced to further substantiate our findings.

Several studies have reported an involvement of other CAMs in the interaction with connexin 43 at gap junctions. For example, connexin 43 has been shown to interact with the tight junction protein ZO-1. Although the functional significance of this interaction is not completely understood, it suggests that there is cross-talk between tight junctions and gap junctions (Dbouk et al.,

2009; Giepmans, 2004). Connexin 43 is also known to interact with the adherens junction proteins N-cadherin, β-catenin, p120 and α-catenin, suggesting that there may also be cross-talk between gap junctions and adherens junctions (Giepmans, 2004, 2006). In a study by Musil et al. (1990), transfection of L-CAM induced the formation of gap junctions in cells which expressed connexin 43 but were otherwise GJIC-deficient. Interestingly, antibodies against L-CAM led to the disassembly of gap junctions, which parallels our findings on hepaCAM in U373 MG cells. In addition to interacting with CAMs, connexin 43 has also been shown to interact with caveolin-1 and caveolin-2, which may regulate GJIC in keratinocytes (Langlois et al., 2008).

A question that needs to be addressed is how the interaction with hepaCAM increases the stability of connexin 43 and its gap junctions in U373 MG cells. As discussed in section 1.7.1, gap junctions are disassembled into individual connexin 43 proteins, which are subsequently degraded by both lysosomal and proteasomal pathways. It would be worthwhile to determine the pathway in which connexin 43 is degraded in U373 MG cells to further understand the mechanisms by which hepaCAM slows down connexin 43 turnover.

4.4.2. Connexin 43-independent functions of hepaCAM in tumour suppression

Since hepaCAM interacts with connexin 43 in U373 MG cells, we also investigated the influence of connexin 43 on the previously published functions of hepaCAM in cell adhesion, migration and proliferation. Although connexin 43 itself has been reported to mediate cell adhesion and migration

(Cotrina et al., 2008; Elias et al., 2007; Lin et al., 2002), its silencing had no significant effects on the increased adhesion and reduced migration of hepaCAM-expressing U373 MG cells. As discussed in section 1.7.3.3, connexin 43 has also been shown to inhibit proliferation, but silencing of connexin 43 did not reverse the anti-proliferative effects of hepaCAM in U373 MG cells. Thus, these functions of hepaCAM in U373 MG cells are independent of connexin 43.

4.4.3. A proposed mechanism of hepaCAM-mediated tumour suppression in U373 MG cells

The loss of GJIC is frequently observed during tumourigenesis. While it was observed in this study that hepaCAM increases GJIC in U373 MG cells, it still remains to be elucidated how this contributes to tumour suppression, as the tumour suppressive properties of connexins by GJIC-dependent mechanisms are not completely understood. It could be that hepaCAM promotes GJIC-mediated exchange of uncharacterised small molecules, which maintain homeostasis in normal healthy tissues as discussed in section 1.7.3.2.

It should be noted that while hepaCAM expression in U373 MG cells targets connexin 43 to cell-cell contacts and promotes GJIC, it did not increase the size of cellular aggregates when the cells were cultured in suspension. It may be because there are different mechanisms in maintaining cell-cell adhesion when cells are attached to a matrix and when cells encounter anchorage-independent conditions. Thus, we postulate that hepaCAM expression increases cell-ECM adhesion, as well as targets connexin 43 to cell-cell contacts to increase GJIC within a primary tumour, making it more difficult

for tumour cells to detach and disseminate during metastasis. On the other hand, when cells do manage to escape from a primary tumour, hepaCAM expression may confer a slightly increased sensitivity to anoikis and cause smaller cellular aggregates to form. It has been shown that tumour cells which formed aggregates when cultured in suspension had lower rates of apoptosis compared to single cells, and that the increased size of aggregates is correlated with increased survival, or resistance to anoikis (Valentinis et al., 1998; Zhang et al., 2004).

4.5. Proteolytic cleavage of the hepaCAM cytoplasmic domain and internalisation of hepaCAM

4.5.1. Functions of the cleaved hepaCAM cytoplasmic domain fragment

The cytoplasmic domain of CAMs such as Ig-CAMs has been shown to undergo proteolytic cleavage, and the resulting cytoplasmic fragment is capable of signal transduction in the absence of the extracellular domain (Cavallaro and Dejana, 2011). It was previously shown that hepaCAM undergoes proteolytic cleavage when exogenously expressed in MCF7 cells, generating a fragment that consists mainly of the cytoplasmic domain with unknown biological functions (Zhang et al., 2010a). In this study, we further show that proteolytic cleavage of the hepaCAM cytoplasmic domain occurs in U373 MG (Figure 33D) and HepG2 cells, thus suggesting that it may be a ubiquitous event in the processing of hepaCAM in different human cancer cell lines. In addition, we show by subcellular fractionation that the cleaved hepaCAM fragment could be found in the nucleus, suggesting that proteolytic cleavage does not occur merely in hepaCAM protein turnover, but also has functions in regulating gene expression. However, the cleaved hepaCAM

fragment does not directly bind to DNA as a transcription factor since it was not detected in the chromatin-bound nuclear fraction. Thus, we postulate that the cleaved hepaCAM fragment may interact with other transcription factors instead, thereby activating and/or stabilising them. We also speculate that the cleaved hepaCAM fragment may be responsible for upregulating the expression of genes such as p53, p21 and p27, since hepaCAM expression was previously shown to increase their protein levels in MCF7 cells (Moh et al., 2008).

The notion of the cleaved cytoplasmic domain fragments of CAMs having functions in regulating gene expression is not novel. For example, the cytoplasmic fragment of L1, an Ig-CAM, is able to regulate the gene expression of β3 integrin, similar to the full-length L1 protein (Riedle et al., 2009). The intracellular domain of epithelial cell adhesion molecule (EpCAM) has been shown to bind to and activate the promoters of the reprogramming factor genes *OCT4*, *SOX2*, *NANOG*, and *c-MYC* (Lin et al., 2012). Since the cytoplasmic domain is important in hepaCAM's functions in inhibiting cell proliferation (Moh et al., 2008), it would be worthwhile to identify the proteins which interact with the cleaved hepaCAM fragment and their downstream signalling pathways to further understand the mechanisms of hepaCAM-mediated tumour suppression.

Presently, we found that the cleaved hepaCAM fragment was not detected in U373 MG cells expressing hepaCAM with the MLC-causing mutations, R92Q and R92W (Figure 33E). It would be interesting to determine whether such a phenomenon is also observed in cells expressing the other MLC-causing

133

mutations. Although these mutations in hepaCAM have not been studied in cancer, our findings may have a wider implication in the understanding of hepaCAM processing in the disease MLC. The pathogenesis of MLC thus far has been attributed to changes in the interactions of hepaCAM with MLC1 and ClC-2, thus leading to modifications in ClC-2 currents (Hoegg-Beiler et al., 2014). We speculate that differences in the cytoplasmic domain cleavage of the hepaCAM mutants may also contribute to the pathogenesis of MLC by affecting gene regulation. Thus, it would be worthwhile to determine whether proteolytic cleavage of the hepaCAM cytoplasmic domain also occurs in other cell types with endogenous hepaCAM expression, for example astrocytes and oligodendrocytes which are implicated in the etiology of MLC, and whether it is affected by MLC-causing mutations in hepaCAM.

4.5.2. Signalling events leading to the internalisation of hepaCAM and the cleavage of its cytoplasmic domain

It is interesting to note that proteolytic cleavage of the hepaCAM cytoplasmic domain in U373 MG cells was also inhibited by treatment with the antibody against the hepaCAM extracellular domain (Figure 33F). Since the antibody against the hepaCAM extracellular domain also disrupts *cis*-interactions with connexin 43 in U373 MG cells, we tested whether the silencing of connexin 43 affects hepaCAM cytoplasmic domain cleavage. This was not the case, however, and led us to two different possibilities: cleavage of the hepaCAM cytoplasmic domain is induced by (1) the binding of the hepaCAM extracellular domain to an extracellular ligand or (2) the *cis*-interaction of hepaCAM with other proteins on the plasma membrane. Presently, we found that the binding of hepaCAM to the integrin ligand fibronectin increased

proteolytic cleavage of its cytoplasmic domain, compared to the non-integrin ligand poly-L-lysine. This suggested that cleavage of the hepaCAM cytoplasmic domain is promoted by the interaction of the hepaCAM extracellular domain with fibronectin. At this point, it is not completely understood whether the binding of hepaCAM to fibronectin is direct or indirect. It is not ruled out that hepaCAM may interact with other known fibronectin receptors such as integrins, and the expression of these adhesion receptors may be upregulated in hepaCAM-expressing cells, hence increasing the affinity of these cells to fibronectin. For example, the integrins α5β1 and αvβ3 are known to bind to the RGD motif on fibronectin (Danen et al., 2002; Wennerberg et al., 1996). The expression of these integrins and their interaction with hepaCAM should be further studied to elucidate the mechanisms by which hepaCAM promotes cell adhesion to fibronectin.

While proteolytic cleavage of the hepaCAM cytoplasmic domain was initially inhibited in cells adhered to the non-integrin ligand poly-L-lysine at 10 and 30 min, it gradually increased over time. It is surmised that this may be due to the eventual secretion of ECM proteins by U373 MG cells themselves on poly-L-lysine-coated plates. The expression of fibronectin and other ECM proteins in U373 MG cells should be determined to further validate this supposition.

Since hepaCAM expression also increased cell spreading on Matrigel (Moh et al., 2005b), a basement membrane preparation containing other ECM proteins such as laminin and collagen, it would be interesting to determine whether hepaCAM also increases the affinity of cells to these ECM proteins, and

whether this promotes proteolytic cleavage of the hepaCAM cytoplasmic domain.

Although silencing of connexin 43 did not inhibit the proteolytic cleavage of the hepaCAM cytoplasmic domain, it still remains to be seen whether the *cis*-interaction of hepaCAM with other proteins on the plasma membrane provides the signal for this phenomenon. We have discussed that the hepaCAM extracellular domain also interacts with caveolin-1, and it would be worthwhile to investigate whether the depletion of caveolin-1 affects hepaCAM cytoplasmic domain processing.

It is still an open question whether the cleaved hepaCAM fragment found in the soluble nuclear fraction is due to its nuclear translocation or proteolytic cleavage of full-length hepaCAM that is present in the same fraction itself. Subcellular fractionation experiments showed that the cleaved hepaCAM fragment is also present in the membrane fraction, which contains the contents of the plasma membrane, mitochondria, ER, Golgi membranes and endosomes. Although the cellular location of hepaCAM proteolytic cleavage has not been identified yet, we postulate that it may occur upon its internalisation from the plasma membrane in the endosomal compartments. We have shown a partial co-localisation of hepaCAM with the early endosomal marker EEA1 in U373 MG cells under normal culture conditions, suggesting that hepaCAM on the plasma membrane is constitutively internalised in endosomes. Furthermore, upon adhesion of U373 MG cells to fibronectin, hepaCAM is internalised and a concomitant increase in hepaCAM cytoplasmic domain cleavage is observed, compared to cells adhered to poly-

L-lysine. Thus, it is likely that internalisation of hepaCAM occurs prior to its proteolytic cleavage in the endosomes, and that the cleaved hepaCAM fragment subsequently translocates to the nucleus. Since hepaCAM is localised to lipid rafts/caveolae and associates with caveolin-1 (Moh et al., 2009a), it is probable that hepaCAM is internalised by caveolin-1-mediated endocytosis.

A question that needs to be addressed is why endocytosis of hepaCAM occurs upon integrin-mediated adhesion of cells to fibronectin. It is known that endocytosis of integrins constantly occurs during cell adhesion and migration, and its function is to recycle the integrins, rather than degrade them (Pellinen and Ivaska, 2006). Interference with the endocytosis and recycling of integrins can inhibit cell adhesion and motility (Proux-Gillardeaux et al., 2005; Roberts et al., 2001). In addition, it has been proposed that the endocytosis of integrins and the ECM proteins ligated to the integrins are important in ECM turnover and remodelling. For example, caveolin-1-dependent endocytosis of both $\beta 1$ integrin and its ligated fibronectin is important in fibronectin matrix turnover (Shi and Sottile, 2008). Thus, it is possible that hepaCAM may be endocytosed as part of ECM turnover and remodelling during cellular adhesion, and proteolytically cleaved as a means of signal transduction into the cell to provide information on its location, local environment and adhesive state, not unlike "outside-in signalling" mediated by integrins (discussed in section 1.2.2).

Using inhibitors of calpain-1 and cathepsin-B, the study by Zhang et al. (2010a) had suggested the possible involvement of these cysteine proteases in

the cleavage of the hepaCAM cytoplasmic domain. However, the exact residue at which hepaCAM is proteolytically cleaved has not been elucidated yet. Calpain-1 is a calcium-dependent, non-lysosomal intracellular protease which cleaves a broad number of substrates but does not appear to recognise a specific amino acid sequence. It has been proposed that cleavage by calpain-1 may be dependent on the higher order structural features of substrates (Cuerrier et al., 2005; Huang and Wang, 2001; Tompa et al., 2004). Cathepsin-B is a lysosomal protease and also has a broad specificity. Several studies have suggested that cathepsin-B has a preference for certain amino acids at specific positions of its substrates, but the understanding of its selectivity is not yet complete (Biniossek et al., 2011; Turk et al., 2012). Thus, further studies are required to determine the amino acid position at which hepaCAM is cleaved. One possible approach would involve purification of the cleaved hepaCAM fragment and N-terminal protein sequencing.

4.6. Future work

As discussed in section 4.5.1, it would be worthwhile to study the downstream signalling pathways of the cleaved hepaCAM cytoplasmic domain fragment to further understand the mechanisms of hepaCAM-mediated tumour suppression. Preliminary studies to transfect MCF7 and U373 MG cells with a construct for residues 260-416 of hepaCAM, which approximates the hepaCAM cytoplasmic domain, were unsuccessful as there was extensive cell death and low expression in surviving cells (data not shown). As this had been observed previously, it is likely that overexpression of the hepaCAM cytoplasmic domain alone leads to far-ranging effects on cell survival and death (Moh Mei Chung, personal communication). Thus, a possible option is

138

to clone the hepaCAM cytoplasmic domain into an expression vector with an inducible promoter. In this way, the downstream activities of the hepaCAM cytoplasmic domain can be studied in transfected cells upon induction of its expression. Alternatively, it may be worthwhile to raise an antibody which specifically recognises the cleaved hepaCAM fragment, but not full-length hepaCAM. For example in studying EpCAM signalling, Lin et al. (2012) utilised an antibody that recognises the soluble intracellular domain of EpCAM but not the full-length protein. Using either method, we can then further verify the nuclear translocation of the cleaved hepaCAM fragment by immunofluorescence staining. The effects of the hepaCAM cytoplasmic domain alone in mediating growth inhibition can also be further studied by proliferation and apoptosis assays, and the downstream effectors of hepaCAM cytoplasmic domain signalling can be identified by proteomics-based technologies.

As previously published studies have utilised *in vitro* cell line models in studying the functions of hepaCAM, it may be worthwhile to perform xenografts in mouse models using control and hepaCAM-expressing cancer cells. Tumour growth and metastasis can be monitored in these xenograft models to better understand the functions of hepaCAM in a physiological setting. It is also interesting to note that while hepaCAM expression increased the motility of MCF7 and HepG2 cells, it reduced the motility of U373 MG cells. Furthermore, as a putative tumour suppressor, hepaCAM has two seemingly contradictory functions of inhibiting proliferation and yet increasing the motility of MCF7 and HepG2 cells, raising the possibility that its expression may be differentially regulated during tumourigenesis (Moh and

Shen, 2009). Hence, the use of xenograft models to profile tumour progression may help to shed light on these questions.

Although it still remains to be elucidated how exactly the hepaCAM-mediated increase in GJIC in U373 MG cells contributes to tumour suppression, it may be useful to profile hepaCAM and connexin 43 expression in clinical samples at different stages of tumour progression to further understand the functional significance of their interaction. This may aid in the development of "bystander effect" therapeutic strategies (briefly discussed in section 1.7.3.2) that utilise GJIC to spread the effects of a therapeutic agent within a tumour mass.

CHAPTER 5   CONCLUSION

HEPACAM is a putative tumour suppressor gene that is frequently downregulated in human HCC and other solid cancers. In this study, a novel interaction of hepaCAM with the gap junction protein connexin 43 in U373 MG glioblastoma cells is observed. Connexin 43, which has an aberrant intracellular localisation in U373 MG cells, is re-targeted to the plasma membrane at cellular junctions upon hepaCAM expression. In addition, hepaCAM expression leads to an increase in connexin 43 protein levels, not due to an increase in its transcription, but due to its enhanced stability from the interaction of these two proteins. The R92Q and R92W mutations in the hepaCAM extracellular domain, which are involved in the leukodystrophy MLC, weaken the interaction of hepaCAM with connexin 43 and fail to target connexin 43 to cellular junctions. This indicates that the interaction of hepaCAM with connexin 43 is important in the proper localisation of connexin 43 to cellular junctions in glioblastoma cells.

The functions of hepaCAM in increasing adhesion, reducing migration and inhibiting proliferation do not appear to be dependent on its interaction with connexin 43. On the other hand, hepaCAM is observed to promote connexin 43-mediated gap junction transfer in U373 MG cells. Although the tumour suppressive properties of connexin 43 by GJIC-dependent mechanisms are not completely understood, we postulate that hepaCAM expression increases cell-cell contact and GJIC within a primary tumour, making it more difficult for tumour cells to detach and disseminate during metastasis.

The hepaCAM cytoplasmic domain undergoes proteolytic cleavage in MCF7, U373 MG and HepG2 cells, indicating that it may be a ubiquitous event in the processing of hepaCAM in different human cancer cell lines. Interestingly, cleavage of the cytoplasmic domain is inhibited by the R92Q and R92W mutations in the hepaCAM extracellular domain, as well as by the treatment with an antibody against the hepaCAM extracellular domain. We further show that upon integrin-mediated adhesion of U373 MG cells to fibronectin, hepaCAM undergoes endocytosis and is concomitantly cleaved. As the cleaved hepaCAM fragment can be found in the nucleus, it is likely that cleavage of the cytoplasmic domain has functions in regulating gene expression and mediating the tumour suppressive activities of hepaCAM. Further research needs to be done to identify the genes that are regulated by the cleaved hepaCAM fragment in order to expand our understanding of hepaCAM-mediated tumour suppression.

REFERENCES

Aijaz, S., Balda, M.S., and Matter, K. (2006). Tight junctions: molecular architecture and function. International review of cytology *248*, 261-298.

Akiyama, S.K. (2002). Functional analysis of cell adhesion: quantitation of cell-matrix attachment. Methods Cell Biol *69*, 281-296.

Anderson, J.M., and Van Itallie, C.M. (2009). Physiology and function of the tight junction. Cold Spring Harbor perspectives in biology *1*, a002584.

Attwell, S., Roskelley, C., and Dedhar, S. (2000). The integrin-linked kinase (ILK) suppresses anoikis. Oncogene *19*, 3811-3815.

Avanzo, J.L., Mesnil, M., Hernandez-Blazquez, F.J., Mackowiak, II, Mori, C.M., da Silva, T.C., Oloris, S.C., Garate, A.P., Massironi, S.M., Yamasaki, H.*, et al*. (2004). Increased susceptibility to urethane-induced lung tumors in mice with decreased expression of connexin43. Carcinogenesis *25*, 1973-1982.

Barclay, A.N. (2003). Membrane proteins with immunoglobulin-like domains--a master superfamily of interaction molecules. Semin Immunol *15*, 215-223.

Barthel, S.R., Gavino, J.D., Descheny, L., and Dimitroff, C.J. (2007). Targeting selectins and selectin ligands in inflammation and cancer. Expert opinion on therapeutic targets *11*, 1473-1491.

Beardslee, M.A., Laing, J.G., Beyer, E.C., and Saffitz, J.E. (1998). Rapid turnover of connexin43 in the adult rat heart. Circulation research *83*, 629-635.

Berthoud, V.M., Minogue, P.J., Laing, J.G., and Beyer, E.C. (2004). Pathways for degradation of connexins and gap junctions. Cardiovasc Res *62*, 256-267.

Biniossek, M.L., Nagler, D.K., Becker-Pauly, C., and Schilling, O. (2011). Proteomic identification of protease cleavage sites characterizes prime and non-prime specificity of cysteine cathepsins B, L, and S. Journal of proteome research *10*, 5363-5373.

Borradori, L., and Sonnenberg, A. (1999). Structure and function of hemidesmosomes: more than simple adhesion complexes. J Invest Dermatol *112*, 411-418.

Brooks, P.C., Clark, R.A., and Cheresh, D.A. (1994). Requirement of vascular integrin alpha v beta 3 for angiogenesis. Science *264*, 569-571.

Calderwood, D.A. (2004). Integrin activation. J Cell Sci *117*, 657-666.

Campbell, K.P. (1995). Three muscular dystrophies: loss of cytoskeleton-extracellular matrix linkage. Cell *80*, 675-679.

Capdevila-Nortes, X., Lopez-Hernandez, T., Apaja, P.M., Lopez de Heredia, M., Sirisi, S., Callejo, G., Arnedo, T., Nunes, V., Lukacs, G.L., Gasull, X., *et al*. (2013). Insights into MLC pathogenesis: GlialCAM is an MLC1 chaperone required for proper activation of volume-regulated anion currents. Hum Mol Genet *22*, 4405-4416.

Cavallaro, U., and Christofori, G. (2004). Cell adhesion and signalling by cadherins and Ig-CAMs in cancer. Nat Rev Cancer *4*, 118-132.

Cavallaro, U., and Dejana, E. (2011). Adhesion molecule signalling: not always a sticky business. Nat Rev Mol Cell Biol *12*, 189-197.

Chen, S.C., Pelletier, D.B., Ao, P., and Boynton, A.L. (1995). Connexin43 reverses the phenotype of transformed cells and alters their expression of cyclin/cyclin-dependent kinases. Cell growth & differentiation : the molecular biology journal of the American Association for Cancer Research *6*, 681-690.

Christofori, G., and Semb, H. (1999). The role of the cell-adhesion molecule E-cadherin as a tumour-suppressor gene. Trends Biochem Sci *24*, 73-76.

Cotrina, M.L., Lin, J.H., and Nedergaard, M. (2008). Adhesive properties of connexin hemichannels. Glia *56*, 1791-1798.

Cottin, S., Ghani, K., and Caruso, M. (2008). Bystander effect in glioblastoma cells with a predominant cytoplasmic localization of connexin43. Cancer gene therapy *15*, 823-831.

Cottin, S., Gould, P.V., Cantin, L., and Caruso, M. (2011). Gap junctions in human glioblastomas: implications for suicide gene therapy. Cancer gene therapy *18*, 674-681.

Cronier, L., Crespin, S., Strale, P.O., Defamie, N., and Mesnil, M. (2009). Gap junctions and cancer: new functions for an old story. Antioxid Redox Signal *11*, 323-338.

Cruz-Munoz, W., and Khokha, R. (2008). The role of tissue inhibitors of metalloproteinases in tumorigenesis and metastasis. Critical reviews in clinical laboratory sciences *45*, 291-338.

Cuerrier, D., Moldoveanu, T., and Davies, P.L. (2005). Determination of peptide substrate specificity for mu-calpain by a peptide library-based approach: the importance of primed side interactions. J Biol Chem *280*, 40632-40641.

Czyz, J., Irmer, U., Schulz, G., Mindermann, A., and Hulser, D.F. (2000). Gap-junctional coupling measured by flow cytometry. Exp Cell Res *255*, 40-46.

Dagli, M.L., Yamasaki, H., Krutovskikh, V., and Omori, Y. (2004). Delayed liver regeneration and increased susceptibility to chemical hepatocarcinogenesis in transgenic mice expressing a dominant-negative mutant of connexin32 only in the liver. Carcinogenesis *25*, 483-492.

Danen, E.H., Sonneveld, P., Brakebusch, C., Fassler, R., and Sonnenberg, A. (2002). The fibronectin-binding integrins alpha5beta1 and alphavbeta3 differentially modulate RhoA-GTP loading, organization of cell matrix adhesions, and fibronectin fibrillogenesis. J Cell Biol *159*, 1071-1086.

Dbouk, H.A., Mroue, R.M., El-Sabban, M.E., and Talhouk, R.S. (2009). Connexins: a myriad of functions extending beyond assembly of gap junction channels. Cell Commun Signal *7*, 4.

Delva, E., Tucker, D.K., and Kowalczyk, A.P. (2009). The desmosome. Cold Spring Harbor perspectives in biology *1*, a002543.

Desgrosellier, J.S., and Cheresh, D.A. (2010). Integrins in cancer: biological implications and therapeutic opportunities. Nat Rev Cancer *10*, 9-22.

Duarri, A., Lopez de Heredia, M., Capdevila-Nortes, X., Ridder, M.C., Montolio, M., Lopez-Hernandez, T., Boor, I., Lien, C.F., Hagemann, T., Messing, A., *et al*. (2011). Knockdown of MLC1 in primary astrocytes causes cell vacuolation: a MLC disease cell model. Neurobiology of disease *43*, 228-238.

Duxbury, M.S., Ito, H., Zinner, M.J., Ashley, S.W., and Whang, E.E. (2004). Focal adhesion kinase gene silencing promotes anoikis and suppresses metastasis of human pancreatic adenocarcinoma cells. Surgery *135*, 555-562.

Eghbali, B., Kessler, J.A., Reid, L.M., Roy, C., and Spray, D.C. (1991). Involvement of gap junctions in tumorigenesis: transfection of tumor cells with connexin 32 cDNA retards growth in vivo. Proceedings of the National Academy of Sciences of the United States of America *88*, 10701-10705.

Elias, L.A., Wang, D.D., and Kriegstein, A.R. (2007). Gap junction adhesion is necessary for radial migration in the neocortex. Nature *448*, 901-907.

Eugenin, E.A., Branes, M.C., Berman, J.W., and Saez, J.C. (2003). TNF-alpha plus IFN-gamma induce connexin43 expression and formation of gap junctions between human monocytes/macrophages that enhance physiological responses. Journal of immunology *170*, 1320-1328.

Favre-Kontula, L., Rolland, A., Bernasconi, L., Karmirantzou, M., Power, C., Antonsson, B., and Boschert, U. (2008). GlialCAM, an immunoglobulin-like cell adhesion molecule is expressed in glial cells of the central nervous system. Glia *56*, 633-645.

Frantz, C., Stewart, K.M., and Weaver, V.M. (2010). The extracellular matrix at a glance. J Cell Sci *123*, 4195-4200.

Frisch, S.M., and Screaton, R.A. (2001). Anoikis mechanisms. Curr Opin Cell Biol *13*, 555-562.

Fu, C.T., Bechberger, J.F., Ozog, M.A., Perbal, B., and Naus, C.C. (2004). CCN3 (NOV) interacts with connexin43 in C6 glioma cells: possible

mechanism of connexin-mediated growth suppression. J Biol Chem *279*, 36943-36950.

Garrod, D., and Chidgey, M. (2008). Desmosome structure, composition and function. Biochim Biophys Acta *1778*, 572-587.

Gast, D., Riedle, S., Issa, Y., Pfeifer, M., Beckhove, P., Sanderson, M.P., Arlt, M., Moldenhauer, G., Fogel, M., Kruger, A., *et al*. (2008). The cytoplasmic part of L1-CAM controls growth and gene expression in human tumors that is reversed by therapeutic antibodies. Oncogene *27*, 1281-1289.

Gaudry, J.P., Arod, C., Sauvage, C., Busso, S., Dupraz, P., Pankiewicz, R., and Antonsson, B. (2008). Purification of the extracellular domain of the membrane protein GlialCAM expressed in HEK and CHO cells and comparison of the glycosylation. Protein Expr Purif *58*, 94-102.

Gellhaus, A., Dong, X., Propson, S., Maass, K., Klein-Hitpass, L., Kibschull, M., Traub, O., Willecke, K., Perbal, B., Lye, S.J., *et al*. (2004). Connexin43 interacts with NOV: a possible mechanism for negative regulation of cell growth in choriocarcinoma cells. J Biol Chem *279*, 36931-36942.

Giepmans, B.N. (2004). Gap junctions and connexin-interacting proteins. Cardiovasc Res *62*, 233-245.

Giepmans, B.N. (2006). Role of connexin43-interacting proteins at gap junctions. Advances in cardiology *42*, 41-56.

Goldberg, G.S., Lampe, P.D., and Nicholson, B.J. (1999). Selective transfer of endogenous metabolites through gap junctions composed of different connexins. Nat Cell Biol *1*, 457-459.

Govindarajan, R., Zhao, S., Song, X.H., Guo, R.J., Wheelock, M., Johnson, K.R., and Mehta, P.P. (2002). Impaired trafficking of connexins in androgen-independent human prostate cancer cell lines and its mitigation by alpha-catenin. J Biol Chem *277*, 50087-50097.

Guan, X., and Ruch, R.J. (1996). Gap junction endocytosis and lysosomal degradation of connexin43-P2 in WB-F344 rat liver epithelial cells treated with DDT and lindane. Carcinogenesis *17*, 1791-1798.

Gumbiner, B.M. (1996). Cell adhesion: the molecular basis of tissue architecture and morphogenesis. Cell *84*, 345-357.

Gumbiner, B.M. (2005). Regulation of cadherin-mediated adhesion in morphogenesis. Nat Rev Mol Cell Biol *6*, 622-634.

Guo, W., and Giancotti, F.G. (2004). Integrin signalling during tumour progression. Nat Rev Mol Cell Biol *5*, 816-826.

Guo, W., Pylayeva, Y., Pepe, A., Yoshioka, T., Muller, W.J., Inghirami, G., and Giancotti, F.G. (2006). Beta 4 integrin amplifies ErbB2 signaling to promote mammary tumorigenesis. Cell *126*, 489-502.

Gupta, N., Wang, H., McLeod, T.L., Naus, C.C., Kyurkchiev, S., Advani, S., Yu, J., Perbal, B., and Weichselbaum, R.R. (2001). Inhibition of glioma cell growth and tumorigenic potential by CCN3 (NOV). Molecular pathology : MP *54*, 293-299.

Hanahan, D., and Weinberg, R.A. (2000). The hallmarks of cancer. Cell *100*, 57-70.

Hanahan, D., and Weinberg, R.A. (2011). Hallmarks of cancer: the next generation. Cell *144*, 646-674.

Hannigan, G., Troussard, A.A., and Dedhar, S. (2005). Integrin-linked kinase: a cancer therapeutic target unique among its ILK. Nat Rev Cancer *5*, 51-63.

Harburger, D.S., and Calderwood, D.A. (2009). Integrin signalling at a glance. J Cell Sci *122*, 159-163.

Hillis, G.S., and Flapan, A.D. (1998). Cell adhesion molecules in cardiovascular disease: a clinical perspective. Heart *79*, 429-431.

Hirschi, K.K., Xu, C.E., Tsukamoto, T., and Sager, R. (1996). Gap junction genes Cx26 and Cx43 individually suppress the cancer phenotype of human mammary carcinoma cells and restore differentiation potential. Cell growth & differentiation : the molecular biology journal of the American Association for Cancer Research *7*, 861-870.

Hoegg-Beiler, M.B., Sirisi, S., Orozco, I.J., Ferrer, I., Hohensee, S., Auberson, M., Godde, K., Vilches, C., de Heredia, M.L., Nunes, V.*, et al*. (2014). Disrupting MLC1 and GlialCAM and ClC-2 interactions in leukodystrophy entails glial chloride channel dysfunction. Nature communications *5*, 3475.

Horwitz, A.R. (2012). The origins of the molecular era of adhesion research. Nat Rev Mol Cell Biol *13*, 805-811.

Huang, R.P., Fan, Y., Hossain, M.Z., Peng, A., Zeng, Z.L., and Boynton, A.L. (1998). Reversion of the neoplastic phenotype of human glioblastoma cells by connexin 43 (cx43). Cancer Res *58*, 5089-5096.

Huang, Y., and Wang, K.K. (2001). The calpain family and human disease. Trends in molecular medicine *7*, 355-362.

Humphries, M.J. (2001). Cell-Substrate Adhesion Assays. In Current Protocols in Cell Biology (John Wiley & Sons, Inc.).

Hynes, R.O. (2002). Integrins: bidirectional, allosteric signaling machines. Cell *110*, 673-687.

Ito, A., Katoh, F., Kataoka, T.R., Okada, M., Tsubota, N., Asada, H., Yoshikawa, K., Maeda, S., Kitamura, Y., Yamasaki, H.*, et al*. (2000). A role for heterologous gap junctions between melanoma and endothelial cells in metastasis. The Journal of clinical investigation *105*, 1189-1197.

Itoh, M., Nagafuchi, A., Moroi, S., and Tsukita, S. (1997). Involvement of ZO-1 in cadherin-based cell adhesion through its direct binding to alpha catenin and actin filaments. J Cell Biol *138*, 181-192.

Jeworutzki, E., Lopez-Hernandez, T., Capdevila-Nortes, X., Sirisi, S., Bengtsson, L., Montolio, M., Zifarelli, G., Arnedo, T., Muller, C.S., Schulte, U., *et al*. (2012). GlialCAM, a protein defective in a leukodystrophy, serves as a ClC-2 Cl(-) channel auxiliary subunit. Neuron *73*, 951-961.

Kamiguchi, H., Hlavin, M.L., Yamasaki, M., and Lemmon, V. (1998). Adhesion molecules and inherited diseases of the human nervous system. Annual review of neuroscience *21*, 97-125.

Kang, H.G., Jenabi, J.M., Zhang, J., Keshelava, N., Shimada, H., May, W.A., Ng, T., Reynolds, C.P., Triche, T.J., and Sorensen, P.H. (2007). E-cadherin cell-cell adhesion in ewing tumor cells mediates suppression of anoikis through activation of the ErbB4 tyrosine kinase. Cancer Res *67*, 3094-3105.

Kapoor, P., Saunders, M.M., Li, Z., Zhou, Z., Sheaffer, N., Kunze, E.L., Samant, R.S., Welch, D.R., and Donahue, H.J. (2004). Breast cancer metastatic potential: correlation with increased heterotypic gap junctional intercellular communication between breast cancer cells and osteoblastic cells. International journal of cancer Journal international du cancer *111*, 693-697.

Kiang, D.T., Kollander, R., Lin, H.H., LaVilla, S., and Atkinson, M.M. (1994). Measurement of gap junctional communication by fluorescence activated cell sorting. In Vitro Cell Dev Biol Anim *30A*, 796-802.

King, T.J., and Lampe, P.D. (2004a). The gap junction protein connexin32 is a mouse lung tumor suppressor. Cancer Res *64*, 7191-7196.

King, T.J., and Lampe, P.D. (2004b). Mice deficient for the gap junction protein Connexin32 exhibit increased radiation-induced tumorigenesis associated with elevated mitogen-activated protein kinase (p44/Erk1, p42/Erk2) activation. Carcinogenesis *25*, 669-680.

Laird, D.W. (2006). Life cycle of connexins in health and disease. Biochem J *394*, 527-543.

Laird, D.W., Fistouris, P., Batist, G., Alpert, L., Huynh, H.T., Carystinos, G.D., and Alaoui-Jamali, M.A. (1999). Deficiency of connexin43 gap junctions is an independent marker for breast tumors. Cancer Res *59*, 4104-4110.

Laird, D.W., Puranam, K.L., and Revel, J.P. (1991). Turnover and phosphorylation dynamics of connexin43 gap junction protein in cultured cardiac myocytes. Biochem J *273(Pt 1)*, 67-72.

Lampugnani, M.G., Orsenigo, F., Gagliani, M.C., Tacchetti, C., and Dejana, E. (2006). Vascular endothelial cadherin controls VEGFR-2 internalization and signaling from intracellular compartments. J Cell Biol *174*, 593-604.

Langlois, S., Cowan, K.N., Shao, Q., Cowan, B.J., and Laird, D.W. (2008). Caveolin-1 and -2 interact with connexin43 and regulate gap junctional intercellular communication in keratinocytes. Molecular biology of the cell *19*, 912-928.

Langlois, S., Cowan, K.N., Shao, Q., Cowan, B.J., and Laird, D.W. (2010). The tumor-suppressive function of Connexin43 in keratinocytes is mediated in part via interaction with caveolin-1. Cancer Res *70*, 4222-4232.

LeBleu, V.S., Macdonald, B., and Kalluri, R. (2007). Structure and function of basement membranes. Experimental biology and medicine *232*, 1121-1129.

Lee, L.H., Moh, M.C., Zhang, T., and Shen, S. (2009). The immunoglobulin-like cell adhesion molecule hepaCAM induces differentiation of human glioblastoma U373-MG cells. J Cell Biochem *107*, 1129-1138.

Lin, C.W., Liao, M.Y., Lin, W.W., Wang, Y.P., Lu, T.Y., and Wu, H.C. (2012). Epithelial cell adhesion molecule regulates tumor initiation and tumorigenesis via activating reprogramming factors and epithelial-mesenchymal transition gene expression in colon cancer. J Biol Chem *287*, 39449-39459.

Lin, J.H., Takano, T., Cotrina, M.L., Arcuino, G., Kang, J., Liu, S., Gao, Q., Jiang, L., Li, F., Lichtenberg-Frate, H., *et al*. (2002). Connexin 43 enhances the adhesivity and mediates the invasion of malignant glioma cells. The Journal of neuroscience : the official journal of the Society for Neuroscience *22*, 4302-4311.

Loewenstein, W.R., and Kanno, Y. (1966). Intercellular communication and the control of tissue growth: lack of communication between cancer cells. Nature *209*, 1248-1249.

Lopez-Hernandez, T., Ridder, M.C., Montolio, M., Capdevila-Nortes, X., Polder, E., Sirisi, S., Duarri, A., Schulte, U., Fakler, B., Nunes, V., *et al*. (2011a). Mutant GlialCAM causes megalencephalic leukoencephalopathy with subcortical cysts, benign familial macrocephaly, and macrocephaly with retardation and autism. Am J Hum Genet *88*, 422-432.

Lopez-Hernandez, T., Sirisi, S., Capdevila-Nortes, X., Montolio, M., Fernandez-Duenas, V., Scheper, G.C., van der Knaap, M.S., Casquero, P., Ciruela, F., Ferrer, I., *et al*. (2011b). Molecular mechanisms of MLC1 and GLIALCAM mutations in megalencephalic leukoencephalopathy with subcortical cysts. Hum Mol Genet *20*, 3266-3277.

Makrilia, N., Kollias, A., Manolopoulos, L., and Syrigos, K. (2009). Cell adhesion molecules: role and clinical significance in cancer. Cancer investigation *27*, 1023-1037.

McLachlan, E., Shao, Q., Wang, H.L., Langlois, S., and Laird, D.W. (2006). Connexins act as tumor suppressors in three-dimensional mammary cell

organoids by regulating differentiation and angiogenesis. Cancer Res *66*, 9886-9894.

McMurray, R.W. (1996). Adhesion molecules in autoimmune disease. Seminars in arthritis and rheumatism *25*, 215-233.

Mechtersheimer, S., Gutwein, P., Agmon-Levin, N., Stoeck, A., Oleszewski, M., Riedle, S., Postina, R., Fahrenholz, F., Fogel, M., Lemmon, V., *et al*. (2001). Ectodomain shedding of L1 adhesion molecule promotes cell migration by autocrine binding to integrins. J Cell Biol *155*, 661-673.

Meng, W., and Takeichi, M. (2009). Adherens junction: molecular architecture and regulation. Cold Spring Harbor perspectives in biology *1*, a002899.

Mesnil, M., Crespin, S., Avanzo, J.L., and Zaidan-Dagli, M.L. (2005). Defective gap junctional intercellular communication in the carcinogenic process. Biochim Biophys Acta *1719*, 125-145.

Mesnil, M., and Yamasaki, H. (2000). Bystander effect in herpes simplex virus-thymidine kinase/ganciclovir cancer gene therapy: role of gap-junctional intercellular communication. Cancer Res *60*, 3989-3999.

Miranti, C.K., and Brugge, J.S. (2002). Sensing the environment: a historical perspective on integrin signal transduction. Nat Cell Biol *4*, E83-90.

Mitic, L.L., and Anderson, J.M. (1998). Molecular architecture of tight junctions. Annual review of physiology *60*, 121-142.

Mograbi, B., Corcelle, E., Defamie, N., Samson, M., Nebout, M., Segretain, D., Fenichel, P., and Pointis, G. (2003). Aberrant Connexin 43 endocytosis by the carcinogen lindane involves activation of the ERK/mitogen-activated protein kinase pathway. Carcinogenesis *24*, 1415-1423.

Moh, M.C., Lee, L.H., and Shen, S. (2005a). Cloning and characterization of hepaCAM, a novel Ig-like cell adhesion molecule suppressed in human hepatocellular carcinoma. J Hepatol *42*, 833-841.

Moh, M.C., Lee, L.H., Yang, X., and Shen, S. (2003). HEPN1, a novel gene that is frequently down-regulated in hepatocellular carcinoma, suppresses cell growth and induces apoptosis in HepG2 cells. J Hepatol *39*, 580-586.

Moh, M.C., Lee, L.H., Zhang, T., and Shen, S. (2009a). Interaction of the immunoglobulin-like cell adhesion molecule hepaCAM with caveolin-1. Biochem Biophys Res Commun *378*, 755-760.

Moh, M.C., and Shen, S. (2009). The roles of cell adhesion molecules in tumor suppression and cell migration: a new paradox. Cell Adh Migr *3*, 334-336.

Moh, M.C., Tian, Q., Zhang, T., Lee, L.H., and Shen, S. (2009b). The immunoglobulin-like cell adhesion molecule hepaCAM modulates cell

adhesion and motility through direct interaction with the actin cytoskeleton. J Cell Physiol *219*, 382-391.

Moh, M.C., Zhang, C., Luo, C., Lee, L.H., and Shen, S. (2005b). Structural and functional analyses of a novel ig-like cell adhesion molecule, hepaCAM, in the human breast carcinoma MCF7 cells. J Biol Chem *280*, 27366-27374.

Moh, M.C., Zhang, T., Lee, L.H., and Shen, S. (2008). Expression of hepaCAM is downregulated in cancers and induces senescence-like growth arrest via a p53/p21-dependent pathway in human breast cancer cells. Carcinogenesis *29*, 2298-2305.

Mott, J.D., and Werb, Z. (2004). Regulation of matrix biology by matrix metalloproteinases. Curr Opin Cell Biol *16*, 558-564.

Musil, L.S., Cunningham, B.A., Edelman, G.M., and Goodenough, D.A. (1990). Differential phosphorylation of the gap junction protein connexin43 in junctional communication-competent and -deficient cell lines. J Cell Biol *111*, 2077-2088.

Naus, C.C., and Laird, D.W. (2010). Implications and challenges of connexin connections to cancer. Nat Rev Cancer *10*, 435-441.

Paznekas, W.A., Boyadjiev, S.A., Shapiro, R.E., Daniels, O., Wollnik, B., Keegan, C.E., Innis, J.W., Dinulos, M.B., Christian, C., Hannibal, M.C., *et al*. (2003). Connexin 43 (GJA1) mutations cause the pleiotropic phenotype of oculodentodigital dysplasia. Am J Hum Genet *72*, 408-418.

Pellinen, T., and Ivaska, J. (2006). Integrin traffic. J Cell Sci *119*, 3723-3731.

Perez-Moreno, M., Jamora, C., and Fuchs, E. (2003). Sticky business: orchestrating cellular signals at adherens junctions. Cell *112*, 535-548.

Pollmann, M.A., Shao, Q., Laird, D.W., and Sandig, M. (2005). Connexin 43 mediated gap junctional communication enhances breast tumor cell diapedesis in culture. Breast cancer research : BCR *7*, R522-534.

Prise, K.M., and O'Sullivan, J.M. (2009). Radiation-induced bystander signalling in cancer therapy. Nat Rev Cancer *9*, 351-360.

Proux-Gillardeaux, V., Gavard, J., Irinopoulou, T., Mege, R.M., and Galli, T. (2005). Tetanus neurotoxin-mediated cleavage of cellubrevin impairs epithelial cell migration and integrin-dependent cell adhesion. Proceedings of the National Academy of Sciences of the United States of America *102*, 6362-6367.

Rhett, J.M., Jourdan, J., and Gourdie, R.G. (2011). Connexin 43 connexon to gap junction transition is regulated by zonula occludens-1. Molecular biology of the cell *22*, 1516-1528.

Riedle, S., Kiefel, H., Gast, D., Bondong, S., Wolterink, S., Gutwein, P., and Altevogt, P. (2009). Nuclear translocation and signalling of L1-CAM in

human carcinoma cells requires ADAM10 and presenilin/gamma-secretase activity. Biochem J *420*, 391-402.

Roberts, M., Barry, S., Woods, A., van der Sluijs, P., and Norman, J. (2001). PDGF-regulated rab4-dependent recycling of alphavbeta3 integrin from early endosomes is necessary for cell adhesion and spreading. Current biology : CB *11*, 1392-1402.

Saitou, M., Furuse, M., Sasaki, H., Schulzke, J.D., Fromm, M., Takano, H., Noda, T., and Tsukita, S. (2000). Complex phenotype of mice lacking occludin, a component of tight junction strands. Molecular biology of the cell *11*, 4131-4142.

Sanchez-Alvarez, R., Paino, T., Herrero-Gonzalez, S., Medina, J.M., and Tabernero, A. (2006). Tolbutamide reduces glioma cell proliferation by increasing connexin43, which promotes the up-regulation of p21 and p27 and subsequent changes in retinoblastoma phosphorylation. Glia *54*, 125-134.

Segretain, D., and Falk, M.M. (2004). Regulation of connexin biosynthesis, assembly, gap junction formation, and removal. Biochim Biophys Acta *1662*, 3-21.

Shao, Q., Wang, H., McLachlan, E., Veitch, G.I., and Laird, D.W. (2005). Down-regulation of Cx43 by retroviral delivery of small interfering RNA promotes an aggressive breast cancer cell phenotype. Cancer Res *65*, 2705-2711.

Shapiro, L., and Weis, W.I. (2009). Structure and biochemistry of cadherins and catenins. Cold Spring Harbor perspectives in biology *1*, a003053.

Shi, F., and Sottile, J. (2008). Caveolin-1-dependent beta1 integrin endocytosis is a critical regulator of fibronectin turnover. J Cell Sci *121*, 2360-2371.

Shin, K., Fogg, V.C., and Margolis, B. (2006). Tight junctions and cell polarity. Annual review of cell and developmental biology *22*, 207-235.

Sirisi, S., Folgueira, M., Lopez-Hernandez, T., Minieri, L., Perez-Rius, C., Gaitan-Penas, H., Zang, J., Martinez, A., Capdevila-Nortes, X., De La Villa, P., *et al*. (2014). Megalencephalic leukoencephalopathy with subcortical cysts protein 1 regulates glial surface localization of GLIALCAM from fish to humans. Hum Mol Genet *23*, 5069-5086.

Smith, J.H., Green, C.R., Peters, N.S., Rothery, S., and Severs, N.J. (1991). Altered patterns of gap junction distribution in ischemic heart disease. An immunohistochemical study of human myocardium using laser scanning confocal microscopy. The American journal of pathology *139*, 801-821.

Solan, J.L., and Lampe, P.D. (2009). Connexin43 phosphorylation: structural changes and biological effects. Biochem J *419*, 261-272.

Spiegel, I., Adamsky, K., Eisenbach, M., Eshed, Y., Spiegel, A., Mirsky, R., Scherer, S.S., and Peles, E. (2006). Identification of novel cell-adhesion molecules in peripheral nerves using a signal-sequence trap. Neuron glia biology *2*, 27-38.

Takeichi, M. (1991). Cadherin cell adhesion receptors as a morphogenetic regulator. Science *251*, 1451-1455.

Takeichi, M. (1995). Morphogenetic roles of classic cadherins. Curr Opin Cell Biol *7*, 619-627.

Tedder, T.F., Steeber, D.A., Chen, A., and Engel, P. (1995). The selectins: vascular adhesion molecules. FASEB journal : official publication of the Federation of American Societies for Experimental Biology *9*, 866-873.

Temme, A., Buchmann, A., Gabriel, H.D., Nelles, E., Schwarz, M., and Willecke, K. (1997). High incidence of spontaneous and chemically induced liver tumors in mice deficient for connexin32. Current biology : CB *7*, 713-716.

Tompa, P., Buzder-Lantos, P., Tantos, A., Farkas, A., Szilagyi, A., Banoczi, Z., Hudecz, F., and Friedrich, P. (2004). On the sequential determinants of calpain cleavage. J Biol Chem *279*, 20775-20785.

Tsai, H., Werber, J., Davia, M.O., Edelman, M., Tanaka, K.E., Melman, A., Christ, G.J., and Geliebter, J. (1996). Reduced connexin 43 expression in high grade, human prostatic adenocarcinoma cells. Biochem Biophys Res Commun *227*, 64-69.

Turk, V., Stoka, V., Vasiljeva, O., Renko, M., Sun, T., Turk, B., and Turk, D. (2012). Cysteine cathepsins: from structure, function and regulation to new frontiers. Biochim Biophys Acta *1824*, 68-88.

Valentinis, B., Reiss, K., and Baserga, R. (1998). Insulin-like growth factor-I-mediated survival from anoikis: role of cell aggregation and focal adhesion kinase. J Cell Physiol *176*, 648-657.

van der Knaap, M.S., Boor, I., and Estevez, R. (2012). Megalencephalic leukoencephalopathy with subcortical cysts: chronic white matter oedema due to a defect in brain ion and water homoeostasis. Lancet Neurol *11*, 973-985.

Van Itallie, C.M., and Anderson, J.M. (1997). Occludin confers adhesiveness when expressed in fibroblasts. J Cell Sci *110 (Pt 9)*, 1113-1121.

van Kilsdonk, J.W., van Kempen, L.C., van Muijen, G.N., Ruiter, D.J., and Swart, G.W. (2010). Soluble adhesion molecules in human cancers: sources and fates. European journal of cell biology *89*, 415-427.

Wang, Q., Luo, C., Wu, X., Du, H., Song, X., and Fan, Y. (2013). hepaCAM and p-mTOR closely correlate in bladder transitional cell carcinoma and hepaCAM expression inhibits proliferation via an AMPK/mTOR dependent

pathway in human bladder cancer cells. The Journal of urology *190*, 1912-1918.

Weng, Z., Xin, M., Pablo, L., Grueneberg, D., Hagel, M., Bain, G., Muller, T., and Papkoff, J. (2002). Protection against anoikis and down-regulation of cadherin expression by a regulatable beta-catenin protein. J Biol Chem *277*, 18677-18686.

Wennerberg, K., Lohikangas, L., Gullberg, D., Pfaff, M., Johansson, S., and Fassler, R. (1996). Beta 1 integrin-dependent and -independent polymerization of fibronectin. J Cell Biol *132*, 227-238.

Wong, C.W., Dye, D.E., and Coombe, D.R. (2012). The role of immunoglobulin superfamily cell adhesion molecules in cancer metastasis. International journal of cell biology *2012*, 340296.

Xu, B., He, Y., Wu, X., Luo, C., Liu, A., and Zhang, J. (2012). Exploration of the correlations between interferon-gamma in patient serum and HEPACAM in bladder transitional cell carcinoma, and the interferon-gamma mechanism inhibiting BIU-87 proliferation. The Journal of urology *188*, 1346-1353.

Yang, S., Wu, X., Luo, C., Pan, C., and Pu, J. (2010). Expression and clinical significance of hepaCAM and VEGF in urothelial carcinoma. World J Urol *28*, 473-478.

Zamir, E., and Geiger, B. (2001). Molecular complexity and dynamics of cell-matrix adhesions. J Cell Sci *114*, 3583-3590.

Zhang, L., Wu, X., Luo, C., Chen, X., Yang, L., Tao, J., and Shi, J. (2013). The 786-0 renal cancer cell-derived exosomes promote angiogenesis by downregulating the expression of hepatocyte cell adhesion molecule. Molecular medicine reports *8*, 272-276.

Zhang, Q.L., Luo, C.L., Wu, X.H., Wang, C.Y., Xu, X., Zhang, Y.Y., Liu, Q., and Shen, S.L. (2011). HepaCAM induces G1 phase arrest and promotes c-Myc degradation in human renal cell carcinoma. J Cell Biochem *112*, 2910-2919.

Zhang, T., Moh, M.C., Lee, L.H., and Shen, S. (2010a). The immunoglobulin-like cell adhesion molecule hepaCAM is cleaved in the human breast carcinoma MCF7 cells. Int J Oncol *37*, 155-165.

Zhang, X., Xu, L.H., and Yu, Q. (2010b). Cell aggregation induces phosphorylation of PECAM-1 and Pyk2 and promotes tumor cell anchorage-independent growth. Mol Cancer *9*, 7.

Zhang, Y., Lu, H., Dazin, P., and Kapila, Y. (2004). Squamous cell carcinoma cell aggregates escape suspension-induced, p53-mediated anoikis: fibronectin and integrin alphav mediate survival signals through focal adhesion kinase. J Biol Chem *279*, 48342-48349.

Zhang, Y.W., Morita, I., Ikeda, M., Ma, K.W., and Murota, S. (2001). Connexin43 suppresses proliferation of osteosarcoma U2OS cells through post-transcriptional regulation of p27. Oncogene *20*, 4138-4149.

APPENDICES

APPENDIX I: SUPPLEMENTARY FIGURES
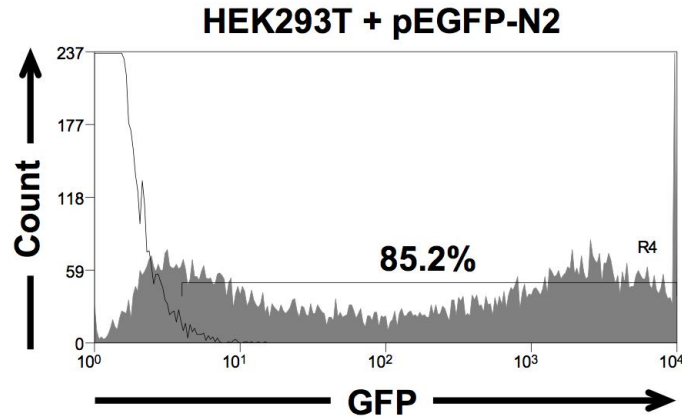
Supplementary Figure 1. Transfection efficiency of HEK293T cells. HEK293T cells were transfected with pEGFP-N2 using Turbofect Transfection Reagent. Cells were analysed by flow cytometry 48 h after transfection to determine the percentage of GFP-expressing cells.

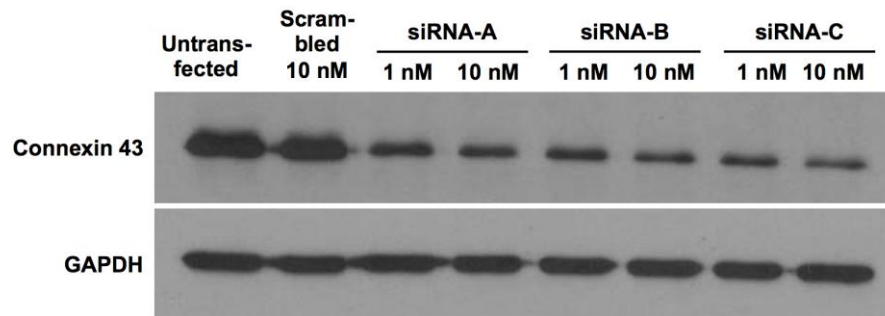**Supplementary Figure 2. Optimisation of siRNA-mediated connexin 43 knockdown in hepaCAM-expressing U373 MG cells.** Wild-type hepaCAM-expressing U373 MG cells were transfected with three different connexin 43 siRNA duplexes from the GJA1 Trilencer-27 Human siRNA kit (OriGene) at two different concentrations, 1 nM or 10 nM. Untransfected cells and cells transfected with 10 nM universal scrambled siRNA were included as controls. Cells were lysed 48 h post-transfection, and 20 μg of cell lysates were subjected to western blot analysis using connexin 43 antibody. GAPDH was used as a loading control. Connexin 43 siRNA duplex C (SR301801C) was selected for subsequent experiments, as the knockdown efficiency was the highest. The concentration used was chosen as 5 nM, as the difference in the knockdown efficiency at 1 nM and 10 nM was slight.
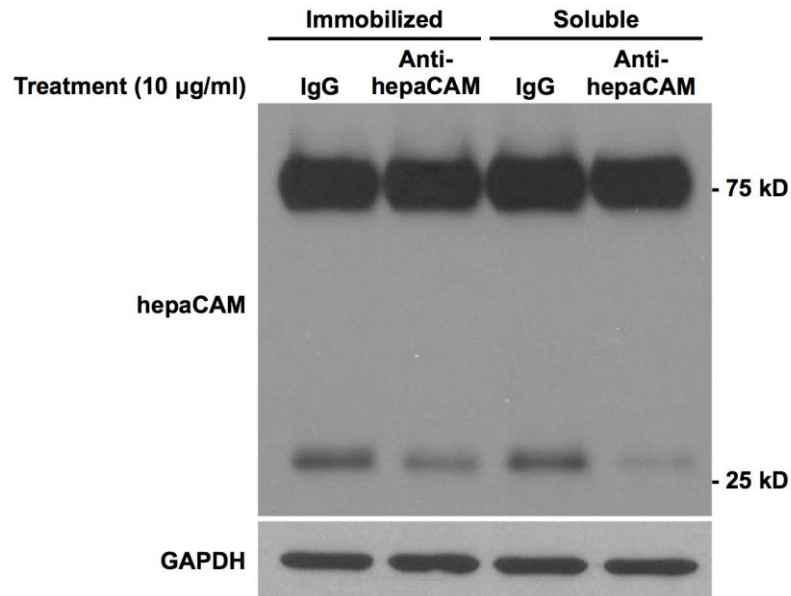
Supplementary Figure 3. Proteolytic cleavage of the hepaCAM cytoplasmic domain is inhibited by the antibody against the hepaCAM extracellular domain in both soluble and immobilised forms. MCF7 cells stably transfected with hepaCAM were treated with an antibody against hepaCAM extracellular domain (10 μg/ml) in immobilised or soluble forms. Mouse IgG (MOPC-21) was included as an isotype control. For the immobilised form, a 24-well plate was coated with the antibodies overnight at 4°C, and rinsed with PBS twice before seeding of cells. For the soluble form, the antibodies were added directly to the cell culture media. Cells were seeded into the respective wells and incubated overnight with the antibodies. The next day, cells were lysed and 20 μg of cell lysates were subjected to Western blot analysis using anti-V5-HRP to detect the V5-tag on the hepaCAM cytoplasmic domain. GAPDH was used as a loading control.

APPENDIX II: BUFFERS AND REAGENTS

Antibiotics stock solutions

Antibiotics	Concentration of stock solution
Ampicillin	100 mg/ml in H_2O
Kanamycin	30 mg/ml in H_2O
Blasticidin	10 mg/ml in H_2O

Filter-sterilised through a 0.22 μm filter.

10× PBS (1 L)

Reagent	Amount	Final concentration
NaCl	80 g	1.37 M
KCl	2 g	27 mM
Na_2HPO_4	14.4 g	100 mM
KH_2PO_4	2.4 g	18 mM
HCl	Adjust to pH 7.4	
ddH_2O	Top up to 1 L	

1× PBS (1 L)

Reagent	Amount	Final concentration
NaCl	8 g	137 mM
KCl	0.2 g	2.7 mM
Na_2HPO_4	1.44 g	10 mM
KH_2PO_4	0.24 g	1.8 mM
HCl	Adjust to pH 7.4	
ddH_2O	Top up to 1 L	

4% paraformaldehyde (100 ml)

Reagent	Amount	Final concentration
Paraformaldehyde	4 g	4%
1× PBS	100 ml	
5 M NaOH	Added dropwise till paraformaldehyde is fully dissolved	
HCl	Adjust to pH 7.4	

Filtered through a 0.22 μm filter and stored at -20°C till use.

0.1% crystal violet (100 ml)

Reagent	Amount	Final concentration
Crystal violet	0.1 g	0.1%
Ethanol	20 ml	20%
ddH_2O	80 ml	

Filtered through a 0.22 μm filter to remove undissolved particulates.

PROTEIN LYSIS AND WESTERN BLOT REAGENTS

RIPA buffer (250 ml)

Reagent	Amount	Final concentration
1 M Tris-HCl, pH 7.4	12.5 ml	50 mM
NaCl	0.73 g	50 mM
NP-40	2.5 ml	1%
Sodium deoxycholate	0.625 g	0.25%
10% SDS	2.5 ml	0.1%
ddH$_2$O	Top up to 250 ml	

Non-denaturing lysis buffer for co-IP (50 ml)

Reagent	Amount	Final concentration
NP-40	0.5 ml	1%
1× PBS	50 ml	

Resolving gel (10 ml)

Reagent	10% gel	12% gel
ddH$_2$O	2.72 ml	2.05 ml
1 M Tris-HCl, pH 8.8	3.75 ml	3.75 ml
30% Acrylamide/bis solution, 29:1	3.33 ml	4.00 ml
10% SDS	100 μl	100 μl
10% Ammonium persulfate	100 μl	100 μl
TEMED	4 μl	4 μl

Stacking gel (4 ml)

Reagent	
ddH$_2$O	2.75 ml
1 M Tris-HCl, pH 6.8	0.50 ml
30% Acrylamide/bis solution, 29:1	0.67 ml
10% SDS	40 μl
10% Ammonium persulfate	40 μl
TEMED	4 μl

Towbin transfer buffer (1 L)

Reagent	Amount	Final concentration
Tris	3.03 g	25 mM
Glycine	14.4 g	192 mM
Ethanol	200 ml	20%
ddH$_2$O	Top up to 1 L	

2× Laemmli sample buffer (50 ml)

Reagent	Amount	Final concentration
1 M Tris-HCl, pH 6.8	6.25 ml	125 mM
Glycerol	10 ml	20%
10% SDS	20 ml	4%
β-mercaptoethanol	1.25 ml (added prior to use)	2.5%
Bromophenol blue	5 mg	0.01%
ddH$_2$O	12.5 ml	

5× Laemmli sample buffer (40 ml)

Reagent	Amount	Final concentration
1 M Tris-HCl, pH 6.8	2.5 ml	62.5 mM
Glycerol	4 ml	10%
10% SDS	8 ml	2%
β-mercaptoethanol	2 ml (added prior to use)	5%
Bromophenol blue	4 mg	0.01%
ddH$_2$O	23.5 ml	

10× TBS (1 L)

Reagent	Amount	Final concentration
NaCl	88 g	1.5 M
Tris base	24.2 g	200 mM
HCl	Adjust to pH 7.4	
ddH$_2$O	Top up to 1 L	

1× TBS (1 L)

Reagent	Amount	Final concentration
NaCl	8.8 g	150 mM
Tris base	2.42 g	20 mM
HCl	Adjust to pH 7.4	
ddH$_2$O	Top up to 1 L	

TBST (1 L)

Reagent	Amount	Final concentration
1× TBS	1 L	
Tween-20	1 ml	0.1%

Stripping buffer (1 L)

Reagent	Amount	Final concentration
Glycine	1.876 g	25 mM
10% SDS	100 ml	1%
HCl	Adjust to pH 2.0	
ddH$_2$O	Top up to 1 L	

APPENDIX III: LIST OF PUBLICATIONS

International Scientific Journals

Wu MH, Moh MC, Schwarz H. hepaCAM associates with connexin 43 and enhances its localization in cellular junctions. (submitted).

Selected Local and International Scientific Conferences

Wu MH, Moh MC, Schwarz H. hepaCAM associates with connexin 43 and enhances its localization in cellular junctions. 6th Models of Physiology and Disease Symposium. Singapore, September 2014. (Poster Presentation).

Wu MH, Moh MC, Schwarz H. hepaCAM associates with connexin 43 and enhances its localization in cellular junctions. Cell Symposia: Hallmarks of Cancer. Beijing, China, November 2014. (Poster Presentation).